UCL DEPARTMENT OF CIVIL, ENVIRONMENTAL & GEOMATIC ENGINEERING

MSc DISSERTATION SUBMISSION

Student Name: BENAZIR ORIHUELA GONZALES

Programme: MSc EEDM

Supervisor: Dr CARMINE GALASSO

Dissertation Title:

Performance assessment of an Earthquake Early Warning System based on real-time Building Response Parameters for Campania, Italy

- I confirm that I have read and understood the guidelines on plagiarism, that I understand the meaning of plagiarism and that I may be penalised for submitting work that has been plagiarised.
- I declare that all material presented in the accompanying work is entirely my own work except where explicitly and individually indicated and that all sources used in its preparation and all quotations are clearly cited.
- I have submitted an electronic copy of the project report through turnitin.

Should this statement prove to be untrue, I recognise the right of the Board of Examiners to recommend what action should be taken in line with UCL's regulations.

Signature: Benazir Orihuela Gonzales **Date** 02/02/2020

LONDON'S GLOBAL UNIVERSITY

University College London
Department of Civil, Environmental & Geomatic Engineering

Performance assessment of an Earthquake Early Warning System based on real-time Building Response Parameters for Campania, Italy

Dissertation submitted in partial fulfilment of the requirements for the Master of Science in
Earthquake Engineering with Disaster Management

Benazir Orihuela Gonzales
Candidate Number: JSYK8
Student Number: 18128207

Supervisor: Dr Carmine Galasso

Academic Year 2018-19

This page is intentionally left in blank

To my family, Orlando and Samin.

*The word cloud has been produced with the content of this dissertation. The size of each word indicates its frequency in the text.

This page is intentionally left in blank

Abstract

In recent times, economic losses due to earthquakes have increased exponentially worldwide mainly due to the extensive development of dense urban areas. Therefore, seismic risk mitigation and reduction are receiving extensive funding for research and application worldwide. One of the innovations are the so-called Earthquake Early Warning Systems (EEWS), which are capable of sending warning alarms before the energetic seismic waves hit a city. Most of the development of these systems has been focused on improving the reliability of the seismic prediction and the suitability of warning times by using alarming thresholds for intensity measure parameters such as Peak Ground Acceleration (PGA). However, mid-rise and high-rise buildings have complex seismic behaviour depending on dynamic characteristics (e.g. fundamental period, lateral stiffness) which are not well correlated with the PGA.

This study has developed Performance Prediction Equations (PPEs) for Engineering Demand Parameters (EDP), such as floor accelerations and inter-storey drifts, which are more suitable to assess the seismic performance of structures. Furthermore, real-time assessment of building response was done by including these equations in the EEWS framework. Finally, a simulation demonstrating the benefits of using the proposed EDP instead of the classical PGA has been carried out for an EEWS for the Campania Region using different building typologies and alarming thresholds.

Keywords: Earthquake Early Warning, Performance Prediction Equation, Real-time Probabilistic Seismic Hazard Analysis, Engineering Demand Parameters, mid-rise and high-rise Buildings, Campania

Acknowledgments

The author would like to acknowledge the following persons for their support in this project.

Dr. Carmine Galasso

For his guidance through the master and especially for being an extraordinary Programme Director on an academic and personal level.

Chevening Scholarship

For believing in me, I would be eternally grateful.

Mr. Omar Velazquez Ortiz

For his suggestions to the work, willingness to answer my questions and patience.

To my friends

Stavroula Stathopoulu, Domenica Iuliano, Kieran O'sullivan, Matthias Fuentes, Michael Rome and Alexandros Tsandoulis. I will always remember you, each one of you made my year in London the best one.

Table of Contents

List of Figures

List of Tables

List of Appendix

List of Acronyms

The acronyms found below are used throughout this dissertation. They are presented by their full name when they are first used, but will later on be referred to by their acronym. In the list, the acronyms are presented in alphabetical order. The list is intended as a help for the reader for refreshing the full name of an acronym after its introduction should occur.

Acronym	Full name
EDP	Engineering Demand Parameter
EDPc	Critical Engineering Demand Parameter
EEWS	Earthquake Early Warning Systems
FEMA	Federal Emergency Management Agency
GMPE	Ground Motion Prediction Equations
GIDS	Generalized Interstorey Drift
NGA	New Generation Attenuation
IM	Intensity Measure
ISNet	Irpinia Seismic Network
MIDR	Maximum Interstorey Drift Ratio
MDOF	Multiple-Degree of Freedom
MRF	Moment Resisting Frame
Mw	Moment Magnitude
PBEEW	Probabilistic-Based Earthquake Early Warning
PBSD	Probabilistic-Based Structural Demand
PDF	Probabilistic Distribution Function
PFA	Peak Floor Acceleration
Pfa	Probability of False Alarm
PGA	Peak Ground Acceleration
Pma	Probability of Missed Alarm
PPE	Performance Prediction Equation
Prc	Critical Exceedance Probability
PSDA	Probabilistic Seismic Demand Assessment
PSHA	Probabilistic Seismic Hazard Analysis

Repi	Epicentral Radius
RTPSHA	Real-time Probabilistic Seismic Hazard Analysis
SDOF	Single-Degree of Freedom

1. Introduction

Urbanization has rapidly progressed worldwide by developing cities in a wide variety of geographic locations including active faults and subduction zones and in this way has posed serious threats to properties and lives. Therefore, the implementation of mitigation measures for seismic risk is needed in large urban areas, which is a complex task that requires multidisciplinary cooperation between scientists, engineers and decision-makers.

In recent times, a new approach has emerged for improving risk mitigation and post-earthquake emergency response based on a network of computerized seismic stations with automatic processing, which provides real-time information on earthquake parameters and expected ground motion. Furthermore, major computational improvements have been able to provide earthquake information before the ground shaking reached a certain target (e.g. a city). This development is currently known as Earthquake Early Warning Systems (EEWS) and is being tested and developed worldwide.

The real-time assessment of an EEWS allows estimating the intensity measure (e.g. Peak Ground Acceleration or PGA) at a target site before the earthquake hits and automatized actions which require milliseconds to seconds can be set. However, engineering demand parameters (e.g. lateral drifts or floor accelerations) have the highest level of structural information available and are best correlated with structural and, non-structural damage (e.g. drift-sensitive components, elevators functionality etc). Furthermore, non-structural damage accounts for 75% of the construction cost (Mondal and Jain, 2005) and its malfunctioning or collapse (e.g. windows, ceilings) pose a threat to the wellbeing and safety of occupants. Therefore, it is specifically reflective to highlight the importance of seismic risk mitigation processes.

Ground motion prediction equations (GMPEs) are commonly used to perform hazard analysis by estimating Peak Ground Accelerations (PGAs). However, PGA is only one component on the seismic behaviour of mid-rise and high-rise buildings. Therefore, the implementation of Performance Prediction Equations that relates more appropriate performance indicators such as floor accelerations or lateral deformations to the earthquake features (e.g. M_w, R_{epi}) is needed.

Most of the current body of research has been focused on improving the real-time estimation of seismic features (e.g. Magnitude, epicentre, acceleration) and another branch of research has focused on the seismic performance and modelling of structures. However, there is still a gap in the knowledge on the combination of both research areas for the implementation of EEWS for engineering applications in buildings. To the knowledge of the author, this investigation presents the first attempt to evaluate the performance of an automatized warning method focused on building response.

2. Literature Review

2.1Earthquake Early Warning Systems

2.1.1. Status of Earthquake Early Warning

EEWS are real-time information systems which take advantage of a network of sensor stations deployed in a region or at a specific site where the target to be protected is located. When an earthquake hits the sensors, seismic waves are registered and then a short time warning (up to tens of seconds) is communicated to the target site in order to take mitigation actions. This system is able to provide a warning on the potentially damaging effects of an impending ground shaking by estimating the magnitude which will occur later. As a result, reduction of deaths, injuries and economic losses are achieved; as well as, a rapid rescue response and damage recovery. The United Nations have recently promoted early warning and response systems, as the most effective strategy for the mitigation of diverse natural hazards and have provided guidelines for the implementation and the deployment of such systems, through the International Strategy for Disaster Reduction (Satriano et al., 2011)
However, as the warning time duration only ranges from a few seconds to a minute, an automatized decision-making approach is needed. With this in mind, a framework has emerged which integrates the seismic hazard analysis to loss models, called Performance-based Earthquake Early Warning (PBEEW). Figure 2.1 presents the general structure of PBEEW.

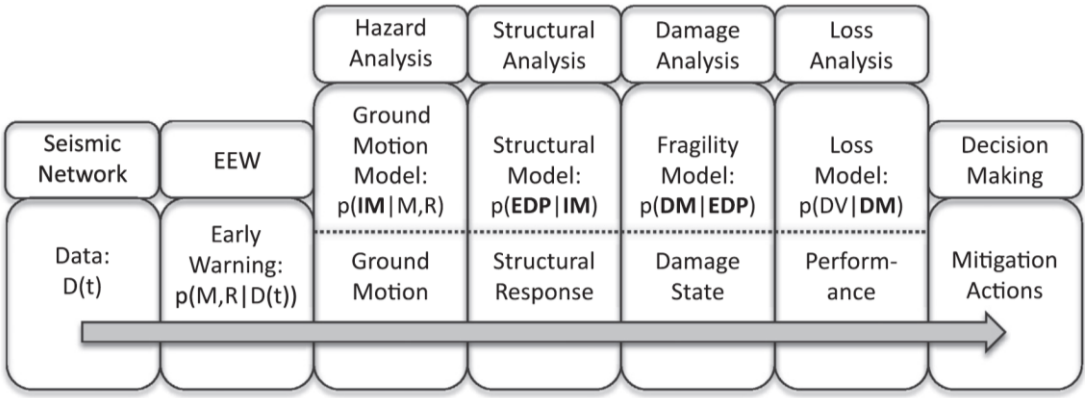

Figure 2.1 Structure of Performance-based Earthquake Early Warning framework (Cheng et al., 2014)

2.1.2 Classification of the EEWS seismic network

Typically, EEWS are classified as regional or site-specific, with recent innovation of combining the two types as a hybrid system. A regional or front detection approach covers a known seismic source zone located close to a threatened area, the information obtained is used to detect and locate an earthquake with a good level of precision. In this approach, the traditional seismological methodology is used to determine the magnitude and intensity

measure (IM) using ground motion prediction equations (GMPE) and a warning alarm can be transmitted to a specified target before the seismic energy arrives. As an outcome, applications such as shake maps, which consist of territorial distributions of ground shakings, are employed for emergency management (Iervolino, 2011).

In case a well-known seismic source is located at a significant distance from a populated area, the system can provide a valuable warning time. However, if the target site is very close to the epicentre, this approach is not viable because the warning time will be too small or even null. This effect, known as the blind zone, affects the area where the warning cannot be issued in time.

Around the world, different regional EEWS configurations exist. For example, the Seismic Alert System in Mexico (Espinosa-Aranda et.al., 2011) which is the first public warning system, the Japan Meteorological Agency (Kubo, et.al., 2011), ElarmS in California (Hellweg et.al. 2009), Presto in Italy (Weber et.al. 2007) and PreSEIS in Turkey (Böse et.al. 2008). In Figure 2.2, a map of global seismic hazard is presented along with active EEWS (blue) that are currently providing warnings to users and real-time seismic system (green) that are still being tested.

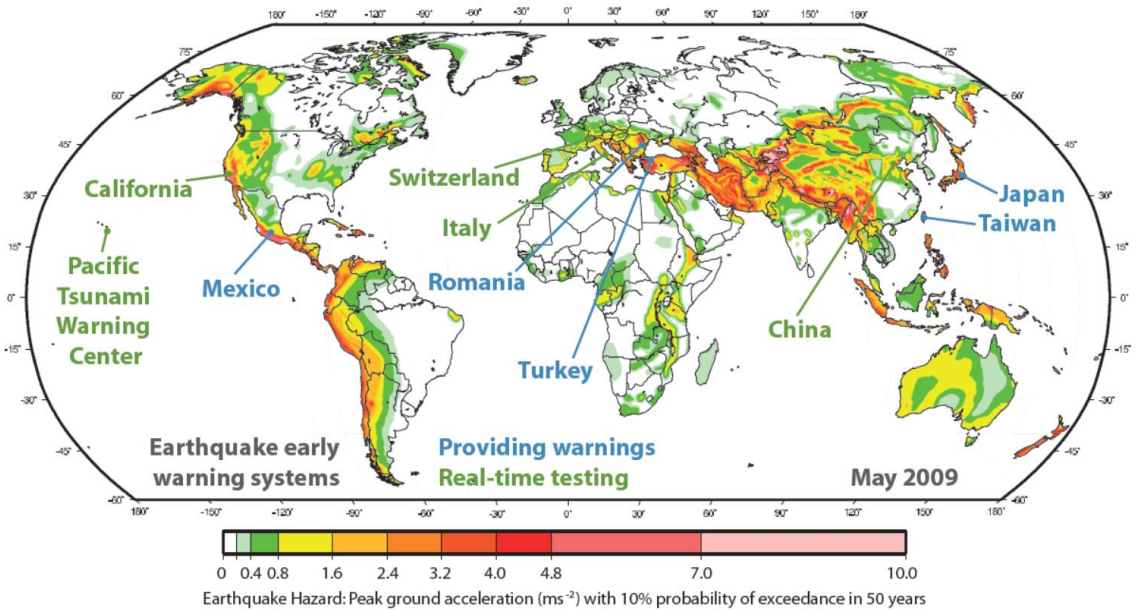

Figure 2.2 Global seismic Hazard and locations where EEWS provide public information (blue) or are being tested (green) (Allen et al., 2009)

Moreover, pre-programmed security actions can be implemented in critical infrastructures (Shut down of nuclear reactors or deceleration of high-speed trains), facilities (controlled shutdown of high- technological manufacturing operations, bringing elevators to a stop at the nearest floor) or at personal level (workers can move away from hazardous positions, students can shelter under their desks).

On the other hand, the network for a site-specific approach is placed around a predetermined target creating a fence, which enhances the safety margin and decreases the vulnerability. In this approach, real-time seismology science is used to estimate the magnitude and intensity measure (IM) using the first few seconds of the earthquake together with ground motion prediction equations (GMPE). Sometimes, seismic sensors are installed within the structure, this is known as a structure-specific system.

The theoretical lead-time for site-specific EEWS is defined as the time difference between the first recorded P-waves at the target site and the arrival of large energy amplitudes (Zollo and Lancieri, 2008). The location of the sensors relies on the lead time required to activate the safety procedures before the arrival of the damaging S-waves. Furthermore, an alarm is issued when the ground motion intensity at one or more sensor exceeds a given threshold (Iervolino, 2011).

Contrary to the regional case, site-specific approaches measure the ground motion and there is no attempt to estimate with precision the seismic features such as magnitude and location due to the lack of computational time. The first portion of the earthquake is normally associated with P-waves, therefore in this approach, the predominant period of the first four seconds (τ_p^{max}) is used to predict the ensuing ground shaking related to S-waves at the same location. This procedure provides a comparatively greater rapid alert which reduces the blind zone and increases the warning time but the parameters are poorly determined. (Iervolino et. al, 2005).

Current efforts to develop and implement EEWS are based on the Peak Ground Acceleration (PGA) as a proxy for the expected level of damage (Iannaccone et. al., 2010, Kanamori, 2005). However, mid-rise and high-rise buildings show a dynamic behaviour that is not only dependent on the PGA, but on their fundamental period (height of the building), and structural system. Few examples exist on the literature about specific applications of EEWS for buildings (Kubo et.al., 2011, Chen et.al., 2014, Primavera, 2016), but there is still a need for more research on this topic.

2.1.3 Hybrid Earthquake Early Warning Approaches in the Campanian Region

A hybrid approach combines regional networks and site-specific applications by estimating real-time predictions of peak ground motion using the information of source features from regional networks, while the earthquake could still be underway (Kanamori, 2005).

For example, in Taiwan, Wu & Teng (2002) used the regional warning system already implemented to locate earthquakes and estimated magnitudes with the site-specific approach, using the first seconds of P-waves. In this way, the system provides 20 seconds of early warning after the earthquake commence and reduces the radius of the blind zone from 70 to 21 km, proving that a hybrid application can enhance the usefulness and reliability of an EEWS.

In 2005, the development and implementation of a hybrid EEWS were started in southern Italy, based on the seismic network deployed along the Apennines belt region where large and destructive earthquakes in Italy have occurred during last centuries. (Weber et al., 2007). The Irpinia Seismic Network (ISNet) constituted by 29 stations, covers an area of

100x70 km^2 and uses a Real-time Probabilistic Seismic Hazard Analysis (RTPSHA) called Presto. As a result, location, magnitude and ground motion parameters are estimated in real-time by combining the P-wave arrival time with the information that some stations have not yet triggered to identify the epicentre of the earthquake. (Iannaccone et al., 2010).

Iervolino (2006) tested this probabilistic framework in the Campanian region for hybrid EEWS. Figure 2.3 presents a scheme of a hybrid EEWS.

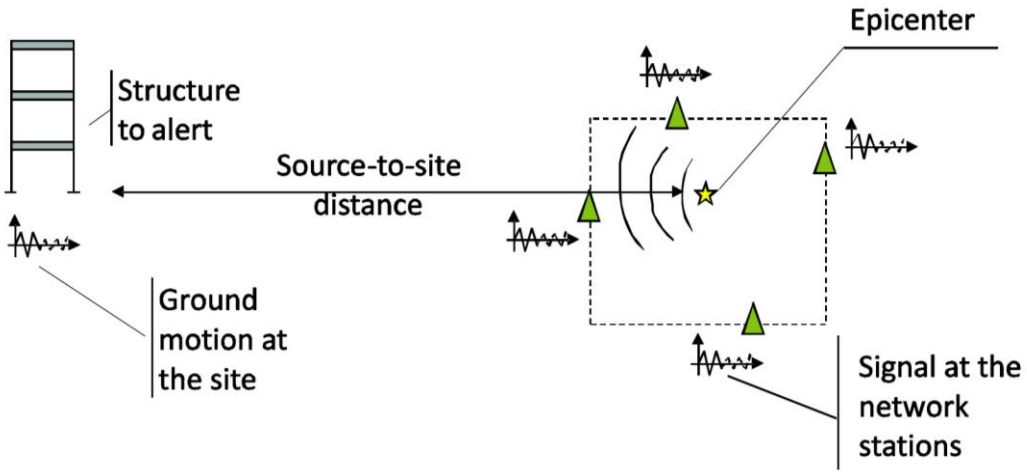

Figure 2.3 Hybrid EWS application for structure-specific (Iervolino, 2011)

Iervolino (2009) carried out a sensitivity analysis to evaluate the sources of uncertainty in an RTPSHA approach in a Hybrid EEWS. The results show how the coefficient of variance is highly dominated by the uncertainty of GMPE compared to those of magnitude and distance. Consequently, the warning decisions taken by using this methodology may present high uncertainty if the GMPE is not well estimated.

When only a few stations are triggered, the blind zone remains small and the lead-times are higher; however, the available information is not enough to estimate accurate parameters of magnitude and source-to-site distance and the probability of issuing false alarms increases. Figure 2.4 presents a hazard curve using the RTPSHA approach, the prediction of the PGA does not benefit from further information and becomes stable after 18 stations are triggered. Therefore, there exists a trade-off compromising the lead-time and information needed to issue an alarm.

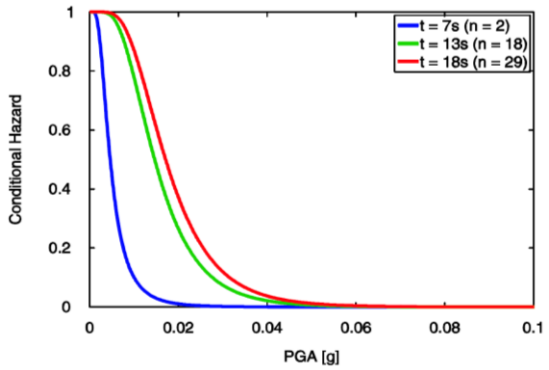

Figure 2.4 PGA Hazard curves via RTPSHA. Iervolino (2011)

Additionally, an analysis considering as many randomly occurring epicentres in the region within the ISNet sensors was computed, Figure 2.5 presents a map with lead-times up to 40 seconds along with real-time risk reduction actions which can be performed in the available time.

A number of different proposals for the refinement of the system have included the set of threshold-based EEWS using the P-waves and initial peak of displacement at the site (Caruso et.al., 2017) or the cost-benefit study of the proposed warning measures through the setting of alarm thresholds based on expected losses (Iervolino et.al., 2007).

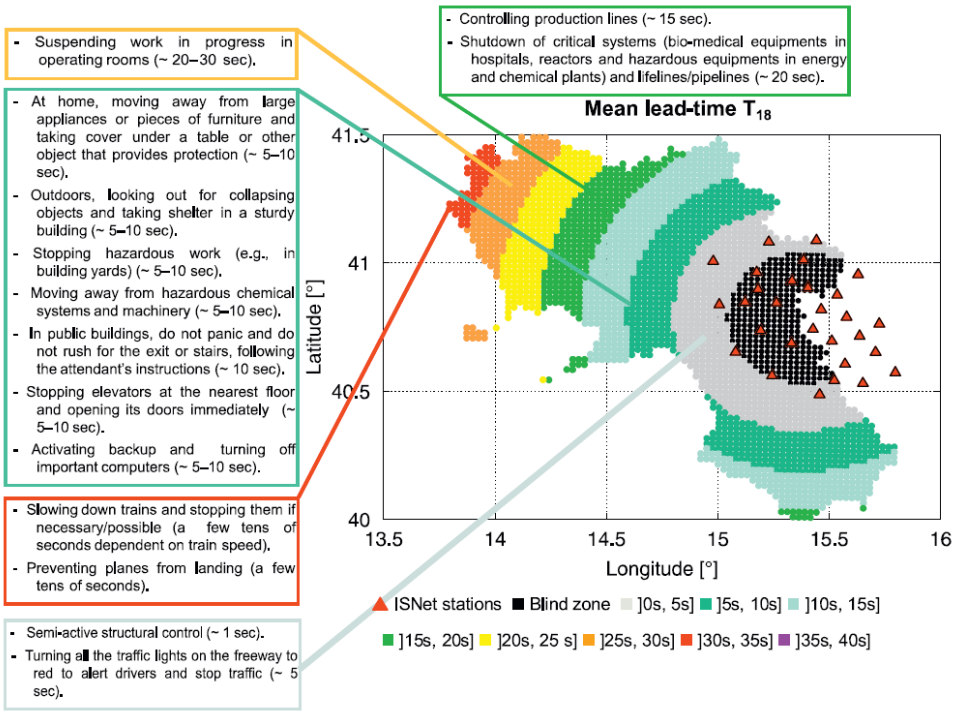

Figure 2.5 Map for the Campania region in the case of an event covered by the ISNet network. Information-dependent average lead-time with possible risk reduction actions. Iervolino (2011)

2.2 Structural Model

2.2.1 Structural response parameter

A growing need has emerged in emergency managers and city officials for a rapid seismic performance assessment of large inventories of buildings in urban areas. The information obtained has to be a valuable tool capable of identifying structural and non-structural damage and trigger mitigation measures.

The objective of Performance-Based Seismic Design (PBSD) is to assure an adequate building performance through the accomplishment of limit states defined along with the importance and function of the structure. For instance, after a seismic event, critical facilities are expected to remain in operational or at immediate occupancy level. Therefore, for this critical infrastructure, it is necessary to estimate, among others, Peak Floor Acceleration (PFA) demands and its distribution along with the building height because it is well correlated with the seismic performance of supports and attachments of building contents.

On the other hand, for less critical infrastructures, structural and non-structural damage is tolerated in life safety and collapse prevention levels, only if no structural collapse happens. In order to achieve the desired performance, it is useful to identify the required lateral stiffness. This parameter is related to the Maximum Interstorey Drift Ratio (MIDR), which is the result of lateral deformations that occur from relative displacement between consecutive floors.

Mid-rise and high-rise buildings can be considered critical because they provide vital services to the functioning of a city such as hospitals, communication towers or government facilities. However, potential losses in more common buildings (i.e. offices or commercial) should not be underestimated because they can concentrate an important density of population. As a result, seismic events can produce large economic losses concentrated within a single building. Given that 75% of the construction cost is associated to non-structural components (Mondal and Jain, 2005; Whittaker and Soong, 2003), it is also important to obtain an accurate prediction of seismic damage on them.

It is known that the shaking experienced by a user in a high-rise building will be completely different from the one on the ground and varies according to the dynamic features of the structure. For example, during the Mw 9 Tohoku earthquake in Japan on 2011, ground motions were amplified by a factor of 3.5 at the roofs of some of the tall buildings (Cheng et al., 2014) causing severe distress on the occupants who did not know which actions to take on such a strong event.

Usually, the procedure of obtaining the dynamic behaviour of a structure is through finite elements modelling approach along with an eigenvalue analysis. However, when the analysis is needed for a wide portfolio of buildings with different structural systems, this procedure is expensive and time-consuming.

In order to address this issue, Miranda (1999) has developed a multiple degrees of freedom (MDOF) model that is able to estimate displacement and acceleration demands for structures which remain elastic with a small number of parameters. The response is obtained

in terms of engineering demand parameters (EDP) which has the highest level of information available of a structure. This robust and fast method produces relatively good results with a small amount of information and computational effort and is useful for rapid evaluation of existing buildings. Other models with non-linear characteristics such as Xiong et. al (2016) and De Luca (2014) are building-specific or used for a determined analysis that requires them (e.g. extensive structural damage and non-linearity).

The Miranda´s linear-MDOF model is an equivalent continuum structure which combines a flexural and a shear cantilever beam which, along the length, (both beams) undergo similar lateral deformations because they are connected by an infinite number of axially rigid members which transmit horizontal forces. Figure 2.6 presents a scheme.

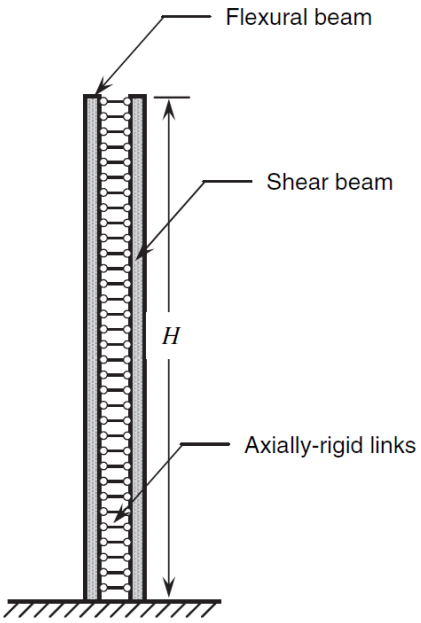

Figure 2.6 Continuum model proposed by Miranda (1999).

The response spectrum is based on an SDOF system which provides an approximate response of acceleration demands on structures. However, it cannot provide maximum interstorey drift demands, which are better related to the structural damages. Miranda and Akkar (2006) proposed a simpler method called the generalized interstorey drift spectrum (GIDS) that considers shear and flexural deformations based on Miranda (1999) model.

2.3 Response prediction equation

Probabilistic Seismic Demand Analysis (PSDA) allows the evaluation of the structural behaviour based on the performance-based seismic assessment methodology. First, ground motion predictions are used within a Probabilistic seismic hazard analysis (PSHA) to derive hazard curves in terms of intensity measures (IM), such as the PGA, on a determined site. Then, the structural analysis uses the IM on the site to estimate an EDP on

the structure and EDP hazard curve presents the probability of exceedance for a critical threshold based on a specified structural parameter (Cornell and Krawinkler, 2000).

The use of IM as an intermediary parameter introduces a source of uncertainty propagation and bias in the calculation (De Bortoli and Zareian, 2018). A novel concept denoted as performance prediction equations (PPEs) aims to merge these two stages by linking engineering demand parameters (EDP) directly to seismic features on the source.

As examples of these innovative efforts, Neam and Taghikhany (2016) performed a regression analysis for maximum inter-storey drift ratio however high standard deviations were obtained and De Bortoli and Zareian (2018) derived equations for floor displacement and inter-storey drift ratio, both studies were based on the NGA-West database.

Moreover, Koleva et al. (2008) derived equations to estimate MIDR only for shear wall structures based on earthquakes occurred in Europe. Primavera (2016) obtained equations from the ITACA database. Nonetheless, both studies presented residual plots with slightly biased trends for increasing magnitude at longer distance and need to be further refined.

2.4 Alarming Thresholds for buildings

As mentioned before, the setting of an early warning alarm is normally based on the probability that a structural parameter (EDPc or PGAc) is exceeding a critical threshold (Prc).

Diverse thresholds can be evaluated on buildings performance including structural and non-structural damage as shown in Tables 2.1 and 2.2 from Hazus-MH 2.1. Structural Damage is classified by model building type and building height and non-structural components criteria are divided into drift sensitive components and acceleration-sensitive components. By selecting a damage state, it is possible to set a structural parameter threshold in terms of PFA or IDR.

Table 2.1 Hazus Average Interstorey Drift Ratio (IDR) of Structural Damage States (Adapted from FEMA, 2013)

Model Building Type	Structural Damage States			
	Slight	Moderate	Extensive	Complete
Mid-Rise Buildings – Moderate Code Design Level				
C1 – Concrete Moment Frame	0.33%	0.60%	1.53%	4.00%
C2 – Concrete Shear Walls	0.27%	0.53%	1.53%	4.00%
High-Rise Buildings - Moderate Code Design Level				
C1 – Concrete Moment Frame	0.25%	0.45%	1.15%	3.00%
C2 – Concrete Shear Walls	0.20%	0.40%	1.15%	3.00%

Table 2.2 Hazus Damage-State Criteria for Non-structural Systems and Contents (Adapted from FEMA, 2013)

Design Level	Non-Structural Damage States – All Building Types			
	Slight	Moderate	Extensive	Complete
Interstorey Drift Ratio (IDR) – Drift Sensitive Components				
All	0.4%	0.8%	2.5%	5%
Peak Floor Acceleration (PFA) – Acceleration Sensitive Components/Contents				
Moderate-Code	0.25g	0.5g	1.0g	2.0g

In one of the few studies specifically setting alarming thresholds for an EEW application to buildings, Picozzi (2012) proposed a interstorey drift threshold of 0.5% for structural and non-structural components based on the damage for RC buildings observed by Ponzo et al. (2010).

On the other hand, it is possible to evaluate other types of damage during a seismic event. For instance, in the scenario that a person is subjected to a varying force with changing acceleration, such as an earthquake, the human body has to continuously adjust to a disturbance in his equilibrium (Cheng et al., 2014) which can produce disequilibrium, stress and fear. Therefore, PFA can help measure human comfort in multi-storey buildings during an earthquake as suggested in Table 2.1. for the relation between human comfort level and PFA.

Table 2.3 Human comfort level to acceleration (Cheng et.al., 2014)

Peak floor acceleration (PFA)	Comfort level	Early warning message
<0.5%g	Not perceptible	No shaking
0.5-1.5%g	Threshold of perceptible	Minor Shaking
1.5-5%g	Annoying	Moderate shaking
>5%g	Very Annoying	Strong shaking

Additionally, elevators are integral to multi-storey buildings and their potential failure due to an earthquake must be considered. For instance, in the State of California is mandatory to install an earthquake sensing device on every elevator which will shut down if an acceleration higher than 0.5g is detected. On the other hand, Japan uses different thresholds (0.08g-0.15g) depending on the use and location of the elevator (Cheng et.al., 2014).

3. Scope of the research

New implementations have been developed for EEWS worldwide, specifically in Italy where the hybrid system has boosted the potential of regional seismic sensors for site-specific applications by estimating real-time predictions of intensity measures (e.g. PGA) using the information gathered in the first seconds of the earthquake record. The developments of real-time seismology have accomplished this important step for risk mitigation, and consequently, a meaningful warning time can be provided to the population.

On the other hand, earthquake engineering has developed models which, using adequate simplifications, can assess the seismic performance of a wide variety of structural typologies with limited data and in a few seconds of computational time.

This research intends to combine both branches of earthquake science to evaluate the potential of EEWS for building applications, where intensity measures are no longer considered to be reliable parameters for their seismic performance and the implementation of real-time assessment in terms of engineering demand parameters (EDPs) such as drift demands and peak floor acceleration is needed.

Due to the fact that typical warning times (tens of seconds) will not allow a complete evacuation for mid-rise and high-rise buildings in case of potential collapse, this dissertation has focused on non-structural damage such as falling hazards (e.g. ceilings and building contents) or elevator serviceability and the mitigation measures that can be taken inside the building.

Therefore, the two main research questions of this study are:

1. How feasible and valuable is it to obtain real-time performance prediction equations for EDPs instead of the classical PGA? The challenge is to obtain reliable equations that directly predict building performance from earthquake features on the source (Mw, distance, etc).
2. How the incorporation of EDPs in the EEWS framework can improve the warning performance? The challenge is to estimate real-time EDPs and including them in an EEW design. Furthermore, a comparison with the PGA-based EEWS will be needed in order to quantitively assess the difference in performance.

In order to investigate those main research questions, this study will carry out two main steps. The first one will develop performance prediction equations for a variety of mid-rise and high-rise buildings (typologies) based upon seismic features. This first step will be applied to Italy using the Italian Accelerometric Archive (ITACA 3.0)
The second step will simulate an EEWS for the Campanian Region by including the performance indicators proposed. In this way, the EEWS will not be able to predict only real-time PGA but additionally other proposed meaningful indicators for buildings and its occupants.

4. Methodology

This dissertation will use a quantitative methodology in order to investigate the research questions outlined in the previous chapter. Figure 4.1 shows the 5 stages which have been briefly summarized below.

Stage 1: Ground motion records from the ITACA database are compiled with their corresponding flat file including M_w, R_{epi}, soil type and fault mechanism.

Stage 2: The seismic records are used as an input to the linear-MDOF model to evaluate the seismic behaviour of a range of building typologies with varying fundamental periods and structural systems.

Stage 3: Prediction equation forms are selected based on specialized literature. Then, non-linear regression analyses are carried out with the structural parameters (e.g. peak floor acceleration, maximum inter-storey drift) and the seismic features. Finally, statistical parameters, equation variability and goodness of fit is analysed in order to select the best equation.

Stage 4: The response prediction equation is derived and validated using historical records. Additionally, a comparison with two models is done.

Stage 5: A simulation of EEWS is developed for the Campania Region for different earthquake scenarios. Alarming thresholds (e.g. elevator functionality) for real-time hazard curves in terms of PGA and structural parameters are set and the warning performance is compared.

The following chapters will cover and develop each of the stages in detail.

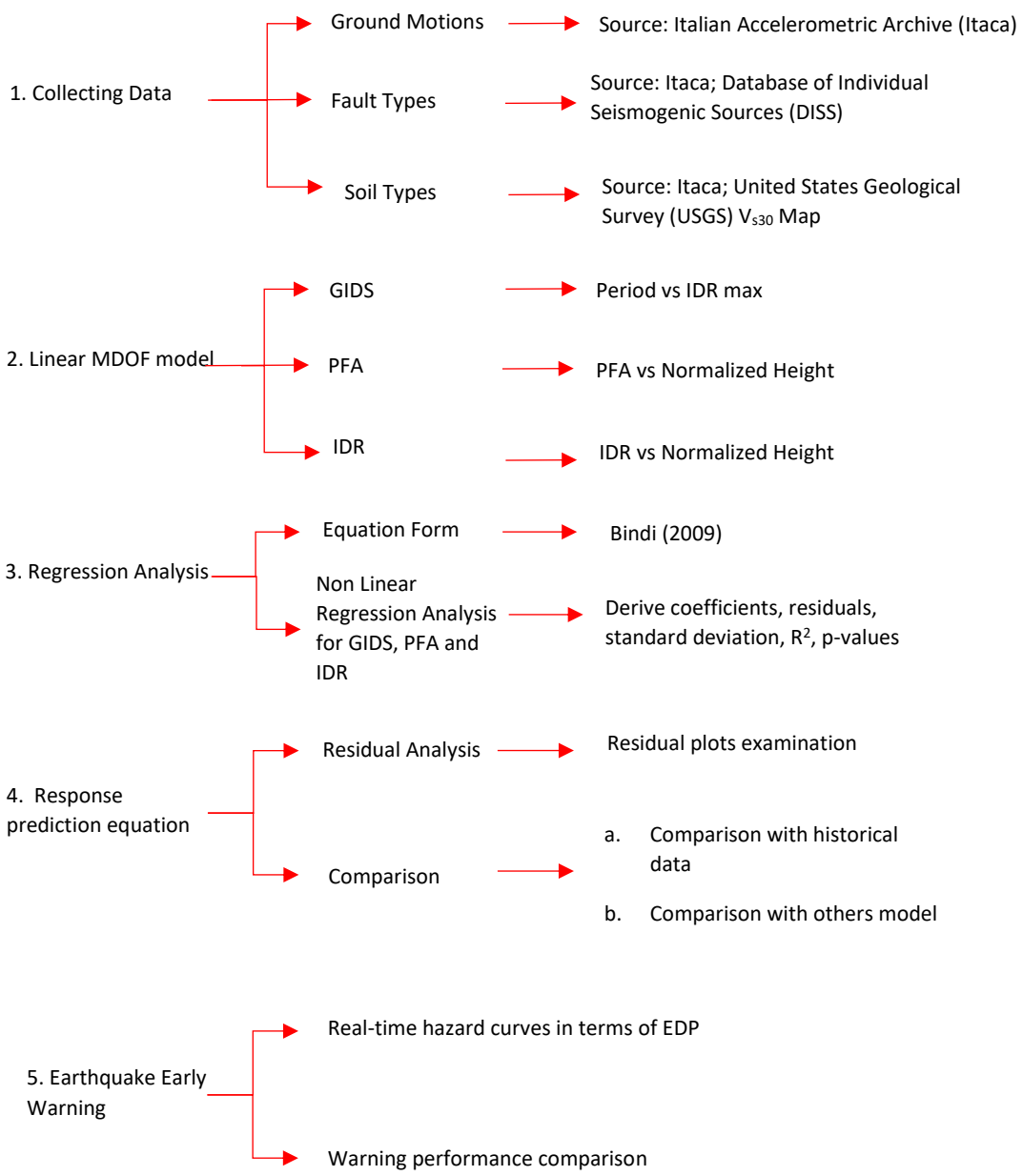

Figure 4.1 Proposed stages of the study.

5. Development of Performance Prediction Equations

5.1 Ground motion Data Selection Criteria

While synthetic earthquakes can be simulated in order to obtain a wide variety of seismic records, real records have been generally considered to provide the best representation of seismic behaviour for structural assessment (Galasso, 2013). Therefore, the first stage was focused on collecting relevant historical data with information about ground motion records, fault types and soil properties.

The Italian Accelerometric Archive (ITACA 3.0) has free access of moderate to severe earthquakes occurred in Italy from 1972 until now. ITACA (http://itaca.mi.ingv.it) was created by the Italian Department of Civil Protection and the Italian Institute for Geophysics and Volcanology (INGV).

The database provides two types of magnitude measurements used: Local Magnitude (M_L) for events up to 4 and Moment Magnitude (M_w) for stronger events. Likewise, two types of distance definitions are evaluated: Epicentral distance (R_{epi}) for events with M_w <5.5 and Joyner-Boore distance (R_{jb}) for severe earthquakes, the best-sampled distance ranges from 5 to 100 km.

In case the R_{epi} or R_{jb} was not given, the distance has been calculated according to Haversine formula where the longitude and latitude of the station are needed along with the earth radius = 6371 km.

$$a = sin^2\left(\frac{\Delta\varphi}{2}\right) + cos\varphi_1 \cdot cos\varphi_2 \cdot sin^2\left(\frac{\Delta\varphi}{2}\right) \qquad \text{(Eq.5-1)}$$

$$c = 2 \cdot atan2(\sqrt{a}, \sqrt{1-a})$$

$$d = r \cdot c$$

The soil types are classified according to Eurocode8 where the average shear-wave velocity in the top 30 m. (V_{s30}) for each class is A: V_{s30}≥800 m/s, B: 360≤ V_{s30}≤800 m/s, C: 180≤ V_{s30}≤360m/s, D: 180≤ V_{s30} and E is a combination of C or D underlain by stiffer material. In case of a soil type characterising a record is not provided the classification has been made from USGS V_{s30} map which estimated the site conditions from the topographic slope.

The main seismic sequences that gathered most data are L'Aquila (2009), Umbria-Marche (1997), Friuli (1976) and Irpinia (1980) where a single station recorded the seismic event with an R_{jb}≤10 km. The historical data obtained is going to be fundamental for the validation of the new building response equation analysed in the next chapter.

From the ITACA database a flat file was created by performing the following criteria:

- Only two-in-plane components (NS, EW) have been considered.
- Events with M_w <5 and R_{epi}>200 km have been removed because their analysis does not represent engineering relevance in this study.

After this procedure 589 horizontal records from 55 seismic events are chosen, the final flat file is compiled in Section A.1 of the Appendix. Since the EEW system have an extremely short time window and it is not possible to predict an accurate fault mechanism these parameters were excluded from the analysis.

The moment magnitude versus R_{epi} distribution according to each soil type is shown in Figure 5.1. It can be seen that most of the available records are soil A (rock) and occurred in a radius between 0 and 50 km epicentral distance.

Furthermore, the epicentre of the earthquakes and the seismic stations distributed along Italy is presented in figure 5.2.

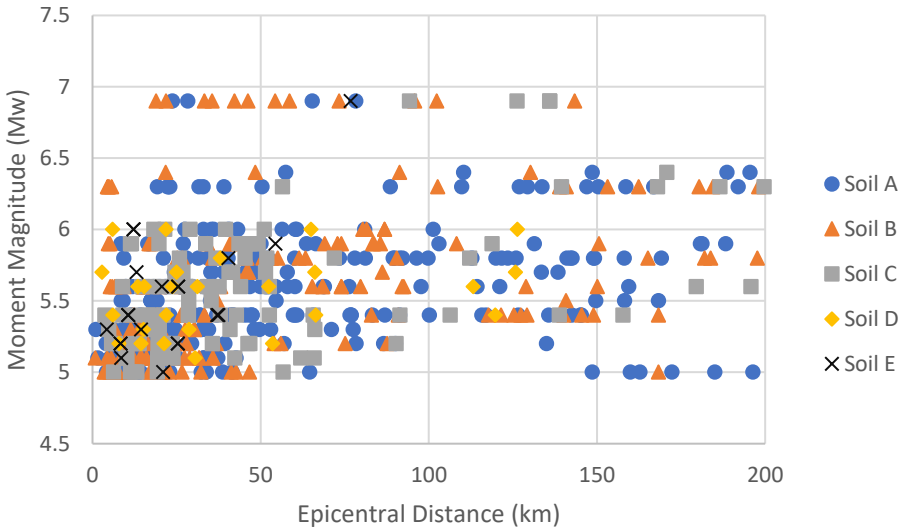

Figure 5.1 Distribution of records with respect to Mw and epicentral distance

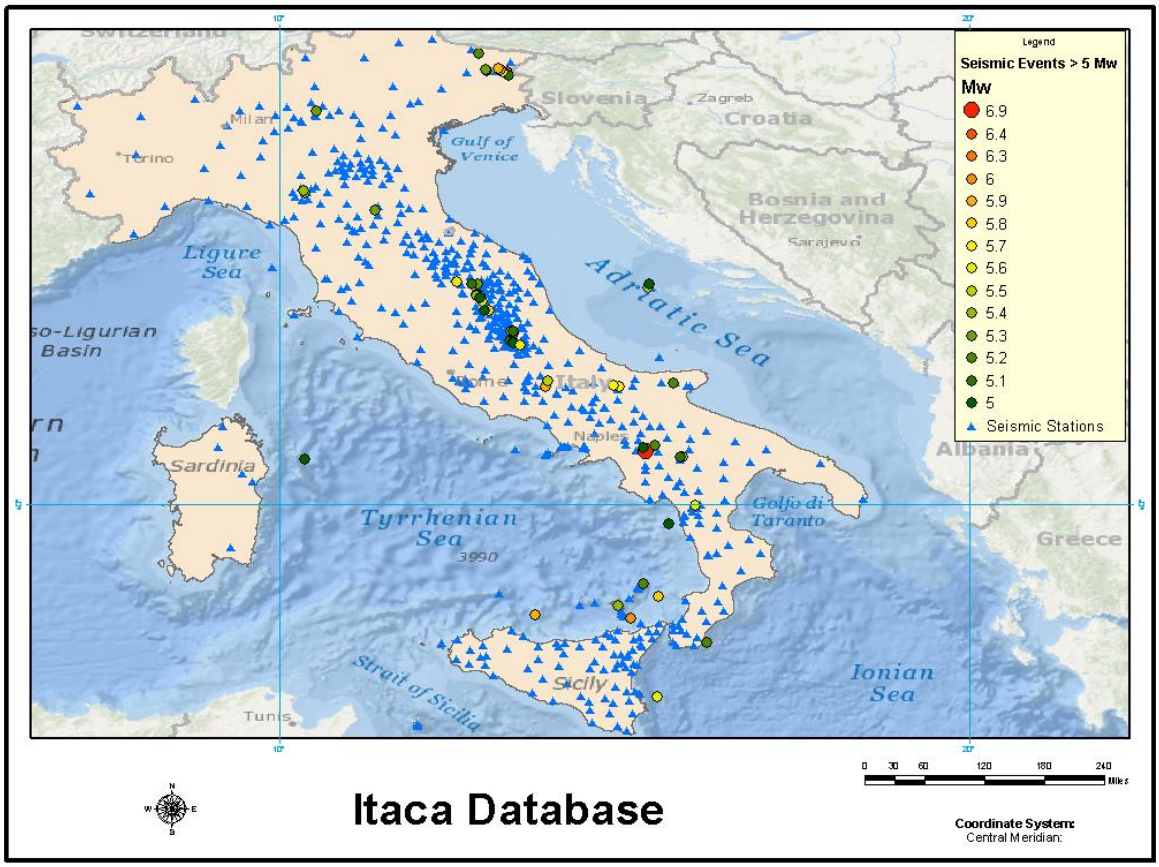

Figure 5.2 Distribution of 55 earthquakes and seismic stations

5.2. Linear MDOF model analysis

In order to obtain the dynamic response of a wide range of structural systems representing the building stock of a city, the linear MDOF model was implemented in the present investigation in Matlab R2018a©, hereafter referred to as Matlab,

This stage was focused on analysing the ground motion records obtained in the previous stage and obtaining the respective building response which are expected to remain on the elastic range or with controlled levels of nonlinearity.

As already mentioned, the linear-MDOF model can present either bending to shear configurations, by just modifying the lateral stiffness ratio (α) which is a dimensionless parameter that controls the degree of participation:

$$\alpha = H\sqrt{\frac{GA}{EI}} \qquad \text{(Eq. 2-5)}$$

Where EI is the flexural rigidity, GA is the shear rigidity and H is the total height. A value of α close to 0 represent a flexural model, an intermediate value corresponds to a configuration that combines shear and flexural deformations, a value equal to ∞ reproduce a pure shear model.

Miranda and Taghavi (2005) proposed an approximate earthquake analysis for a continuous structure with elastic behaviour, where the response can be computed as the superposition of individual modes of vibration as the following:

$$u(x,t) = \sum_{i=1}^{n} u_i(x,t) = \sum_{i=1}^{n} \Gamma_i \Phi_i(x) D_i(t) \qquad \text{(Eq. 2-6)}$$

Where *n* corresponds to the number of modes needed, $u_i(x,t)$ is the lateral displacement of the ith mode at non-dimensional height *x* at a time *t* varying between 0 to 1 at roof level. Additionally, Γ_i is called the modal participation factor, $\Phi_i(x)$ is the mode shape at height *x* and $D_i(t)$ is the displacement at time *t* of single-degree-of freedom (SDOF) system with a period and damping ratio corresponding to the *ith* mode of vibration of the building. Likewise, absolute acceleration can be calculated by adding the ground vibrations to the relative acceleration:

$$\ddot{u}(x,t) = \ddot{u}_g(t) + \sum_{i=1}^{n} \Gamma_i \Phi_i(x) \ddot{D}_\iota(t) \qquad \text{(Eq. 2-7)}$$

Miranda and Taghavi (2005) presented for the continuum model approximate modes shapes and modal participation factors:

$$\Phi_i(x) = \sin(\gamma_i x) - \frac{\gamma_i}{\beta_i}\sinh(\beta_i x) - \eta_i \cos(\gamma_i x) + \eta_i \cosh(\beta_i x) \qquad \text{(Eq. 2-8)}$$

Where β_i and η_i are defined as:

$$\beta_i = \sqrt{{\alpha_o}^2 + {\gamma_i}^2} \qquad \text{(Eq. 2-9)}$$

$$\eta_i = \frac{{\gamma_i}^2 \sin(\gamma_i) + \gamma_i \beta_i \sinh(\beta_i)}{{\gamma_i}^2 \cos(\gamma_i) + {\beta_i}^2 \cosh(\beta_i)} \qquad \text{(Eq. 2-10)}$$

Roots of equation 2.11 give the eigenvalue parameter γ_i in ascending order corresponding to the modes of vibration of the building as a function of α_o.

$$0 = 2 + \left[2 + \frac{{\alpha_o}^4}{{\gamma_i}^2 {\beta_i}^2}\right]\cos(\gamma_i)\cosh(\beta_i) + \left[\frac{{\alpha_o}^2}{\gamma_i \beta_i}\right]\sin(\gamma_i)\sinh(\beta_i) \qquad \text{(Eq. 2-11)}$$

The continuum model permits to obtain vibration periods for higher modes if the fundamental period is known by using:

$$\frac{T_i}{T_1} = \frac{\gamma_1 \beta_1}{\gamma_i \beta_i} \qquad \text{(Eq. 2-12)}$$

The modal participation factors can be computed as:

$$\Gamma_i = \frac{\int_0^1 \Phi_i(x)dx}{\int_0^1 {\Phi_i}^2(x)dx} \qquad \text{(Eq. 2-13)}$$

The interstorey drift ratio (IDR) is approximated as:

$$IDR(x,t) \approx \theta(x,t) = \frac{1}{H}\sum_{i=1}^{n} \Gamma_i {\Phi'}_i(x) D_i(t) \qquad \text{(Eq. 2-14)}$$

Where $\theta(x,t)$ is the rotation of the structure at a time t and at a non-dimensional height corresponding to the middle of the storey and ${\Phi'}_i(x)$ is the first derivative of the mode shape $\Phi_i(x)$

The GIDS provides an estimation of peak interstorey drift demand for different periods of vibration, which is a parameter better correlated with damages. The maximum IDR (MIDR) is computed as:

$$MIDR \quad = \max|\theta(x,t)| \qquad \text{(Eq. 2-15)}$$

In brief, the model is defined by using three parameters:

- the fundamental period of vibration of the building (T_1)
- modal damping ratio (ξ)
- lateral stiffness ratio (α_o)

In order to evaluate a wide range of different building typologies, the following considerations have been used:

- 6 translational modes of vibrations in each direction were examined because these provide a better contribution to the acceleration demands and contain at least 90% of the system total mass. An accurate building response is expected for low to high rise buildings as stated by Reinoso and Miranda (2005)
- 15 fundamental periods were considered for capturing different building heights. The range was tested for 0.1 to 0.5 s with a 0.1 s step, 0.75 s and then for 1 to 5 s with a 0.5 step.

- 3 lateral stiffness ratio (α) considering shear to flexural configurations have been analysed. Taking into account the consideration given by Miranda and Reyes (2002) the values selected for shear walls ($\alpha = 0.1$), dual systems ($\alpha = 8$) and moment-resisting frames ($\alpha = 30$)
- Masses and stiffness distribution along the height were considered uniform and linear.
- The total height of the structure given a fundamental period is calculated using the empirical relationship suggested for ACE7-2010 for generic structures

$$H = \left(\frac{T_1}{0.0488}\right)^{1/0.75}$$

- A constant modal damping ratio characterizing the structure in both directions was set to ξ=5%
- The analysis of IDR and PFA was done considering a 0.01-unit step for the normalized height for better accuracy.

The function modal analysis presented in Section A.7 of Appendix, describe the equations (2.8 to 2.13) used to obtain the modal shapes, modes of vibrations and modal participation factors for the linear-MDOF model.

The process describes a linear-MDOF system, with each translational mode of vibrations previously calculated, subjected to different ground motion records from the flat file. Each script presented in Section A.8 and A:9 of Appendix calculates relative displacement and acceleration, respectively.

Taking into consideration equation 2.6 to 2.7, the computations of generalised inter-storey drift, inter-storey drift ratio and peak floor acceleration for different lateral stiffness ratios and fundamental periods have been presented in Section A.5 and A.6.

As a result, a total of 26505 analyses have been performed using the aforementioned Matlab scripts. The final response has been calculated by combining the two horizontal components (X and Y) using the geometric mean.

Three performance indicators were estimated for the different building typologies:

- The Generalized Inter-storey Drift provided maximum inter-storey drift ratio (MIDR), which is the maximum deformation between adjacent floors during the seismic motion.
- Inter-storey Drift Ratio (IDR), which is the deformation between adjacent floors for each of the storeys computed for the building.
- Peak Floor Acceleration (PFA), which is the maximum acceleration obtained in one of the storeys along with the building height during the seismic motion.

5.2.1 Generalized Inter-storey Drift

The MIDR was computed for all ground motion records listed in Table 5.1. The main outcomes are commented below. In the interest of quantifying the effect of α, MIDR was normalized by using MIDR for α=30. Figure 5.3 shows the influence of α where ordinates which are greater than one indicate a MIDR larger than those computed for a moment-

resisting frame (MRF) system (α=30) and vice versa. For fundamental periods less than 2 s, MIDR for different values of α are smaller than those computed for MRF and do not change more than 15%. However, after this limit MIDR using α=8 starts to increase up to 10% more and IDR ratio using α=0.1 start to reduce.

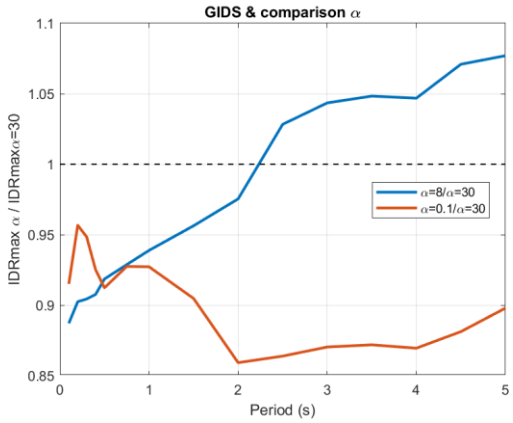

Figure 5.3 Mean IDRmax ratio for different α values

Therefore, we can consider that the influence of α in IDR is low, therefore, the following results are obtained by adopting a value of α=30. In order to evaluate the importance of R_{epi}, the analysis of MIDR was distributed in four groups. Figure 5.4(a) presents the GIDS for ground motion records with R_{epi}<50 km, the MIDR is 0.82% for T= 0.75 s and it is reasonable that the mean has small values since the vast majority of records have low magnitudes. Figure 5.4(b) display the MIDR ratio for different R_{epi}, the distribution occurs as expected, the response attenuates as R_{epi} increases. The response for IDR with R_{epi} >150 represents 20% of R_{epi} <50, for fundamental periods greater than 2s. The response for IDR with 100<R_{epi} <150 and 50<R_{epi} <100 become similar at approximately 40% of R_{epi} <50.

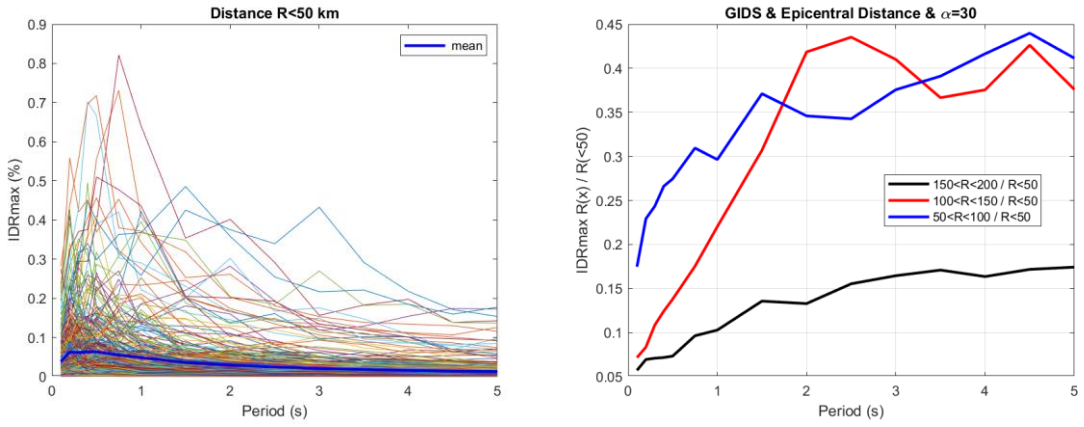

(a) (b)

Figure 5.4 Influence of R_{epi} in the GIDS response: (a) Generalized Interstorey Drift Spectrum for earthquakes with R_{epi}<50km and α = 30. (b) Mean IDRmax ratio for ground motions with different R_{epi}

Likewise, the relevance of soil type in MIDR was evaluated for α=30. Figure 5.5(a) present the MIDR for stiff soil, the graphics turn out to be almost identical to Figure 5.4(a) which

implies that MIDR happens in stiff soil and R_{epi} <50. Figure 5.5(b) shows MIDR ratio normalized by MIDR for stiff soil, as expected, the response with rock soil was considerably less in the range of 30%. On the other hand, stiff and soft soil present a similar response with a maximum difference of 10%.

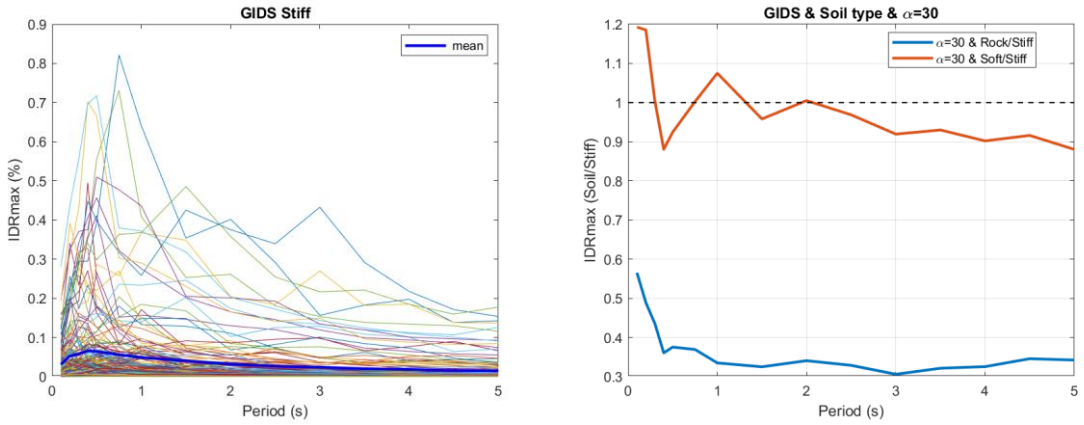

(a) (b)

Figure 5.5 Influence of soil type in the GIDS response: (a) Generalized Interstorey Drift Spectrum for earthquakes with stiff soil and $\alpha = 30$. (b) Mean IDRmax ratio for ground motions with different soil types

5.2.2 Interstorey Drift Ratio

For buildings where flexural deformations (α=0.1) govern, maximum interstorey drift demands occurred near the top as shown in Figure 5.6(a). In contrast, Figure 5.6(b) presents structures that combine shear and flexural deformations (α=8) where larger IDR are experienced near mid-height. While, buildings in which shear deformations (α=30) dominated, IDR happen near the bottom as display in Figure 5.6(c). These results are consistent with plots presented by Miranda (1999) and Galasso (2013).

The Federal Emergency Management Agency (FEMA) earthquake loss estimation methodology, commonly known as Hazus, has developed the estimation of various damage states for structural and non-structural components for 36 generic model buildings types that are classified in terms of their structural systems. The following plots validated the use of the linear-MDOF model because the estimation of seismic demands generally remains on the elastic range.

The average IDR of structural damage states can be found in the Table 5.9a through 5.9d in Hazus-MH 2.1 Technical Manual and are presented as thresholds for the aforementioned figures. In this study, α=30 and α=8 correspond to Concrete Moment Frame (C1M) and α=0.1 correlated to Concrete Shear Walls (C2M) both mid-rise buildings with moderate code design level.
It can be observed that building response with moderate damage represents less than 1% of the total database and only one ground motion record, Friuli (1976), presents complete

damage. Consequently, the building response of the flat file remains on the elastic range and the use of a linear-MDOF model is valid.

Furthermore, a comparison of different values of α is presented in Figure 5.6 (d). From base to mid-height of the building, IDR analysed with α=0.1 and α=8 is less than IDR computed with α=30. On the contrary, from mid-height to the top IDR ratio with α=0.1 and α=8 are up to 4 and 2 times greater, respectively.

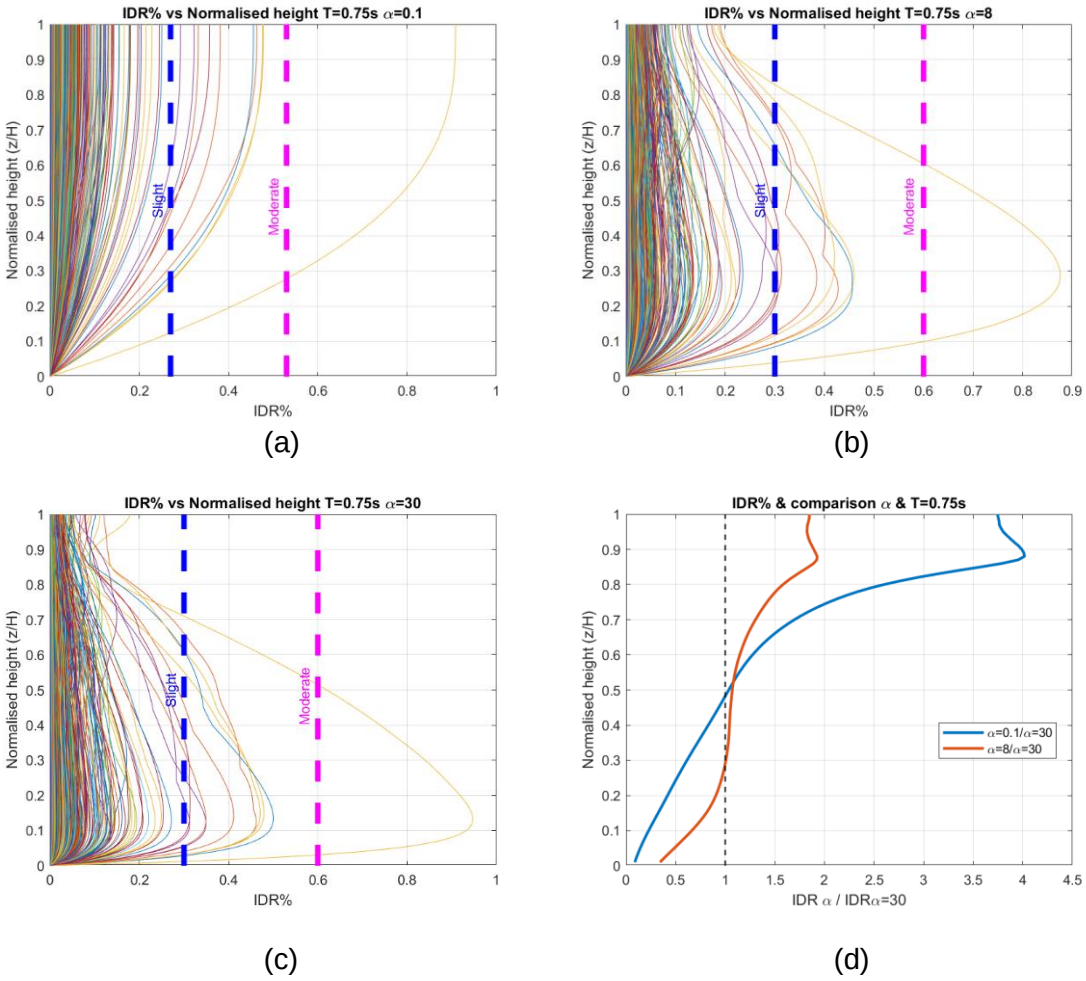

Figure 5.6 Interstorey Drift Ratio vs Normalised height for T=0.75 s and structural damage state thresholds. (a) $\alpha = 0.1$ (b) $\alpha = 8$ (c) $\alpha = 30$ (d) IDR ratio for different α values

4.2.3 Peak Floor Acceleration (PFA)

Multiple non-structural components and building contents, necessary for the functionality of critical facilities, are damaged as a result of large floor acceleration demands which represent a considerable cost for buildings operation. Default threshold values of PFA for each of the damage states are summarized in Table 6.3 of Hazus-MH 2.1 Technical Manual.

Figure 5.7 shows PFA vs normalised height for different α and display the thresholds for each damage state which remain constant for all building types. A considerable amount of ground motion records still present slight damage, and an increase of building responses with moderate damage has occurred. ; however non-structural damage is tolerated in life safety and collapse prevention levels, only if no structural collapse happens as presented in figure 5.6

Figure 5.7(d) shows the influence of the fundamental period for PFA along with the height, the accelerations are amplified as the period decreases and the height increases and regardless the value of α, small periods present higher floor accelerations. Additionally, the thresholds of human comfort discussed in Table 2.1 are presented, where the acceleration on the roof for small periods start to be annoying and the elevators should be shut down for acceleration greater than 0.08g as has been recommended.

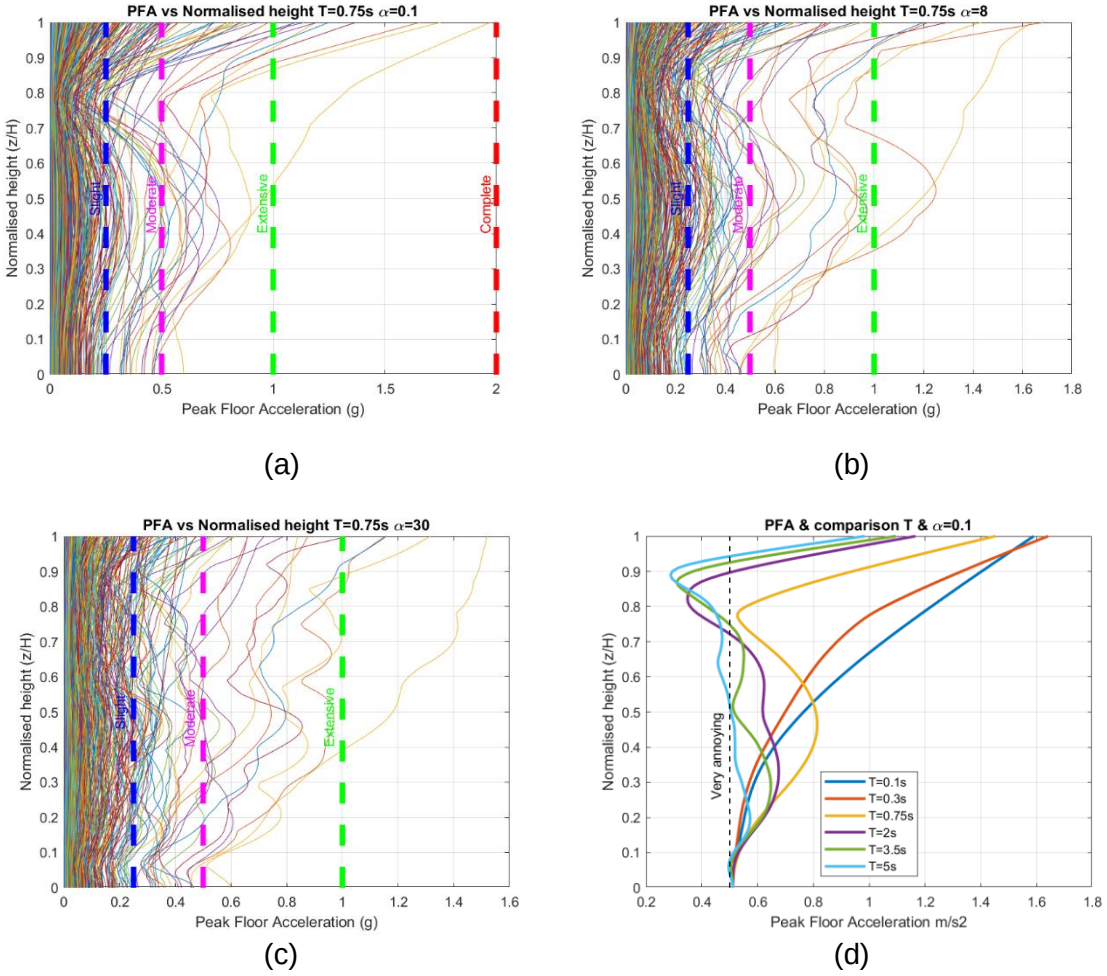

Figure 5.7 Peak floor acceleration vs Normalised height for T=0.75 s and structural damage state thresholds. (a) $\alpha = 0.1$ (b) $\alpha = 8$ (c) $\alpha = 30$ (d) comparison of different periods with $\alpha = 0.1$ and human comfort threshold

To sum up, a number of different analyses and comparisons have been done in order to show the complex seismic response of different building typologies. The analysed models

show different acceleration propagation (reduction or amplification) and inter-storey deformations along with the height. These estimates vary in magnitude and location (along the height of the building) due to the fundamental period, structural typology and soil type. Therefore, it is not possible to use a single performance indicator (e.g. PGA) to assess potential real-time damages during an earthquake and the indicators showed above will be tested on the next sections.

5.3. Regression Analysis

In order to obtain a Performance Prediction Equation (PPE), which could relate EDP to earthquake features, an empirical non-linear regression analysis based on the ITACA database was developed to determine the coefficients, residuals and standard deviations. The equation was formulated for IDR(x), MIDR and PFA(x) for three different lateral resisting systems with fundamental periods ranging from 0.05 to 5 s.

The seismic features considered in the functional form need to be rapidly predicted in real-time since they are going to be incorporated in an EEW framework. For that reason, only earthquake magnitude, epicentral distance and soil type were considered as dependent variables. The verification of the results is compared with historical data and validated by econometric tests. Additionally, a comparison with two additional complex models is performed in order to evaluate the influence of the fault mechanism type in the model.

5.3.1 Functional form

The equation selected to perform the empirical regression is the model adopted by Bindi (2009) where Y relates to magnitude $F_M(M)$, distance $F_D(R, M)$, and soil amplification F_S. The function is as follows:

(Eq. 4-2)

$$log_{10}Y = b_1 + b_2 \cdot M + b_3 log_{10}\sqrt{{R_{epi}}^2 + {b_4}^2} + b_5 S_s + b_6 S_A + \varepsilon\sigma$$

- $Y = \sqrt{Y_x \cdot Y_Y}$ represent the geometric mean of both EDP horizontal components such as IDR(x) and MIDR expressed in percentage and PFA(x) expressed in m/s^2
- b_i regression coefficients to be computed
- $F_M(M) = b_2 \cdot M$ Magnitude scaling
- $F_D(R, M) = (b_3) log_{10}\sqrt{{R_{epi}}^2 + {b_6}^2}$ Distance function
- $F_S = b_9 \cdot S_s + b_{10} \cdot S_A$ Soil amplification

Table 5.5 Dummy variables for soil amplification

Fault Mechanism	S_S	S_A
Soft Soil	1	0
Stiff Soil	0	1
Rock	0	0

- ε is the fractional number of standard deviations and σ is standard deviations

5.3.2 Statistical Measurements

In the performance prediction equation, earthquake features represent predictor variables (independent) and EDP constituted response variables (dependent), as can be observed in equation 3.2, the relationship between these variables is not linear. In order to determine the coefficients a non-linear regression analysis was performed in Matlab, the scripts are presented in Section A.10 to A.12 of the Appendix.

In the following paragraphs, the goodness of fit will be evaluated by statistical parameters obtained from the model. For example, the standard deviation (σ) represents how the calculated values are spread out from the mean. Consequently, the variation of standard deviation versus the fundamental period is analysed for each EDP and different α. Figure 5.8(a) shows σ associated with MIDR. Figure 5.8(b), Figure 5.8(c) and Figure 5.8(d), presents σ associated with IDR(x=0.05), IDR(x=0.30), IDR(x=1.00), where the maximum response happens for α=30, α=8 and α=0.1,respectively. Figure 5.8(e) and Figure 5.8(f) shows σ associated with PFA(x=0.50) and PFA(x=1.00) where larger acceleration has been found.

In general, the aforementioned standard deviation plots display a stable trend for fundamental periods larger than 1 s with an average value of 0.35, as a result, it can be concluded that the standard deviation is not affected by fundamental periods or lateral stiffness ratio. In a similar work, Neam and Taghikhany (2016) derived a new prediction equation for MIDR considering near-fault ground motions where higher standard deviations (0.5 to 0.6) were obtained.

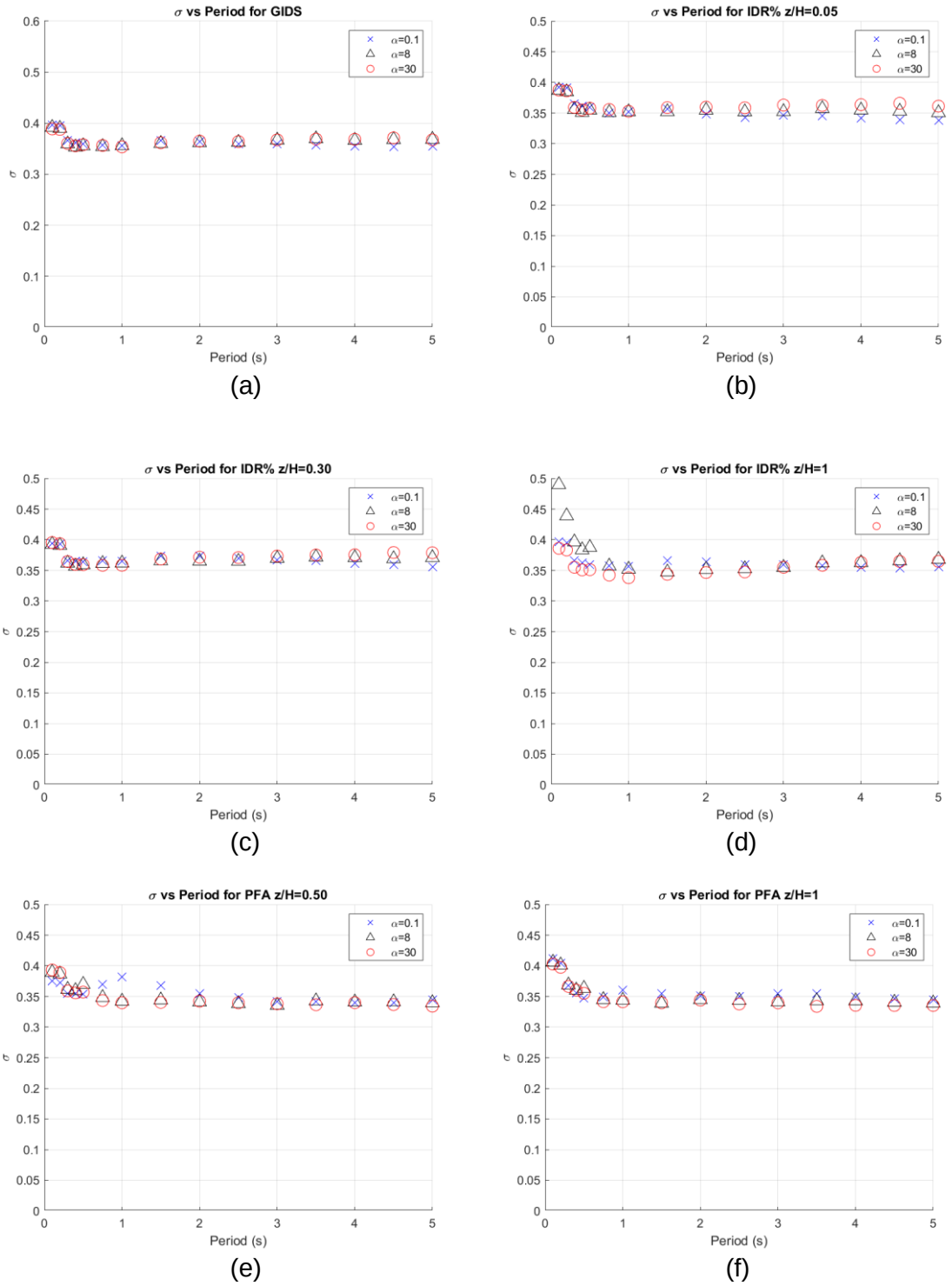

Figure 5.8 Standard deviations of $\log_{10}Y$ (IDRmax, IDR(x) and PFA(x)) at different periods (a) GIDS (b) IDR(x=0.05) (c) IDR(x=0.30) (d) IDR(x=1) (e) PFA (x=0.5) (f) PFA (x=1)

The stochastic error from the model is represented by residual values which indicate the difference between the observed and predicted values. In order to assess the appropriateness of the model, residual values are plotted versus independent variables.

Figure 5.9 and Figure 5.10 present the distribution of residual values against M_w and R_{epi} for T=0.75 s. considering (a) GIDS α=8 (b) IDR(x=1) α=8 (c) PFA(x=1) α=30. As can be observed, the scatter plot is equally and randomly spread around the horizontal axis throughout the range of fitted values. This indicates that the derived equation has produced unbiased estimates.

Additionally, a linear trend of the residual plot has been computed and the output shows that the scatter is normally distributed with a symmetrical pattern around zero. Several ground motions records have R_{epi}<50 km and it is expected that Figure 5.10 display more data on the left side. It is worth mentioning that similar results have been obtained for other fundamental periods, α and normalized height.

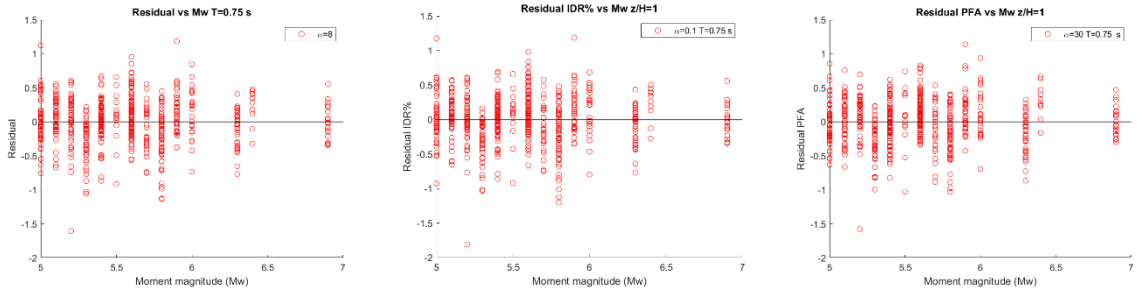

(a) (b) (c)

Figure 5.9 Residual from prediction model against M_w for T=0.75 s. (a) GIDS α=8 (b) IDR(x=1) α=0.1 (c) PFA(x=1) α=30

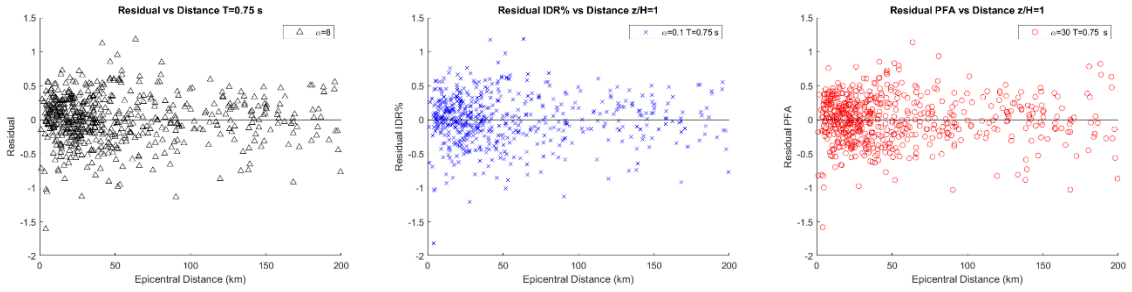

(a) (b) (c)

Figure 5.10 Residual from prediction model against R_{epi} for T=0.75 s. (a) GIDS α=8 (b) IDR(x=1) α=0.1 (c) PFA(x=1) α=30

R^2 or coefficient of determination measures the strength of the relationship between the model and the dependent variable, it represents the percentage of the variance and how good the data fit the regression model. The values fluctuate between 0 and 100% where higher values of R^2 indicate that greater variation is accounted for and the data points are

closer to the regression line. The overall R^2 is in the range of 70 to 75%, which indicates a good fit of the data.

The standard errors, the residual plots and R^2 indicate a good fit for the non-linear regression and now it is possible to evaluate the statistical output in order to estimate the reliability of the function. The coefficients explain the relationship between the independent and dependent variables; on the other hand, p-values show whether these relationships are statistically significant in a larger population.

The null hypothesis tests indicate that no correlation exists between the independent and each of the dependent variables, in other words, that the coefficients of each of the variables have no effects in the equation and are cumulatively zero (0). In case the p-value is less than the significance level, the null hypothesis is rejected and the variable is considered statistically significant and meaningful addition to the fit of the model.

However, a larger p-value indicates that there is not sufficient evidence to conclude that a correlation exists at the population level. The significance level is a measure of the strengths of the evidence that must be obtained in order to reject the null hypothesis, in this case, a value of 0.05 (5%) was taken.

Table 5.6 presents P-values for the coefficients from the regression analysis for EDP, it can be seen that all values are less than the significance level near zero, so in general, the coefficients improve the fit of the model.

Table 5.6 P-values for coefficients

Coefficients	IDR	PFA	MIDR
b_1	1.31E-95	1.10E-27	1.71E-102
b_2	3.10E-87	1.17E-70	1.91E-97
b_3	2.07E-54	2.84E-77	6.29E-50
b_4	8.35E-07	1.72E-10	4.08E-06
b_5	7.85E-20	3.65E-21	2.13E-20
b_6	1.82E-14	4.69E-14	5.36E-14

5.3.3 Determination of coefficients

The regression coefficients, standard deviation and R^2 corresponding to the main response of MIDR, IDR(x) and PFA(x) for α=0.1,8,30 are presented in section A2 to A4 of the Appendix.

5.3.4 Comparison between Historical earthquake data and New Performance Prediction equation

A comparison is performed between the new performance prediction equations characterized by different lateral resisting systems and the building response parameters subjected to historical earthquake data for different soil types. The analysis is evaluated for

a fundamental period of 0.75 s where the higher response has been found. In order to validate the equation, the following seismic events with relevant data are selected:

- Friuli Third Shock 1976 M_w=5.9 Stiff Soil
- Irpinia 1980 M_w=6.9 Stiff Soil
- Umbria-Marche Second Shock 1997 M_w=6.0 Soft Soil
- L'Aquila 2009 M_w=6.3 Rock Soil

Figure 5.11 presents the comparison for MIDR, Figure 5.12 shows the variation for IDR(x) for different heights where the maximum drift happens and Figure 5.13 displays the trend for PFA (x) for the roof where the acceleration is higher.

The building response is well captured for data with an epicentral distance greater than 10 km; however, due to the lack of data, it is complicated to be reproduced with accuracy, a seismic event with small epicentral distance. Moreover, the error given by prediction equations and building responses for historical data identified with the same soil type is minimum. On the other hand, historical data identified with different soil type follows the prediction equation trend and often fall within the mean ± σ zone.

The prediction equation trend happens as expected, the building response decreases as the distance increases. In general terms, the comparison suggests that the predictive model captures with reliability the building response of historical data with different soil conditions

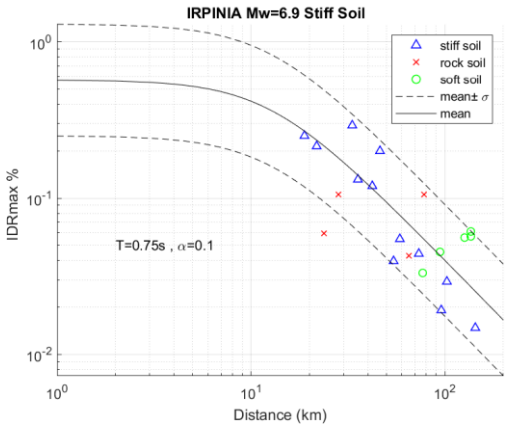

(a)

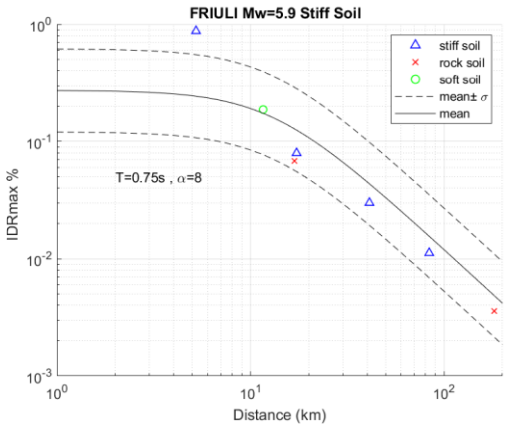

(b)

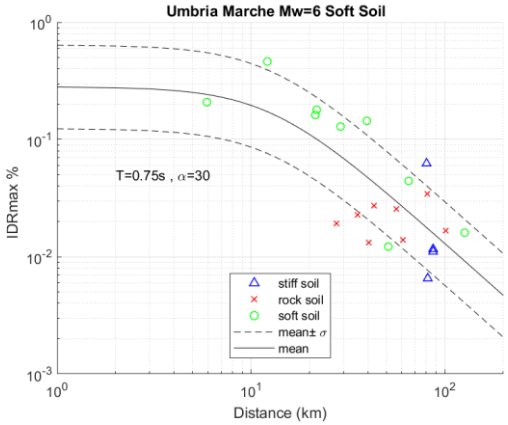

(c)

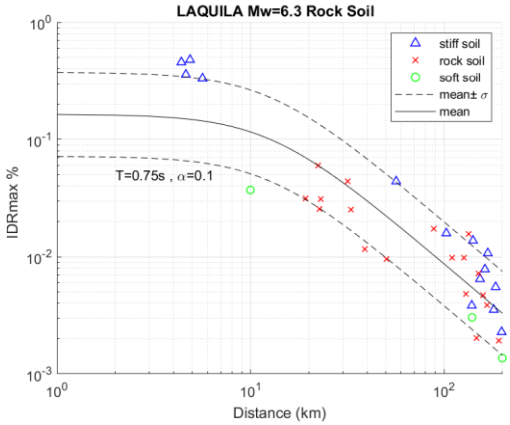

(d)

Figure 5.11 Performance prediction equation for GIDS with T=0.75 s. (a) Irpinia Mw=6.9 α=0.1 (b) Friuli Mw=5.9 α=8 (c) Umbria Marche Mw=6.0 α=30 (d) L'Aquila Mw=6.3 α=0.1

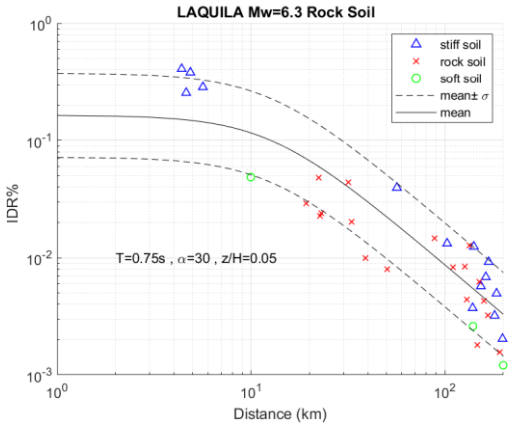

(a)

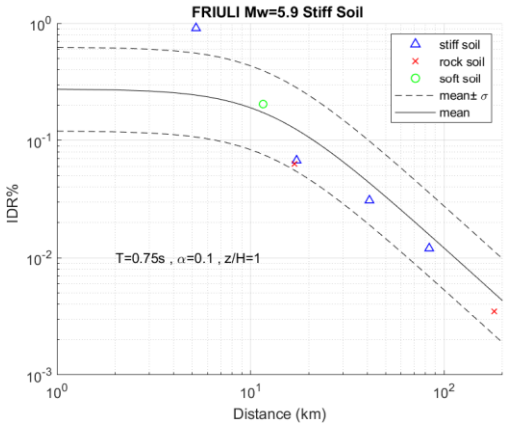

(b)

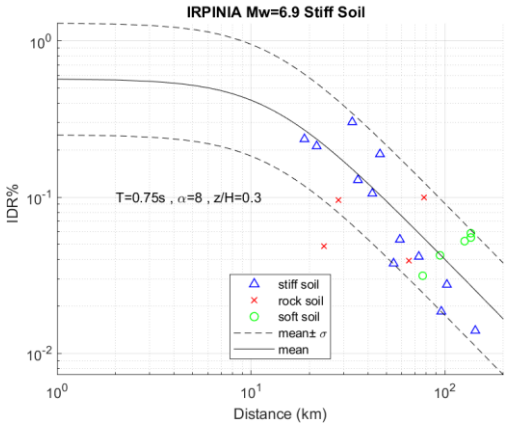

(c)

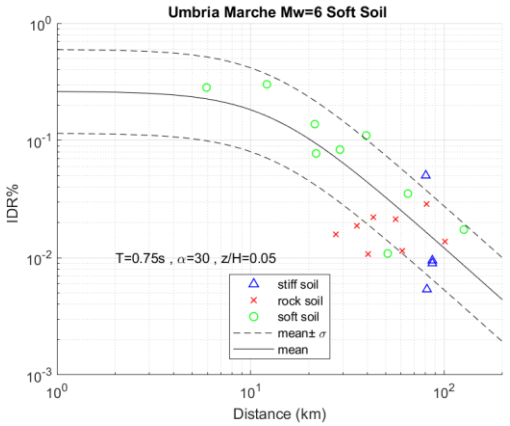

(d)

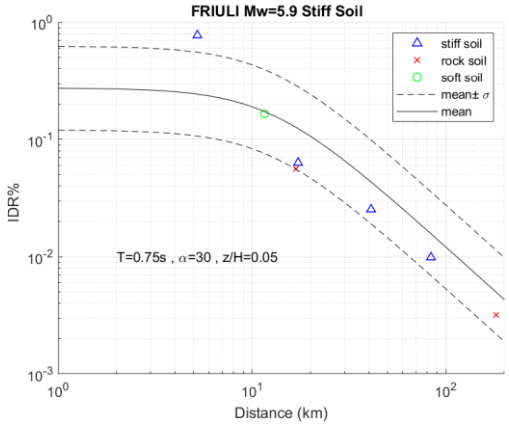

(e)

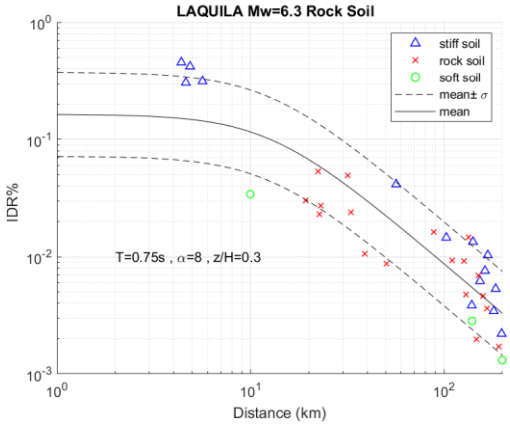

(f)

Figure 5.12 Performance prediction equation for IDR(x) with T=0.75 s. (a) L'Aquila Mw=6.3 α=30 z/H=0.05 (b) Friuli Mw=5.9 α=0.1 z/H=1 (c) Irpinia Mw=6.9 α=8 z/H=0.30 (d) Umbria Marche Mw=6.0 α=30 z/H=0.05 (e) Friuli Mw=5.9 α=30 z/H=0.05 (f) L'Aquila Mw=6.3 α=8 z/H=0.30

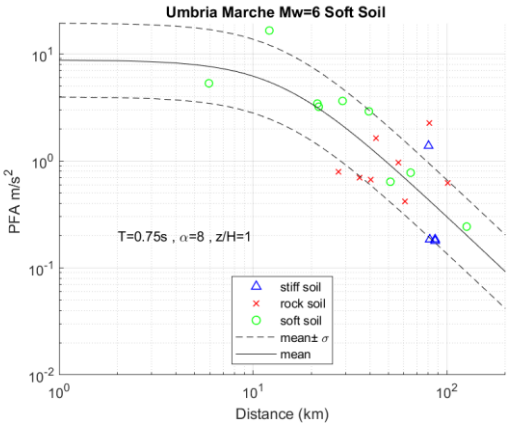

(a)

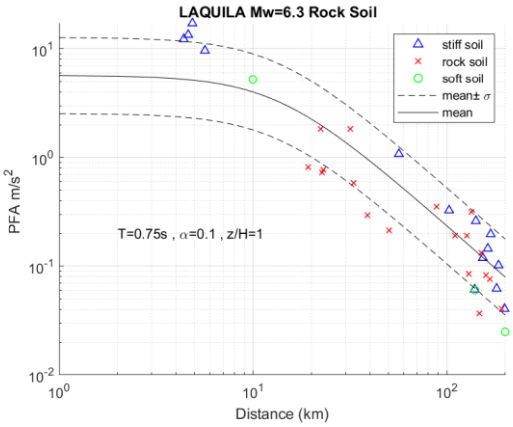

(b)

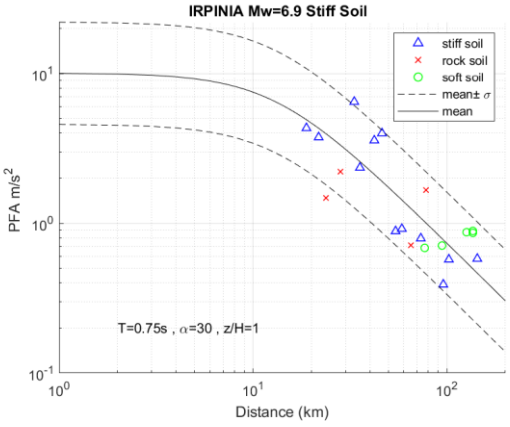

(c)

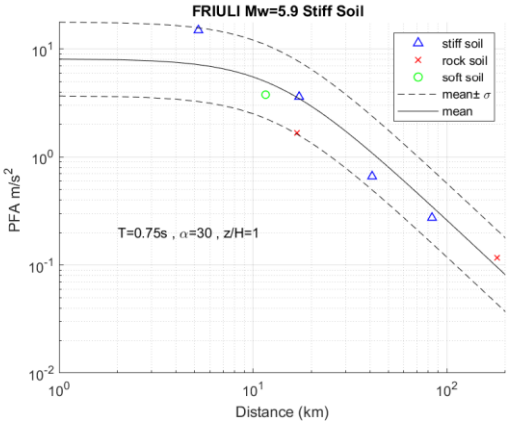

(d)

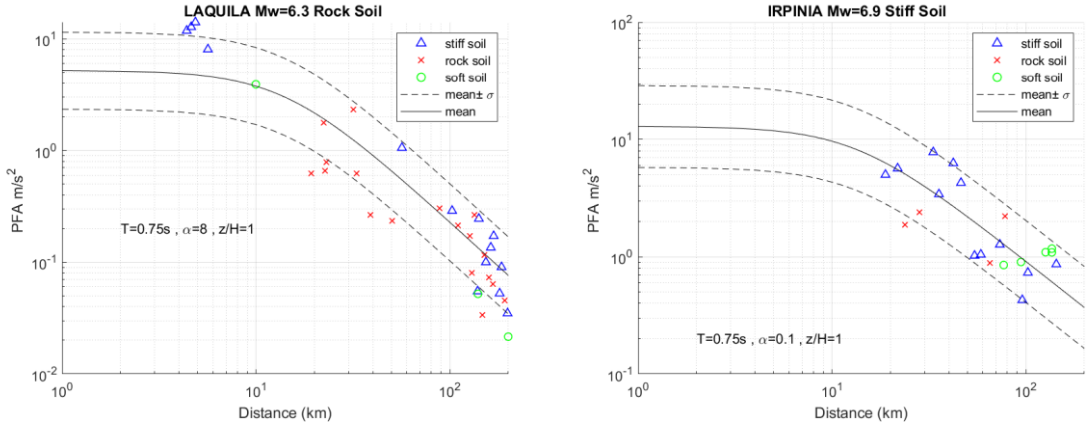

Figure 5.13 Performance prediction equation for PFA(x) with T=0.75 s. (a) Umbria Marche Mw=6.0 α=8.0 z/H=1.0 (b) L'Aquila Mw=6.3 α=0.1 z/H=1.0 (c) Irpinia Mw=6.9 α=30 z/H=1.0 (d) Friuli Mw=5.9 α=30 z/H=1.0 (e) L'Aquila Mw=6.3 α=8.0 z/H=1.0 (f) Irpinia Mw=6.9 α=0.1 z/H=1.0

5.3.4 Comparison with more complex models

A common error is to develop a model too complex to fit a particular set of data points or for a particular application. Sometimes, the size of the sample limits the number of variables that can be added to ensure reliable results. Overfitting can cause a misleading R^2 and regression coefficients; as a result, the model is improbable to describe the relationship between variables for a whole population.

For that reason, two more complex functional forms are investigated and statistical parameters are compared with the previous model. Bommer (2003) is presented in eq. 4-3 and includes the fault mechanism type, on the other hand, Akkar and Bommer (2010) have been shown in eq. 4-4 and neglects the effect of M and R_{epi} coupling terms.

$$log_{10}Y = b_1 + b_2 \cdot M + b_3 log_{10}\sqrt{{R_{epi}}^2 + {b_4}^2} + b_5 F_N + b_6 F_R + b_7 S_s + b_8 S_A + \varepsilon\sigma \quad \text{(Eq.4-3)}$$

$$log_{10}Y = b_1 + b_2 \cdot M + b_3 \cdot M^2 + (b_4 + b_5 \cdot M) log_{10}\sqrt{{R_{epi}}^2 + {b_6}^2} + b_7 \cdot F_N + b_8 \cdot F_R + b_9 \cdot S_s + b_{10} \cdot S_A + \varepsilon \cdot \sigma \quad \text{(Eq.4-4)}$$

The main statistical parameters σ and R^2 are presented in table 5.16 and Table 5.17, respectively. The two complex models have more variables to analyse, it is expected that the standard deviation and R^2 present higher values; however, the difference between them is less than 3% which indicates that the models are reliable.

Furthermore, Table 5.18 displays the p-values obtained for both complex models, the p-value for fault mechanism type (coefficient b_8) indicates a low contribution to the model and a high possibility that multicollinearity has been occurring. The results suggest that an overfitting problem has been taking place as well. In order to improve the p-values presented

for the new equation model, more historical data that include different fault type mechanism is needed.

To sum up, the new performance prediction equation presents reliable statistical parameters and predicts with accuracy the response of historical data. The analysis for the three prediction models was performed for historical seismic events where the highest response occurred for MIDR, IDR(x) and PFA(x) and it is presented in Figure 5.14. Akkar and Bommer (2003) overestimated the response and some historical data falls outside the mean ± σ zone. The building response is better captured specially for the prediction equation of Bindi (2009).

Table 5.16 R^2 for IDR(x)=1 and PFA(x)=1

	IDR(x)=1		PFA(x)=1	
T(s)	(2003)	(2009)	(2003)	(2009)
0.10	0.7356	0.7264	0.7325	0.7233
0.20	0.7185	0.7076	0.7183	0.7078
0.30	0.7332	0.7200	0.7352	0.7229
0.40	0.7303	0.7171	0.7317	0.7199
0.50	0.7201	0.7071	0.7295	0.7181
0.75	0.7285	0.7173	0.7395	0.7288
1.00	0.7301	0.719	0.7391	0.7274
1.50	0.7149	0.7075	0.7326	0.7246
2.00	0.7125	0.7029	0.7286	0.7197
2.50	0.7079	0.696	0.7335	0.7238
3.00	0.6936	0.6822	0.7305	0.7217
3.50	0.6922	0.6808	0.7351	0.727
4.00	0.6874	0.6749	0.7382	0.7298
4.50	0.6854	0.6734	0.7389	0.7301
5.00	0.6839	0.6720	0.7397	0.7303

Table 5.17 σ for IDR(x)=1 and PFA(x)=1

	IDR(x)=1		PFA(x)=1	
T(s)	(2003)	(2009)	(2003)	(2009)
0.10	0.3913	0.3973	0.4078	0.4141
0.20	0.3871	0.3938	0.4009	0.4076
0.30	0.3582	0.3663	0.3692	0.3771
0.40	0.3541	0.3620	0.3638	0.3711
0.50	0.3544	0.3619	0.3581	0.3650
0.75	0.3457	0.3522	0.3455	0.3519
1.00	0.3403	0.3467	0.3438	0.3509
1.50	0.3474	0.3513	0.3439	0.3483
2.00	0.3507	0.3559	0.3482	0.3532

2.50	0.3498	0.3562	0.3405	0.3461
3.00	0.3576	0.3635	0.3428	0.3478
3.50	0.3611	0.3671	0.3381	0.3427
4.00	0.3647	0.3713	0.3389	0.3437
4.50	0.3666	0.3729	0.3395	0.3445
5.00	0.3669	0.3731	0.3396	0.3452

Table 5.18 P-values for MIDR, IDR(X) and PFA(x)

	GIDS		IDR(x)		PFA(x)	
Coefficients	(2003)	(2009)	(2003)	(2009)	(2003)	(2009)
b_1	3.35E-98	1.71E-102	2.70E-92	1.31E-95	3.30E-26	1.10E-27
b_2	6.10E-99	1.91E-97	1.47E-90	3.10E-87	4.79E-74	1.17E-70
b_3	2.02E-50	6.29E-50	5.09E-56	2.07E-54	2.31E-78	2.84E-77
b_4	2.52E-06	4.08E-06	2.98E-07	8.35E-07	4.38E-11	1.72E-10
b_5	0.05	2.13E-20	0.02	7.85E-20	0.04	3.65E-21
b_6	0.96	5.36E-14	0.82	1.82E-14	0.65	4.69E-14
b_7	3.60E-21	-	5.87E-21	-	2.59E-22	-
b_8	1.12E-13	-	3.47E-14	-	8.78E-14	-

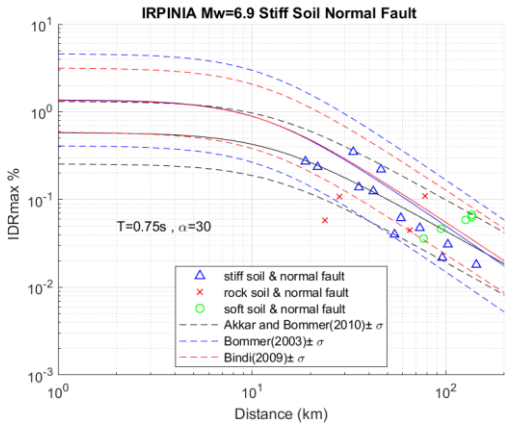

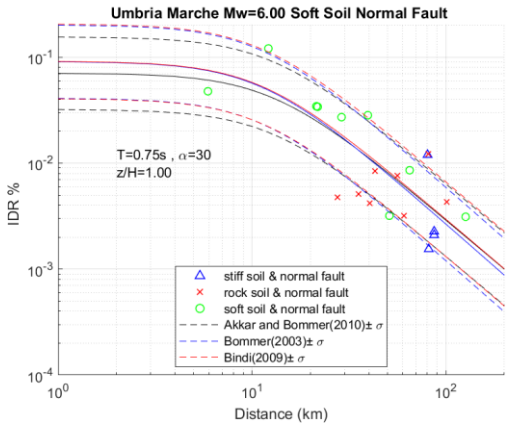

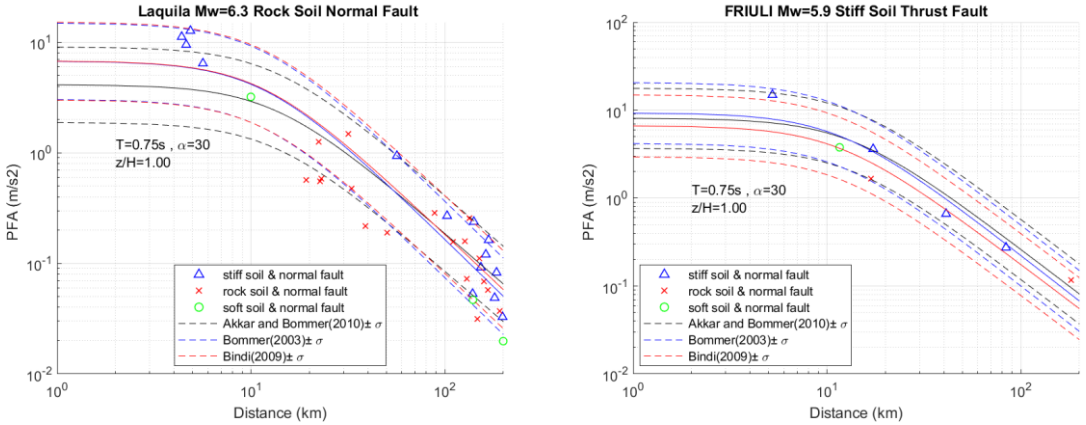

Figure 5.14 Comparison between simplified equation model for α=30, z/H=1, T=0.75 s. (a) Irpinia Mw=6.9 (b) Umbria Marche Mw=6.0 (c) L'Aquila Mw=6.3 (d) Friuli Mw=5.9

6. Performance Assessment of the EEWS Application to Campania

6.1. Problem Formulation

The Performance-based Earthquake Early Warning framework, displayed in Figure 2.1, presents the ground motion prediction equation and the structural model to describe two separate stages comprising the hazard and structural analysis. As a result, a new performance prediction equation that merges these two stages and connects the corresponding seismic features with the building structural characteristics were formulated in the previous chapter.

For decision making and seismic risk management purposes, a representative measure of the earthquake potential has to be obtained. At a given time *t,* real-time information of magnitude (Mw) and distance (R) is predicted by EEWS, and the probability that a ground motion intensity measure (e.g. PGA), can be exceeded is calculated via a Real-time Probabilistic Seismic Hazard Analysis (RTPSHA).

The prediction process is based on a Bayesian framework in which the posterior probabilistic density function $f(m|\tau_1, \tau_2, \ldots, \tau_n)$ represent the magnitude calculated at a given time by the triggering sequence of a developing earthquake in a seismic network via the Bayes theorem. The Gutenberg-Richter recurrence relationship incorporates data from past earthquakes where the seismic features of the Campania region are described by {β=1.69, M_{min}=4, M_{max}=7}.

The seismic stations provide a vector (τ) with information of the predominant period from the first four seconds of P-waves records which are analysed on the frequency domain and the maximum amplitude of the record that is extracted with the associated frequency. (Convertito et. al, 2008).

In this application, the magnitude is a predetermined parameter, so the posterior PDF was obtained with an inverse procedure and the vector τ have been generated by a Monte Carlo approach using the function elaborated by Allen and Kanamori (2003), presented in equation 6-1. However these parameters were computed for California, and further research is recommended to adapt or test the validity of this approach to Italy.

$$\mu_{\log(\tau)} = \frac{(M-5.9)}{7\log e};\ \sigma_{\log(\tau)} = \frac{0.16}{\log e} \qquad \text{(Eq. 6-1)}$$

The posterior PDF is presented in equation 6-2 It can be observed that it is time-dependent and the quantity of data processed will increase with time as the earthquake triggers more seismic stations. Figure 6.1(b) shows the real-time PDF for M and how the prediction becomes stable on the magnitude simulated (Mw=6).

$$f(m|\tau_1,\tau_2,\ldots,\tau_n)=\frac{e^{(2\mu_{\ln(\tau)}\cdot(\sum_{i=1}^{n}\ln(\tau_i)-n\mu_{\ln(\tau)^2}))/2\sigma_{\ln(\tau)}}e^{-\beta m}}{\int_{M_{min}}^{M_{max}}e^{(2\mu_{\ln(\tau)}\cdot(\sum_{i=1}^{n}\ln(\tau_i)-n\mu_{\ln(\tau)^2}))/2\sigma_{\ln(\tau)}}e^{-\beta m}dm}$$ (Eq. 6-2)

Likewise, the PDF of source-to-site distance is calculated at a given time by the triggering sequence of a developing earthquake given by a vector $\{S_1, S_{2,..,} S_n\}$. The RTLoc algorithm developed by Satriano (2008) is normally used for the real-time localisation of the hypocentre, this approach creates a dense grid point located inside the region where the network works. In order to obtain the probability that the hypocentre match that grid point, a volume that is likely to contain the hypocentre is calculated known as the Voronoi cell of that station. In this case, the PDF for the source-to-site distance was considered a deterministic parameter, because the analysis was performed for a target site with a known epicentre.

Iervolino et al. (2009) investigated the uncertainty of the parameters used in a real-time hazard analysis and concluded that the dominating variability was associated with the ground motion prediction equations The new performance prediction equations have shown similar levels of variability, and it is expected that the simplified process of obtaining EDPS directly can reduce the overall uncertainty of EEWS for buildings. A new real-time hazard analysis has been computed in terms of the building response in the hybrid EEWS for the Campania region using equation 6-3.

$$f_n(im)=\iint_{M\,R} f(edp|m,r)f(m|\tau_1,\tau_2,\ldots,\tau_n)f(r|\,s_1,s_2,\ldots,s_n)drdm$$ (Eq. 6-3)

6.2. EEWS design for Campania

In this chapter, a simulation of the development of an EEWS on the Campania region was carried out and real-time hazard curves in terms of building response are derived. The classical approach of setting alarms using the PGA as the warning threshold was compared with different performance parameters or EDPs such as Peak Floor Acceleration (PFA) and Maximum Interstorey Drift (MIDR).

Given that the simulation is focused on mid-rise to high-rise buildings, the analysis has been carried out for the two biggest urban areas in Campania: Naples, the capital, and Salerno. Saint Angelo De Lombardi, a small town affected by the Irpinia earthquake, was also considered for comparison reasons even though only small buildings are expected to be located in the town as shown in Table 6.1. Figure 6.1 (a) presents the target sites, the epicentre location and the geographical distribution of 29 seismic stations from the ISNet network.

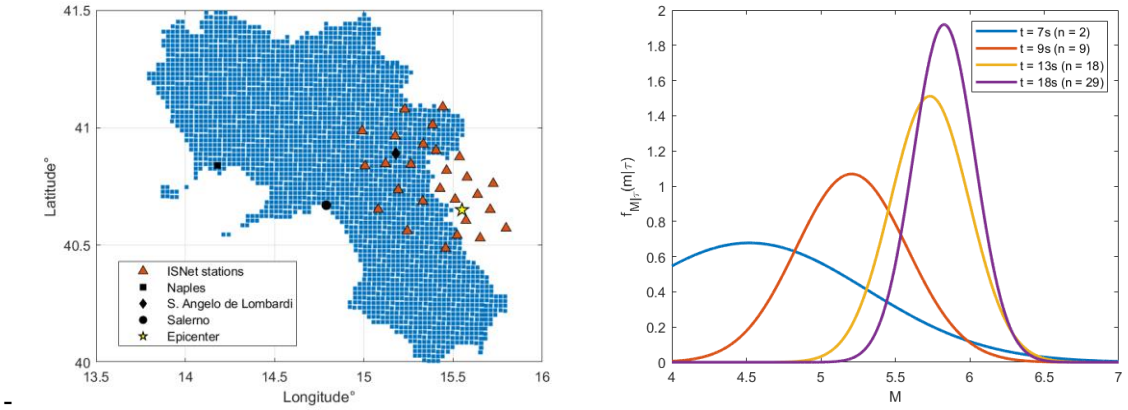

(a) (b)

Figure 6.1 (a) Map of the campania region with the ISNet network, three target sites and the epicentre (b) Real-time probabilistic density function of Mw=6

Table 6.1 Building characteristics for the analysed cities

City	Population	Expected building height	Fundamental Periods for analysis
Naples	3,084,890	Up to 129m	T= 0.3, 0.75 and 1.5s
Salerno	1,098,513	Up to 55m	T= 0.3 and 0.75
Saint Angelo De Lombardi	4,203	Up to 10m	T= 0.3

In order to obtain the RTPSHA, the analysis was performed using a Matlab script provided by the supervisor of this investigation, Dr Carmine Galasso. Three seismic events were simulated with an M_w= 6, 6.5 and 7 in order to evaluate the warning performance for a strong shaking. The seismic event follows this triggering sequence after 4 seconds of the seismic motion have been recorded: 2 stations (t=7 s), 9 stations (t=9 s), 18 stations (t=13 s), 29 stations (t=18 s).

The simulation evaluates three different warning scenarios by comparing real-time EEWS performance by using alarming rules based on the PGA and EDPs for elevator failure, non-structural damage and human comfort during the shaking as follows:

1: Elevator failure

Failure is understood as the potential trapping of occupants during an earthquake or the malfunctioning of the system and slow restoration afterwards. These risks can be mitigated by implementing an automated early warning system that provides enough time to stop or shut down an elevator depending on the available warning time.

For instance, 50% of the Otis elevators in Japan are equipped with earthquake detectors so passengers can exit safely. During the Tohoku-Oki earthquake, several elevators performed an emergency shutdown (Layne,2011).

A threshold of 0.08g has been selected for the warning based on the Japanese Regulation (Cheng, 2014), and the differences in the EEWS outcome was evaluated with two parameters: PGA and PFA.

In this case, the warning will be twofold: an automated system to stop the elevator in the nearest floor so passengers can exit; and a warning message to the occupants of the elevator saying: “An earthquake is expected to arrive in x seconds, the elevator will stop at the nearest floor”.

2: Non-structural components collapse hazard

Non-structural components can pose a threat on the occupants if the seismic shaking is strong, therefore, an early warning to shelter or go to a safety zone is proposed.

These components are classified in drift-sensitive components which are affected by building displacement with a corresponding MIDR threshold of 0.4%; also, acceleration-sensitive components which are affected by building shaking with a corresponding PFA threshold of 0.25g. Both thresholds were selected based on the start of the damage as the “slight level” based on Table 6.4 of Hazus-MH 2.1. A similar MIDR threshold of 0.5% was selected by Picozzi (2012) for damage of structural and non-structural elements within a building.

In this case, the warning will be a message to the occupants of the building saying: “An earthquake is expected to arrive in x seconds, stay away from windows and look for a safe area on your floor”.

3: The occupants’ comfort during an earthquake.

Several studies have demonstrated a relationship between peak accelerations and human comfort (Griffis, 1993). Therefore, a strong shaking can cause an important level of distress and fear even though the structural integrity of the building is not compromised.

A threshold of 0.05g has been selected for a “very annoying” comfort level (Cheng, 2014), a comparison was performed in terms of PGA and PFA regarding the outcomes of the EEWS.

In this case, the warning will be a message to the occupants of the building saying: “An earthquake is expected to arrive in x seconds, the structure of the building is safe so please remain calm”.

Having established the alarming thresholds as EDP critical values “EDPc”, the alarming decisional rule, using the RTPSHA, will be to alarm if the probability of exceedance of EDPc, is higher than a critical probability threshold, Prc.

$$Pr[EDP > EDP_c] \geq Pr_c \qquad \text{(Eq. 6-3)}$$

These thresholds should be set in order to prevent a significative number of false alarms and missed alarms(Iervolino et.al., 2011; Grasso et.al., 2007) which can not be reduced

together. Therefore, the alarm setting needs to take into account the trade-off between the benefits of a correct decision and the costs of a wrong decision. The probability of false and missed alarms are defined as follows (Grasso et.al., 2007):

Pma = probability of missed alarm, that is, the probability of having critical threshold exceedance but no alarm activation.

Pfa = probability of false alarm, that is, the probability of having no threshold exceedance but alarm activation.

This issue become of importance when the consequence of implementing a warning is costly, for instance when the alarming decision can trigger the shutdown of critical infrastructures such as nuclear plants, energy generators or high-speed railways.

However, in the proposed cases of setting early warnings in buildings, the cost of a false alarm is considered not significant in comparison to a missed alarm. For instance, the cost of stopping the elevator during a harmless earthquake (false alarm) is not a big concern; but to be trapped in an elevator during a seismic event (missed alarm) produces considerable damages. Therefore, the alarming decision was set prioritizing the minimisation of missed alarms.

Iervolino et.al. (2006) recommends to set a low Prc in order to reduce the probability of missed alarms, therefore, a 10% probability of exceedance was selected for the three cases considered in this simulation. A more refined threshold can be estimated based on a cost-benefit analysis (including expected loss and expected utility) as done in Iervolino et.al (2007). This potential improvement is an area of further research.

The real-time hazard curves in terms of PGA and building response EDPs for the three earthquake scenarios are presented in section A.13 to A.16.

6.3. Simulation Results

In this section, the outcomes of the EEWS application will be compared. In order to evaluate the performance of the PGA as a warning indicator, the following terms are defined:

- A correct alarm will happen if both the PGA and the evaluated EDP activates the warning alarm together.
- An incorrect alarm by underestimation will happen if the PGA does not activate the alarm while the EDP does it.
- An incorrect alarm by overestimation will happen if the PGA activates the alarm while the EDP does not.

For each earthquake event (Mw=6, 6.5 and 7), 15 EEW simulations have been done in order to assess the variability in building typologies (7 for Naples, 5 for Salerno and 3 for Saint Angelo). These simulations were used to assess the triggering of early warnings for human comfort, elevator failure and non-structural damage (by using two EDPs). Therefore, in the following paragraphs 180 cases are evaluated (60 for each Mw event).

The simulation results for an Mw=6 earthquake are shown in Table 6.2. Green cells show that the warning has not been triggered by the respective PGA or EDP indicator, while red cells show an alarming trigger. It can be seen that 15 out of 60 cases have triggered the warning alarm. For human comfort and non-structural damage by MIDR, the PGA has predicted correctly in every case. However, for the elevator failure case, 3 out of 12 cases (25%) were underestimated by the PGA, this means, the alarm was not triggered even though it should have been triggered by using the predicted PFA. In a similar manner, for the non-structural damage by PFA, 1 out of 12 cases (8%) was underestimated by using the PGA as an early warning indicator.

To sum up, from the 48 cases predicted by using EDPs, the PGA was able to activate the warning correctly in 44 cases (92%) but failed in the other 4 (8%).

Table 6.2 Simulation Results for Mw=6

	Mw=6										
	Human Comfort										
Target	**PGAc = 0.05g**	**PFAc = 0.05g**						**PGA alarming performance**			
		T=0.3		**T=0.75**		**T=1.5**		**Correct**	**Incorrect**		**Error %**
		α=0.1	**α=30**	**α=0.1**	**α=30**	**α=0.1**	**α=30**		**Under**	**Over**	
Naples	*No alarm*	*No alarm*	*No alarm*	*No alarm*	*No alarm*	*No alarm*	*No alarm*	6	0	0	0%
Salerno	*Alarm*	*Alarm*	*Alarm*	*Alarm*	*Alarm*	*x*	*x*	4	0	0	0%
St. Ang.	*Alarm*	*Alarm*	*Alarm*	*x*	*x*	*x*	*x*	2	0	0	0%
							Subtotal	**12**	**0**	**0**	**0%**
	Elevator Failure										
Target	**PGAc = 0.08g**	**PFAc = 0.08g**						**PGA alarming performance**			
		T=0.3		**T=0.75**		**T=1.5**		**Correct**	**Incorrect**		**Error %**
		α=0.1	**α=30**	**α=0.1**	**α=30**	**α=0.1**	**α=30**		**Under**	**Over**	
Naples	*No alarm*	*No alarm*	*No alarm*	*No alarm*	*No alarm*	*No alarm*	*No alarm*	6	0	0	0%
Salerno	*No alarm*	*Alarm*	*Alarm*	*Alarm*	*No alarm*	*x*	*x*	1	3	0	75%
St. Ang.	*Alarm*	*Alarm*	*Alarm*	*x*	*x*	*x*	*x*	2	0	0	0%
							Subtotal	**9**	**3**	**0**	**25%**
	Nonstructural damage by PFA										
Target	**PGAc = 0.25g**	**PFAc = 0.25g**						**PGA alarming performance**			
		T=0.3		**T=0.75**		**T=1.5**		**Correct**	**Incorrect**		**Error %**
		α=0.1	**α=30**	**α=0.1**	**α=30**	**α=0.1**	**α=30**		**Under**	**Over**	
Naples	*No alarm*	*No alarm*	*No alarm*	*No alarm*	*No alarm*	*No alarm*	*No alarm*	6	0	0	0%
Salerno	*No alarm*	*No alarm*	*No alarm*	*No alarm*	*No alarm*	*x*	*x*	4	0	0	0%
St. Ang.	*No alarm*	*Alarm*	*No alarm*	*x*	*x*	*x*	*x*	1	1	0	50%

							Subtotal	11	1	0	8%
	Nonstructural damage by MIDR										
Target	PGAc = 0.25g	MIDRc = 0.4%						PGA alarming performance			
		T=0.3		T=0.75		T=1.5		Correct	Incorrect		Error %
		α=0.1	α=30	α=0.1	α=30	α=0.1	α=30		Under	Over	
Naples	No alarm	No alarm	No alarm	No alarm	No alarm	No alarm	No alarm	6	0	0	0%
Salerno	No alarm	No alarm	No alarm	No alarm	No alarm	x	x	4	0	0	0%
St. Angelo	No alarm	No alarm	No alarm	x	x	x	x	2	0	0	0%
							Subtotal	12	0	0	0%
							Total	44	4	0	8%

The simulation results for an Mw=6.5 earthquake are shown in Table 6.3. It can be seen that 22 out of 60 cases have triggered the warning alarm. For the elevator failure and non-structural damage by MIDR, the PGA has predicted the warning correctly in every case. However, for human comfort, 4 out of 12 cases (33%) were underestimated by the PGA, this means, the alarm was not triggered even though it should have been triggered according to the predicted PFA. In a similar manner, for the non-structural damage by PFA, 2 out of 12 cases (17%) were underestimated by using the PGA as an early warning indicator.

To sum up, from the 48 cases predicted by using EDPs, the PGA was able to activate the warning correctly in 42 cases (87%) but failed in the other 6 (13%).

Table 6.3 Simulation Results for Mw=6.5

	Mw=6.5										
	Human Comfort										
Target	PGAc = 0.05g	PFAc = 0.05g						PGA alarming performance			
		T=0.3		T=0.75		T=1.5		Correct	Incorrect		Error %
		α=0.1	α=30	α=0.1	α=30	α=0.1	α=30		Under	Over	
Naples	No alarm	Alarm	Alarm	Alarm	No alarm	Alarm	No alarm	2	4	0	67%
Salerno	Alarm	Alarm	Alarm	Alarm	Alarm	x	x	4	0	0	0%
St. Angelo	Alarm	Alarm	Alarm	x	x	x	x	2	0	0	0%
							Subtotal	8	4	0	33%
	Elevator Failure										
Target	PGAc = 0.08g	PFAc = 0.08g						PGA alarming performance			
		T=0.3		T=0.75		T=1.5		Correct	Incorrect		Error %
		α=0.1	α=30	α=0.1	α=30	α=0.1	α=30		Under	Over	

Naples	*No alarm*	*No alarm*	*No alarm*	*No alarm*	*No alarm*	*No alarm*	*No alarm*	6	0	0	0%
Salerno	*Alarm*	*Alarm*	*Alarm*	*Alarm*	*Alarm*	*x*	*x*	4	0	0	0%
St. Angelo	*Alarm*	*Alarm*	*Alarm*	*x*	*x*	*x*	*x*	2	0	0	0%
						Subtotal		**12**	**0**	**0**	**0%**
	Nonstructural damage by PFA										
Target	**PGAc = 0.25g**	**PFAc = 0.25g**						**PGA alarming performance**			
		T=0.3		**T=0.75**		**T=1.5**		**Correct**	**Incorrect**		**Error %**
		α=0.1	**α=30**	**α=0.1**	**α=30**	**α=0.1**	**α=30**		**Under**	**Over**	
Naples	*No alarm*	*No alarm*	*No alarm*	*No alarm*	*No alarm*	*No alarm*	*No alarm*	6	0	0	0%
Salerno	*No alarm*	*No alarm*	*No alarm*	*No alarm*	*No alarm*	*x*	*x*	4	0	0	0%
St. Angelo	*No alarm*	*Alarm*	*Alarm*	*x*	*x*	*x*	*x*	0	2	0	100%
						Subtotal		**10**	**2**	**0**	**17%**
	Nonstructural damage by MIDR										
Target	**PGAc = 0.25g**	**MIDRc = 0.4%**						**PGA alarming performance**			
		T=0.3		**T=0.75**		**T=1.5**		**Correct**	**Incorrect**		**Error %**
		α=0.1	**α=30**	**α=0.1**	**α=30**	**α=0.1**	**α=30**		**Under**	**Over**	
Naples	*No alarm*	*No alarm*	*No alarm*	*No alarm*	*No alarm*	*No alarm*	*No alarm*	6	0	0	0%
Salerno	*No alarm*	*No alarm*	*No alarm*	*No alarm*	*No alarm*	*x*	*x*	4	0	0	0%
St. Angelo	*No alarm*	*No alarm*	*No alarm*	*x*	*x*	*x*	*x*	2	0	0	0%
						Subtotal		**12**	**0**	**0**	**0%**
						Total		**42**	**6**	**0**	**13%**

The simulation results for an Mw=7 earthquake are shown in Table 6.4. It can be seen that 36 out of 60 cases have triggered the warning alarm. For human comfort, the PGA has alarmed correctly in every case. However, for the elevator failure case, 6 out of 12 cases (50%) were underestimated by the PGA. It is important to note that all of the incorrect alarms were located in Naples where the PGA was low enough to not trigger an alarm, even though the buildings were receiving a strong shaking. In the non-structural damage cases, 6 out of 12 (50%) and 1 out of 12 cases (8%) were underestimated by the PGA instead of PFA and MIDR, respectively.

To sum up, from the 48 cases predicted by using EDPs, the PGA was able to activate the warning correctly in 35 cases (73%) but failed in the other 13 (27%).

Table 6.4 Simulation Results for Mw=7

	Mw=7										
	Human Comfort										
Target	**PGAc = 0.05g**	**PFAc = 0.05g**						**PGA alarming performance**			
		T=0.3		**T=0.75**		**T=1.5**		**Correct**	**Incorrect**		**Error %**
		α=0.1	**α=30**	**α=0.1**	**α=30**	**α=0.1**	**α=30**		**Under**	**Over**	
Naples	*Alarm*	*Alarm*	*Alarm*	*Alarm*	*Alarm*	*Alarm*	*Alarm*	6	0	0	0%
Salerno	*Alarm*	*Alarm*	*Alarm*	*Alarm*	*Alarm*	*x*	*x*	4	0	0	0%
St. Angelo	*Alarm*	*Alarm*	*Alarm*	*x*	*x*	*x*	*x*	2	0	0	0%
							Subtotal	**12**	**0**	**0**	**0%**
	Elevator Failure										
Target	**PGAc = 0.08g**	**PFAc = 0.08g**						**PGA alarming performance**			
		T=0.3		**T=0.75**		**T=1.5**		**Correct**	**Incorrect**		**Error %**
		α=0.1	**α=30**	**α=0.1**	**α=30**	**α=0.1**	**α=30**		**Under**	**Over**	
Naples	*No alarm*	*Alarm*	*Alarm*	*Alarm*	*Alarm*	*Alarm*	*Alarm*	0	6	0	100%
Salerno	*Alarm*	*Alarm*	*Alarm*	*Alarm*	*Alarm*	*x*	*x*	4	0	0	0%
St. Angelo	*Alarm*	*Alarm*	*Alarm*	*x*	*x*	*x*	*x*	2	0	0	0%
							Subtotal	**6**	**6**	**0**	**50%**
	Nonstructural damage by PFA										
Target	**PGAc = 0.25g**	**PFAc = 0.25g**						**PGA alarming performance**			
		T=0.3		**T=0.75**		**T=1.5**		**Correct**	**Incorrect**		**Error %**
		α=0.1	**α=30**	**α=0.1**	**α=30**	**α=0.1**	**α=30**		**Under**	**Over**	
Naples	*No alarm*	*No alarm*	*No alarm*	*No alarm*	*No alarm*	*No alarm*	*No alarm*	6	0	0	0%
Salerno	*No alarm*	*Alarm*	*Alarm*	*Alarm*	*Alarm*	*x*	*x*	0	4	0	100%
St. Angelo	*No alarm*	*Alarm*	*Alarm*	*x*	*x*	*x*	*x*	0	2	0	100%
							Subtotal	**6**	**6**	**0**	**50%**
	Nonstructural damage by MIDR										
Target	**PGAc = 0.25g**	**MIDRc = 0.4%**						**PGA alarming performance**			
		T=0.3		**T=0.75**		**T=1.5**		**Correct**	**Incorrect**		**Error %**
		α=0.1	**α=30**	**α=0.1**	**α=30**	**α=0.1**	**α=30**		**Under**	**Over**	
Naples	*No alarm*	*No alarm*	*No alarm*	*No alarm*	*No alarm*	*No alarm*	*No alarm*	6	0	0	0%
Salerno	*No alarm*	*No alarm*	*No alarm*	*No alarm*	*No alarm*	*x*	*x*	4	0	0	0%
St. Angelo	*No alarm*	*No alarm*	*Alarm*	*x*	*x*	*x*	*x*	1	1	0	50%
							Subtotal	**11**	**1**	**0**	**8%**
							Total	**35**	**13**	**0**	**27%**

The cross-case analysis of the simulation results brings important insights. A logical result is that the stronger the shaking, the more warnings are triggered, with 15 out 60 (25%) for Mw=6 to 36 out 60 (60%) for MW=7. This demonstrates the overall importance of having an operational EEWS in the region of Campania, especially during strong events. Furthermore, the stronger the shaking, the more incorrect alarms by using the PGA, from 8% for an MW=6 to 27% for an Mw=7. This agrees with structural theory, because the stronger the shaking, the more complex the seismic behaviour and therefore, the building performance prediction by using PGAs is poor.

Every warning case can also be assessed across event magnitudes as follows:

- For human comfort, a low PFA threshold of 0.05g has been set. The results show that 4 out of 36 cases (11%) were incorrectly predicted by the PGA. For the strongest event (Mw=7) all the predictions were correct because both PGA and PFA thresholds were surpassed by the strong shaking.
- For elevator failure, a moderate PFA threshold of 0.08g has been set. The results show that 9 out of 36 cases (25%) were incorrectly predicted by the PGA. Most of the incorrect warnings belong to the strongest event (Mw=7).
- For non-structural damage, a high PFA threshold of 0.25g has been set. The results show that 9 out of 36 cases (25%) were incorrectly predicted by the PGA. Most of the incorrect warnings belong to the strongest event (Mw=7).
- For non-structural damage, a MIDR threshold of 0.4% has also been set. The results show that just 1 out of 36 cases (3%) were incorrectly predicted by the PGA. This case is found for the strongest shaking affecting a 4 floor RC building in Saint Angelo.

This overall comparison shows an important result: that the higher the PFA threshold, the poorer the PGA alarming decision. On the other hand, the results for the MIDR parameter does not seem conclusive due to the lack of alarms triggered (just 1 out 36).

Finally, a comparison across city targets shows:

- The distant and dense Naples presents 10 out of 72 (14%) incorrect predictions by the PGA.
- The city of Salerno present 7 out of 48 (15%) incorrect predictions by the PGA.
- The small town of Saint Angelo di Lombardi presents 6 out of 24 (25%) incorrect predictions by the PGA.

These results show that the PGA as an alarming indicator have had a poor performance in every analysed city which increases for regions located close to the epicentre.

7. Discussion and Further Research

While the estimation of M and Repi has important variability (significant for the first few stations), the GMPE has been noted as the main source of uncertainty (Iervolino,2009) for RTPSHA in EEWS. In the current effort of linking directly EDPs and seismic features on the source through performance prediction equations, this study carried the risk of increasing the uncertainty in EEWS and therefore losing reliability. However, the variability calculated for the prediction equations developed herein is similar to traditional GMPEs. Therefore, the uncertainty of the prediction has not increased and two stages (seismological prediction and structural modelling) in the EEW framework have been successfully merged.

In the few literature cases of EEWS for buildings, these two stages are clearly separated (first a seismological prediction of PGA and then structural analysis through the building). These two-staged processes have an inherent uncertainty propagation process that may be reduced by the direct link developed for this study. A proper comparison of the uncertainty in these two-stages processes and the framework proposed here remain as a further area of research.

The goodness of fit of the prediction equations was evaluated as acceptable by current econometric standards, therefore automatized estimation of building performance can be carried out with seismic parameters estimated in real-time. Some further refinements for the prediction equations can certainly be made. For instance, the inclusion of the fault mechanism as a relevant variable has been discarded due to their poor significance indicators in the regression model. This finding can mean that the data, on fault type, is not large enough to fit the model and a synthetic strong-motion database might provide better insights.

On the topic of intensity prediction using the first P-wave seconds, it is important to point out that the τ parameter is based on California data. The question of whether or not this parameter can become representative for the Italian case remains as a source of uncertainty and future studies for the Italian case are needed.

On the evaluation of the time-dependent warning reliability, Iervolino et.al. (2011) proposed 18 stations out of 29 as the number in which the PGA prediction stabilizes for an Mw=6 and there is no need to include subsequent stations. This study has used the same number of stations for the prediction of EDPs. While the few performed simulations suggest a similar pattern (stabilization before 18 stations), an uncertainty analysis for a larger set of simulations is needed in order to generalize this criterion.

The implementation of the EEWS for buildings was mainly simulated for Naples and Salerno, the two biggest urban areas of Campania. The location of these cities allows warning time of 5 to 10 seconds in Salerno and 15 to 20 seconds in Naples (Iervolino et.al., 2011) which are large enough to implement the proposed mitigation measures. However, nearest cities such as Saint Angelo have insignificant warning times or are located in the denominated blind zone if waiting for 18 stations to be hit. Furthermore, the few simulations carried out for Saint Angelo show the importance of having EEWS for these close-to-the-fault cities, in

fact, some simulations show extensive structural damage as can be seen in the Appendix. The development of warning measures for these sites can be possible if the lead-time is increased at the cost of losing reliability (usage of only a couple of stations). On the other hand, two main measures that can improve this reliability were pointed out by Iervolino et.al. (2006): Improving the prediction performance of the parameter τ and installing a larger set of seismic stations. This last proposal can make EEWS for nearest sites as Saint Angelo viable.

The EEWS simulation was based upon the selection of "EDPc" thresholds from the literature. However, these thresholds can vary depending on the specific features of each building. For instance, some elevators and windows can be more or less resistant by design and some building components might be more acceleration or drift sensitive. Therefore, a real application should rely on a proper estimation of thresholds for the particular case. The results showed in this study can vary if these thresholds change, so, they should be seen as a specific case and not as a demonstrated generalization.

The EEWS simulation has shown a large number of incorrect predictions by using the PGA as the warning indicator instead of more appropriate EDPS. However, it can be seen that all the incorrect predictions are defined as underestimations, this means, the predicted PGA was not strong enough to trigger a warning. One proposal to improve this PGA-based EEWS can be to lower the PGAc threshold so as to reduce the incorrect predictions found in this study. With this in mind, an exercise of reducing the PGAc in 50%. In fact, the results show a reduction of underestimations (only 7 from 23 in the base case), but at the cost of producing overestimations (11 from zero in the base case) maintaining the overall level of inaccuracy. Therefore, a tarde-off exists between underestimations and overestimations in a similar manner as false alarms and missed alarms. More important, the poor performance of the PGA is not an issue in the setting of the threshold, but an inherent lack of building performance prediction reliability.

The implementation of EEWS on buildings can be costly and take an important adaptation time for the occupants. However, mid-rise and high-rise buildings may have the financial capacity to undertake such infrastructure improvements. On the other hand, these buildings normally have automatized systems and communication systems (e.g. speakers) on each space, so, the implementation of the warnings described in this study can take advantage of this existing infrastructure. Furthermore, the wording of the warnings and the way of communicating them (lights, verbal, SMS, etc) might be refined for each particular application.

While the proper trade-off analysis between the probability of false alarms (Pfa) and missed alarms (Pma) was not carried out for this study, a lower exceedance threshold of 10% was set looking for a reduction on missed alarms. Given that mid-rise and high-rise buildings are an important economic component of the city, the cost of interrupting their activities can be not negligible. Therefore, cost-benefit analysis of the alarming decision remains as an area for further research. This is even more important for critical buildings such as hospitals in which elevators are certainly a life-safety component and should remain operational especially after an earthquake hit.

8. Conclusions

First of all, this dissertation has shown the importance of using appropriate EDPs for the seismic performance of buildings by finding a wide and complex variation of performance along with their height and in agreement with earthquake engineering literature. This performance cannot be predicted by the PGA and more refined EDPs, as has been proposed in this study, are required to be utilised.

In order to estimate these EDPs in real-time, this study has developed and validated performance prediction equations for Italy. These equations have shown a good fit and an acceptable level of variability. These performance prediction equations have been used for a real-time probabilistic seismic hazard analysis (RTPSHA) in the region of Campania for different structural typologies and earthquake magnitudes. Furthermore, three potential early warnings cases for human comfort, elevator failure and non-structural damage in buildings were proposed based on available warning times and thresholds from the literature. The application of RTPSHA has been valuable and alarming decisional rules (EDPc and Prc) were set based on hazard curves.

The simulation results show the unreliable performance of using an intensity measure, like the PGA, instead of EDPs for early warning systems in buildings. EDPs are much better correlated with structural and non-structural damages and therefore its real-time estimation and implementation in EEWS is a big improvement to prevent incorrect alarming decisions. Particularly striking results are the 27% of incorrect predictions for all the Mw=7 simulated cases, and 25% of incorrect predictions for the elevator failure across different cities and magnitudes.

To the knowledge of the author, this is the first study assessing the different performance of EEWS in buildings by comparing PGA and EDPs as performance indicators. The results show a strong pattern of incorrect predictions by the widely used PGA in EEWS and therefore, more studies are needed in this important and complex topic.

9. Bibliography

Allen, R.M., Gasparini, P., Kamigaichi, O., Bose, M., 2009. The Status of Earthquake Early Warning around the World: An Introductory Overview. Seismol. Res. Lett. 80, 682–693. https://doi.org/10.1785/gssrl.80.5.682

Akkar, S. & Bommer, J.J., 2010. Empirical Equations for the Prediction of PGA, PGV, and Spectral Accelerations in Europe, the Mediterranean Region, and the Middle East. Seismological Research Letters, 81(2), pp.195–206.

Bindi, D. et al., 2009. Towards a new reference ground motion prediction equation for Italy: Update of the Sabetta-Pugliese (1996). Bulletin of Earthquake Engineering, 7(3), pp.591–608.

Bommer, J.J., Douglas, J. & Strasser, F.O., 2003. Style-of-Faulting in Ground-Motion Prediction Equations. Bulletin of Earthquake Engineering, 1(2), pp.171–203.

Böse, M.,Wenzel, F., Erdik, M., 2008. PreSEIS: a neural network-based approach to earthquake early warning for finite fault. Bull Seis Soc Am 98:366–382

Cheng, M.H., Wu, S., Heaton, T.H., Beck, J.L., 2014. Earthquake early warning application to buildings. Eng. Struct. 60, 155–164. https://doi.org/10.1016/j.engstruct.2013.12.033

Convertito, V., Iervolino, I., Manfredi, G., Zollo, A., 2008. Prediction of response spectra via real-time earthquake measurements. Soil Dynamics and Earthquake Engineering. 28(6):492–505.

Cornell, C.A., Krawinkler, H., 2000. Progress and Challenges in Seismic Performance Assessment. PEER Center News, 3, 1-3.

De Bortoli, M., & Zareian, F., 2018. Performance Prediction Equations for Linear Planar Structural Systems: Concept, Formulation, and Validation. Earthquake Spectra, 34(2), 697–718. https://doi.org/10.1193/110716EQS194M

De Luca, F., 2014. Toward Validation of Simulated Accelerograms Via Prediction Equations for Nonlinear Sdof Response. BGTA. https://doi.org/10.4430/bgta0114

Espinosa-Aranda, J.M., Cuéllar, A., Rodríguez, F.H., Frontana, B., Ibarrola, G., Islas, R., García, A., 2011. The seismic alert system of Mexico (SASMEX): Progress and its current applications. Soil Dynamics and Earthquake Engineering. Volume 31, Issue 2, Pages 154-162, ISSN 0267-7261. https://doi.org/10.1016/j.soildyn.2010.09.011.

FEMA, 2013. Hazus-MH 2.1 Technical Manual. Multi-hazard Loss Estimation Methodology

FEMA, 2013. Hazus-MH 2.1 User Manual. Multi-hazard Loss Estimation Methodology

Galasso, C. et al., 2013. Validation of ground-motion simulations for historical events using MDoF systems. Earthquake Engineering & Structural Dynamics, 42(9), pp.1395–1412.

Grasso, V., Beck, J.L., Manfredi, G. Seismic Early Warning Systems: Procedure for Automated Decision Making. In: Paolo Gasparini, Gaetano Manfredi, Jochen Szchau, editors. Earthquake Early Warning. Springer; 2007. ISBN:978-3-540-72240-3.

Griffis, L.G., 1993. Serviceability limit states under wind load. AISC Eng J. 30(1):1–16.

Hellweg, M., Allen, R.M., Brown, H., Neuhauser, D.S., Khainovsky,O., 2010. CISN ShakeAlert: progress toward using early warnings for earthquakes in California, Abstract NH33A-1368 presented at 2010 fall meeting, AGU, San Francisco, California, 13–17 Dec 2010

Iannaccone, G., Zollo, A., Elia, L., Convertito, V., Satriano, C., Martino, C., Festa, G., Lancieri, M., Bobbio, A., Stabile, T.A., Vassallo, M., Emolo, A., 2010. A prototype system for earthquake

early-warning and alert management in southern Italy. Bull. Earthq. Eng. 8, 1105–1129. https://doi.org/10.1007/s10518-009-9131-8

Iervolino, I., Convertito, V., Giorgio, M., Manfredi, G., Zollo, A., 2006. Real time risk analysis for hybrid earthquake early warning systems. Journal of Earthquake Engineering; 10(6):867–85.

Iervolino, I., Manfredi, G., Cosenza, E., 2007a. Earthquake early warning and engineering application prospects. In: Paolo Gasparini, Gaetano Manfredi, Jochen Szchau, editors. Earthquake Early Warning. Springer. ISBN:978-3-540-72240-3.

Iervolino, I., Giorgio, M., Manfredi, G., 2007b. Expected loss-based alarm threshold set for earthquake early warning systems. Earthquake Engineering and Structural Dynamics; 36(9):1151–68.

Iervolino, I., Giorgio, M., Galasso, C., Manfredi, G., 2009. Uncertainty in early warning predictions of engineering ground motion parameters: what really matters? Geophysical Research Letters. doi:10.1029/2008GL036644.

Iervolino, I., 2011. Performance-based earthquake early warning. Soil Dyn. Earthq. Eng. 31, 209–222. https://doi.org/10.1016/j.soildyn.2010.07.010

Kanamori, H., 2005. Real-time seismology and earthquake damage mitigation. Annual Review of Earth and Planetary Sciences. 3(5.1–):5.20.

Koleva, G., Sandu, I. & Akkar, S., 2008. An Estimation of the Maximum Interstory Drift Ratio For Shear-Wall Type Structures. In International Workshop On: Seismic Hazard And Seismic Risk Reduction In The Countries Influenced By Vrancea Earthquakes. Chisinau, Moldova.

Kubo, T., Hisada, Y., Murakami, M., Kosuge, F., Hamano, K., 2011. Application of an earthquake early warning system and a real-time strong motion monitoring system in emergency response in a high-rise building. Soil Dynam Earthquake Eng. 31:231–9.

Lancieri, M., Zollo, A., 2008. A Bayesian approach to the real-time estimation of magnitude from the early *P* and *S* wave displacement peaks. J. Geophys. Res. 113, B12302. https://doi.org/10.1029/2007JB005386

Miranda, E., 1999. Approximate Seismic Lateral Deformation Demands in Multistory Buildings. Journal of Structural Engineering, 125(4), pp.417–425.

Miranda, E. & Reyes, C.J., 2002. Approximate Lateral Drift Demands in Multistory Buildings with Nonuniform Stiffness. Journal of Structural Engineering, 128(7), pp.840–849.

Miranda, E. & Taghavi, S., 2005. Approximate Floor Acceleration Demands in Multistory Buildings. I: Formulation. Journal of Structural Engineering, 131(2), pp.203–211.

Miranda, E. & Akkar, S., 2005. Rapid Assessment of Building Response Using Generalized Interstory Drift Spectra. In Directions in Strong Motion Instrumentation. Berlin/Heidelberg: Springer-Verlag, pp. 107–121.

Miranda, E. & Akkar, S.D., 2006. Generalized Interstory Drift Spectrum. Journal of Structural Engineering, 132(6), pp.840–852.

Mondal, G. & Jain, S., 2005. Proposed draft for IS 1893 on design of non-structural elements. Indian Concrete Journal. 79. 39-45.

Neam, A.S. & Taghikhany, T., 2016. Prediction equations for generalized interstory drift spectrum considering near-fault ground motions. Natural Hazards, 80(3), pp.1443–1473.

Pacor, F., Paolucci, R., Ameri, G., Massa, M., Puglia, R., 2011. Italian strong motion records in ITACA: overview and record processing. Bull. Earthq. Eng. 9, 1741–1759. https://doi.org/10.1007/s10518-011-9295-x

Primavera, P., 2016. Real-Time Assessment of Building Response for Earthquake Early Warning (EEW) Applications. Dissertation submitted in partial fulfilment of the requirements for the Master of Science in Earthquake Engineering with Disaster Management. University College London. Department of Civil, Environmental & Geomatic Engineering

Picozzi, M., 2012. An attempt of real-time structural response assessment by an interferometric approach: A tailor-made earthquake early warning for buildings. Soil Dynamics and Earthquake Engineering, Volume 38, Pages 109-118, ISSN 0267-7261, https://doi.org/10.1016/j.soildyn.2012.02.003.

Ponzo, F.C., Ditommaso, R., Auletta, G., Mossucca, A., 2010. A fast method for structural health monitoring of Italian reinforced concrete strategic buildings. Bulletin of Earthquake Engineering. 8:1421–34. doi:10.1007/s10518-010-9194-6.

Reinoso, E., Miranda, E., 2005. Estimation of floor acceleration demands in high-rise buildings during earthquakes. Struct. Des. Tall Spec. Build. 14, 107–130. https://doi.org/10.1002/tal.272

Satriano, C., Lomax, A., Zollo, A., 2008. Real-time evolutionary earthquake location for seismic early warning. Bulletin of the Seismological Society of America. 98(3):1482–94.

Satriano, C., Wu, Y.-M., Zollo, A., Kanamori, H., 2011. Earthquake early warning: Concepts, methods and physical grounds. Soil Dyn. Earthq. Eng. 31, 106–118. https://doi.org/10.1016/j.soildyn.2010.07.007

Weber, E., Iannaccone, G., Zollo, A., Bobbio, A., Cantore, L., Corciulo, M., Convertito, V., Di Crosta, M., Elia, L., Emolo, A., Martino, C., Romeo, A., Satriano, C., 2007. Development and testing of an advanced monitoring infrastructure (ISNet) for seismic early-warning applications in the Campania region of southern Italy. In: Gasparini P, Manfredi G, Zschau J (eds) Earthquake Early Warning Systems. Springer

Whittaker, A. & Soong, T., 2003. An overview of nonstructural research at three U.S. Earthquake Engineering Research Centers.

Wu Y.M., Teng, T.L., 2002. A virtual sub-network approach to earthquake early warning. Bull Seism Soc Am 92:2008-2018

Xiong, C. et al., 2016. A nonlinear computational model for regional seismic simulation of tall buildings. Bulletin of Earthquake Engineering, 14(4), pp.1047–1069.

APPENDIX

A.1 FLAT FILE

N° GM	EQ ID	Date	Hour	M_w	Fault type	R_{epi}	Ss	SA
1	Friuli First Shock	06/05/1976	20:00:12	6.4	Thrust	148.6196	0	0
2	Friuli First Shock	06/05/1976	20:00:12	6.4	Thrust	57.3909	0	0
3	Friuli First Shock	06/05/1976	20:00:12	6.4	Thrust	48.4145	0	1
4	Friuli First Shock	06/05/1976	20:00:12	6.4	Thrust	91.2975	0	1
5	Friuli First Shock	06/05/1976	20:00:12	6.4	Thrust	130.2500	0	1
6	Friuli First Shock	06/05/1976	20:00:12	6.4	Thrust	110.3704	0	0
7	Friuli First Shock	06/05/1976	20:00:12	6.4	Thrust	195.5086	0	0
8	Friuli First Shock	06/05/1976	20:00:12	6.4	Thrust	170.7381	1	0
9	Friuli First Shock	06/05/1976	20:00:12	6.4	Thrust	21.7205	0	1
10	Friuli First Shock	06/05/1976	20:00:12	6.4	Thrust	188.6022	0	0
11	Friuli-Aftershock	09/05/1976	00:53:44	5.1	Thrust	24.9471	0	1
12	Friuli-Aftershock	09/05/1976	00:53:44	5.1	Thrust	31.7127	0	1
13	Friuli-Aftershock	09/05/1976	00:53:44	5.1	Thrust	19.3947	0	1
14	Friuli-Aftershock	11/05/1976	22:44:00	5.0	Thrust	7.6747	0	1
15	Friuli-Aftershock	11/05/1976	22:44:00	5.0	Thrust	10.3021	0	0
16	Friuli-Aftershock	11/05/1976	22:44:00	5.0	Thrust	18.3694	1	0
17	Friuli-Aftershock	11/05/1976	22:44:00	5.0	Thrust	13.1622	0	1
18	Friuli-Aftershock	11/09/1976	16:31:10	5.1	Thrust	10.2740	0	0
19	Friuli-Aftershock	11/09/1976	16:31:10	5.1	Thrust	16.0768	0	1
20	Friuli-Aftershock	11/09/1976	16:31:10	5.1	Thrust	15.6904	0	0
21	Friuli-Aftershock	11/09/1976	16:31:10	5.1	Thrust	4.3876	1	0
22	Friuli-Aftershock	11/09/1976	16:31:10	5.1	Thrust	7.4623	0	1
23	Friuli Second Shock	11/09/1976	16:35:01	5.6	Thrust	19.5285	0	0
24	Friuli Second Shock	11/09/1976	16:35:01	5.6	Thrust	26.2079	0	1
25	Friuli Second Shock	11/09/1976	16:35:01	5.6	Thrust	25.8944	0	0
26	Friuli Second Shock	11/09/1976	16:35:01	5.6	Thrust	14.9642	0	1
27	Friuli Second Shock	11/09/1976	16:35:01	5.6	Thrust	60.2007	0	0
28	Friuli Second Shock	11/09/1976	16:35:01	5.6	Thrust	92.0663	1	0
29	Friuli Second Shock	11/09/1976	16:35:01	5.6	Thrust	20.1752	0	1
30	Friuli Third Shock	15/09/1976	03:15:18	5.9	Thrust	11.6159	0	0
31	Friuli Third Shock	15/09/1976	03:15:18	5.9	Thrust	17.2939	0	1
32	Friuli Third Shock	15/09/1976	03:15:18	5.9	Thrust	16.8908	0	1
33	Friuli Third Shock	15/09/1976	03:15:18	5.9	Thrust	5.2292	0	1
34	Friuli Third Shock	15/09/1976	03:15:18	5.9	Thrust	41.1175	0	0
35	Friuli Third Shock	15/09/1976	03:15:18	5.9	Thrust	83.7262	1	0
36	Friuli Third Shock	15/09/1976	03:15:18	5.9	Thrust	181.2345	0	1
37	Friuli Fourth Shock	15/09/1976	09:21:18	5.9	Thrust	11.2659	0	0
38	Friuli Fourth Shock	15/09/1976	09:21:18	5.9	Thrust	16.8309	0	1
39	Friuli Fourth Shock	15/09/1976	09:21:18	5.9	Thrust	16.4207	0	0
N° GM	EQ ID	Date	Hour	5.9	Fault type	R_{epi}	Ss	SA

40	Friuli Fourth Shock	15/09/1976	09:21:18	5.9	Thrust	4.6987	0	1
41	Friuli Fourth Shock	15/09/1976	09:21:18	5.9	Thrust	50.1405	0	1
42	Friuli Fourth Shock	15/09/1976	09:21:18	5.9	Thrust	40.9112	0	1
43	Friuli Fourth Shock	15/09/1976	09:21:18	5.9	Thrust	83.2759	0	0
44	Friuli Fourth Shock	15/09/1976	09:21:18	5.9	Thrust	85.6129	0	0
45	Friuli Fourth Shock	15/09/1976	09:21:18	5.9	Thrust	103.0089	0	0
46	Friuli Fourth Shock	15/09/1976	09:21:18	5.9	Thrust	188.2510	0	0
47	Friuli Fourth Shock	15/09/1976	09:21:18	5.9	Thrust	8.4677	0	1
48	Friuli Fourth Shock	15/09/1976	09:21:18	5.3	Thrust	180.7569	0	0
49	Friuli Aftershock	16/09/1977	23:48:07	5.3	Thrust	6.6708	0	0
50	Friuli Aftershock	16/09/1977	23:48:07	5.3	Thrust	6.1246	0	0
51	Friuli Aftershock	16/09/1977	23:48:07	5.3	Thrust	34.4784	0	0
52	Friuli Aftershock	16/09/1977	23:48:07	5.3	Thrust	9.1310	0	1
53	Friuli Aftershock	16/09/1977	23:48:07	5.3	Thrust	9.1310	0	0
54	Friuli Aftershock	16/09/1977	23:48:07	5.2	Thrust	11.3944	1	0
55	Ferruzzano	11/03/1978	19:20:43	5.2	Normal	9.1934	0	1
56	Ferruzzano	11/03/1978	19:20:43	5.2	Normal	46.7837	0	0
57	Ferruzzano	11/03/1978	19:20:43	6.0	Normal	54.0385	1	0
58	Patti Gulf	15/04/1978	23:33:47	6.0	Strike-slip	60.3129	0	0
59	Patti Gulf	15/04/1978	23:33:47	6.0	Strike-slip	12.2187	0	0
60	Patti Gulf	15/04/1978	23:33:47	6.0	Strike-slip	35.9987	1	0
61	Patti Gulf	15/04/1978	23:33:47	6.0	Strike-slip	33.0147	0	0
62	Patti Gulf	15/04/1978	23:33:47	5.8	Strike-slip	18.2642	1	0
63	Nerina Valley	19/09/1979	21:35:37	5.8	Normal	21.0469	0	0
64	Nerina Valley	19/09/1979	21:35:37	5.8	Normal	38.0126	0	0
65	Nerina Valley	19/09/1979	21:35:37	5.8	Normal	9.2711	0	0
66	Nerina Valley	19/09/1979	21:35:37	5.8	Normal	31.4922	1	0
67	Nerina Valley	19/09/1979	21:35:37	5.8	Normal	39.4547	1	0
68	Nerina Valley	19/09/1979	21:35:37	5.8	Normal	40.4011	0	0
69	Nerina Valley	19/09/1979	21:35:37	5.8	Normal	25.7996	0	0
70	Nerina Valley	19/09/1979	21:35:37	5.0	Normal	50.0888	0	1
71	Nerina Valley Aftershock	28/02/1980	21:04:40	5.0	Normal	5.8515	0	0
72	Nerina Valley Aftershock	28/02/1980	21:04:40	6.9	Normal	10.6285	1	0
73	Irpinia	23/11/1980	18:34:53	6.9	Normal	23.7807	0	1
74	Irpinia	23/11/1980	18:34:53	6.9	Normal	76.7522	0	1
75	Irpinia	23/11/1980	18:34:53	6.9	Normal	21.8028	0	1
76	Irpinia	23/11/1980	18:34:53	6.9	Normal	58.5384	0	0
77	Irpinia	23/11/1980	18:34:53	6.9	Normal	42.2094	0	1
78	Irpinia	23/11/1980	18:34:53	6.9	Normal	28.3030	0	1
79	Irpinia	23/11/1980	18:34:53	6.9	Normal	54.3341	1	0
80	Irpinia	23/11/1980	18:34:53	6.9	Normal	18.8553	1	0
81	Irpinia	23/11/1980	18:34:53	6.9	Normal	135.9557	1	0
N° GM	EQ ID	Date	Hour	6.9	Fault type	R_{epi}	Ss	SA

82	Irpinia	23/11/1980	18:34:53	6.9	Normal	135.9557	0	1
83	Irpinia	23/11/1980	18:34:53	6.9	Normal	94.2737	0	1
84	Irpinia	23/11/1980	18:34:53	6.9	Normal	95.7349	1	0
85	Irpinia	23/11/1980	18:34:53	6.9	Normal	46.2283	0	1
86	Irpinia	23/11/1980	18:34:53	6.9	Normal	126.2149	0	0
87	Irpinia	23/11/1980	18:34:53	6.9	Normal	35.5811	0	1
88	Irpinia	23/11/1980	18:34:53	6.9	Normal	65.3037	0	1
89	Irpinia	23/11/1980	18:34:53	6.9	Normal	102.3163	0	0
90	Irpinia	23/11/1980	18:34:53	6.9	Normal	33.2615	0	1
91	Irpinia	23/11/1980	18:34:53	6.9	Normal	78.2734	0	1
92	Irpinia	23/11/1980	18:34:53	5.0	Normal	73.3225	0	1
93	Irpinia	23/11/1980	18:34:53	5.0	Normal	143.3392	0	1
94	Irpinia Aftershock	24/11/1980	00:24:00	5.0	Normal	17.0110	0	1
95	Irpinia Aftershock	24/11/1980	00:24:00	5.0	Normal	17.3497	0	1
96	Irpinia Aftershock	24/11/1980	00:24:00	5.0	Normal	42.7021	0	1
97	Irpinia Aftershock	24/11/1980	00:24:00	5.0	Normal	26.6295	0	0
98	Irpinia Aftershock	24/11/1980	03:03:54	5.0	Normal	6.8445	0	1
99	Irpinia Aftershock	25/11/1980	17:06:44	5.2	Normal	8.1652	0	1
100	Irpinia Aftershock	25/11/1980	17:06:44	5.2	Normal	32.1909	1	0
101	Basilicata	16/01/1981	00:37:45	5.2	Normal	16.3882	1	0
102	Basilicata	16/01/1981	00:37:45	5.2	Normal	21.4515	0	1
103	Basilicata	16/01/1981	00:37:45	5.2	Normal	21.7424	0	1
104	Basilicata	16/01/1981	00:37:45	5.2	Normal	8.7919	0	1
105	Basilicata	16/01/1981	00:37:45	5.2	Normal	10.4556	0	1
106	Basilicata	16/01/1981	00:37:45	5.2	Normal	10.1286	1	0
107	Basilicata	16/01/1981	00:37:45	5.2	Normal	13.4638	0	1
108	Basilicata	16/01/1981	00:37:45	5.2	Normal	12.1291	0	1
109	Basilicata	16/01/1981	00:37:45	5.2	Normal	10.4939	0	1
110	Basilicata	16/01/1981	00:37:45	5.2	Normal	9.4759	0	1
111	Basilicata	16/01/1981	00:37:45	5.0	Normal	24.5342	0	1
112	Basilicata	16/01/1981	00:37:45	5.0	Normal	25.3069	0	0
113	International waters	21/03/1982	09:44:00	5.0	Normal	41.2365	0	1
114	International waters	21/03/1982	09:44:00	5.0	Normal	41.5084	0	1
115	International waters	21/03/1982	09:44:00	5.6	Normal	46.6661	0	0
116	Frignano	09/11/1983	16:29:52	5.6	Thrust	20.9220	0	0
117	Gubbio	29/04/1984	05:03:00	5.6	Normal	36.6749	1	0
118	Gubbio	29/04/1984	05:03:00	5.6	Normal	16.7602	0	0
119	Gubbio	29/04/1984	05:03:00	5.6	Normal	20.6330	0	0
120	Gubbio	29/04/1984	05:03:00	5.6	Normal	54.4388	0	0
121	Gubbio	29/04/1984	05:03:00	5.6	Normal	26.1323	0	0
122	Gubbio	29/04/1984	05:03:00	5.9	Normal	25.8397	1	0
123	Gubbio	29/04/1984	05:03:00	5.9	Normal	38.1316	0	1
124	Comino Valley	07/05/1984	17:49:43	5.9	Normal	10.2931	1	0
N° GM	EQ ID	Date	Hour	5.9	Fault type	R_{epi}	Ss	SA

125	Comino Valley	07/05/1984	17:49:43	5.9	Normal	19.7303	0	1
126	Comino Valley	07/05/1984	17:49:43	5.9	Normal	72.8077	1	0
127	Comino Valley	07/05/1984	17:49:43	5.9	Normal	54.3709	1	0
128	Comino Valley	07/05/1984	17:49:43	5.9	Normal	69.0569	1	0
129	Comino Valley	07/05/1984	17:49:43	5.9	Normal	49.1946	1	0
130	Comino Valley	07/05/1984	17:49:43	5.9	Normal	49.1946	0	1
131	Comino Valley	07/05/1984	17:49:43	5.9	Normal	43.5194	0	0
132	Comino Valley	07/05/1984	17:49:43	5.9	Normal	33.6101	1	0
133	Comino Valley	07/05/1984	17:49:43	5.9	Normal	74.0321	0	0
134	Comino Valley	07/05/1984	17:49:43	5.9	Normal	27.0005	0	0
135	Comino Valley	07/05/1984	17:49:43	5.9	Normal	46.9185	0	1
136	Comino Valley	07/05/1984	17:49:43	5.9	Normal	66.3771	0	0
137	Comino Valley	07/05/1984	17:49:43	5.5	Normal	63.6384	0	0
138	Comino Valley	07/05/1984	17:49:43	5.5	Normal	34.2133	0	0
139	Comino Valley Aftershock	11/05/1984	10:41:48	5.5	Normal	19.2026	0	0
140	Comino Valley Aftershock	11/05/1984	10:41:48	5.5	Normal	17.4122	1	0
141	Comino Valley Aftershock	11/05/1984	10:41:48	5.5	Normal	17.4122	1	0
142	Comino Valley Aftershock	11/05/1984	10:41:48	5.5	Normal	17.4122	0	0
143	Comino Valley Aftershock	11/05/1984	10:41:48	5.5	Normal	28.6206	0	0
144	Comino Valley Aftershock	11/05/1984	10:41:48	5.5	Normal	35.2164	0	1
145	Comino Valley Aftershock	11/05/1984	10:41:48	5.5	Normal	9.0799	0	0
146	Comino Valley Aftershock	11/05/1984	10:41:48	5.5	Normal	54.5789	0	0
147	Comino Valley Aftershock	11/05/1984	10:41:48	5.5	Normal	37.0984	0	1
148	Comino Valley Aftershock	11/05/1984	10:41:48	5.8	Normal	35.0775	0	1
149	Comino Valley Aftershock	11/05/1984	10:41:48	5.8	Normal	8.5659	1	0
150	Potenza	05/05/1990	07:21:20	5.8	Strike-slip	26.7062	0	1
151	Potenza	05/05/1990	07:21:20	5.8	Strike-slip	45.7023	0	1
152	Potenza	05/05/1990	07:21:20	5.8	Strike-slip	36.6763	1	0
153	Potenza	05/05/1990	07:21:20	5.6	Strike-slip	35.7432	0	0
154	Potenza	05/05/1990	07:21:20	5.6	Strike-slip	25.1852	0	0
155	East Sicily	13/12/1990	00:24:26	5.6	Strike-slip	31.1773	0	1
156	East Sicily	13/12/1990	00:24:26	5.6	Strike-slip	52.4968	0	0
157	East Sicily	13/12/1990	00:24:26	5.6	Strike-slip	46.7633	0	1
158	East Sicily	13/12/1990	00:24:26	5.6	Strike-slip	65.3146	0	0
N° GM	EQ ID	Date	Hour	5.9	Fault type	R_{epi}	Ss	SA

159	East Sicily	13/12/1990	00:24:26	5.6	Strike-slip	28.3352	1	0
160	East Sicily	13/12/1990	00:24:26	5.1	Strike-slip	79.7031	0	1
161	East Sicily	13/12/1990	00:24:26	5.1	Strike-slip	51.5436	0	1
162	Potentino	26/05/1991	12:26:01	5.1	Strike-slip	42.2713	1	0
163	Potentino	26/05/1991	12:26:01	5.2	Strike-slip	28.9119	0	0
164	Potentino	26/05/1991	12:26:01	5.2	Strike-slip	31.6771	0	0
165	Gargano	30/09/1995	10:14:34	5.2	Thrust	46.2501	1	0
166	Gargano	30/09/1995	10:14:34	5.4	Thrust	28.4980	1	0
167	Gargano	30/09/1995	10:14:34	5.4	Thrust	22.5407	1	0
168	Parma	15/10/1996	09:56:01	5.4	Thrust	13.2501	1	0
169	Parma	15/10/1996	09:56:01	5.4	Thrust	28.4663	0	1
170	Parma	15/10/1996	09:56:01	5.7	Thrust	28.4663	1	0
171	Parma	15/10/1996	09:56:01	5.7	Thrust	16.4736	1	0
172	Umbria-Marche 1st Shock	26/09/1997	00:33:12	5.7	Normal	86.1191	1	0
173	Umbria-Marche 1st Shock	26/09/1997	00:33:12	5.7	Normal	125.7864	1	0
174	Umbria-Marche 1st Shock	26/09/1997	00:33:12	5.7	Normal	24.9465	0	0
175	Umbria-Marche 1st Shock	26/09/1997	00:33:12	5.7	Normal	2.8130	0	0
176	Umbria-Marche 1st Shock	26/09/1997	00:33:12	5.7	Normal	24.5455	1	0
177	Umbria-Marche 1st Shock	26/09/1997	00:33:12	5.7	Normal	35.2103	1	0
178	Umbria-Marche 1st Shock	26/09/1997	00:33:12	5.7	Normal	39.0549	0	0
179	Umbria-Marche 1st Shock	26/09/1997	00:33:12	5.7	Normal	40.5731	1	0
180	Umbria-Marche 1st Shock	26/09/1997	00:33:12	5.7	Normal	51.4244	1	0
181	Umbria-Marche 1st Shock	26/09/1997	00:33:12	5.7	Normal	24.3423	1	0
182	Umbria-Marche 1st Shock	26/09/1997	00:33:12	5.7	Normal	26.9363	0	0
183	Umbria-Marche 1st Shock	26/09/1997	00:33:12	5.7	Normal	13.1263	0	1
184	Umbria-Marche 1st Shock	26/09/1997	00:33:12	6.0	Normal	66.0702	0	1
185	Umbria-Marche 1st Shock	26/09/1997	00:33:12	6.0	Normal	35.3372	0	1
186	Umbria-Marche 2nd Shock	26/09/1997	09:40:25	6.0	Normal	81.4977	1	0
187	Umbria-Marche 2nd Shock	26/09/1997	09:40:25	6.0	Normal	86.8731	1	0
N° GM	EQ ID	Date	Hour	5.9	Fault type	R_{epi}	Ss	SA

188	Umbria-Marche 2nd Shock	26/09/1997	09:40:25	6.0	Normal	86.8688	0	0
189	Umbria-Marche 2nd Shock	26/09/1997	09:40:25	6.0	Normal	126.3155	1	0
190	Umbria-Marche 2nd Shock	26/09/1997	09:40:25	6.0	Normal	21.8114	1	0
191	Umbria-Marche 2nd Shock	26/09/1997	09:40:25	6.0	Normal	60.6417	0	0
192	Umbria-Marche 2nd Shock	26/09/1997	09:40:25	6.0	Normal	5.9275	0	0
193	Umbria-Marche 2nd Shock	26/09/1997	09:40:25	6.0	Normal	21.4721	0	0
194	Umbria-Marche 2nd Shock	26/09/1997	09:40:25	6.0	Normal	35.3531	1	0
195	Umbria-Marche 2nd Shock	26/09/1997	09:40:25	6.0	Normal	40.5168	1	0
196	Umbria-Marche 2nd Shock	26/09/1997	09:40:25	6.0	Normal	43.1876	0	0
197	Umbria-Marche 2nd Shock	26/09/1997	09:40:25	6.0	Normal	39.5737	1	0
198	Umbria-Marche 2nd Shock	26/09/1997	09:40:25	6.0	Normal	51.0826	1	0
199	Umbria-Marche 2nd Shock	26/09/1997	09:40:25	6.0	Normal	27.4906	0	0
200	Umbria-Marche 2nd Shock	26/09/1997	09:40:25	6.0	Normal	28.9605	0	0
201	Umbria-Marche 2nd Shock	26/09/1997	09:40:25	6.0	Normal	12.1474	0	0
202	Umbria-Marche 2nd Shock	26/09/1997	09:40:25	6.0	Normal	80.9460	1	0
203	Umbria-Marche 2nd Shock	26/09/1997	09:40:25	6.0	Normal	101.2495	0	1
204	Umbria-Marche 2nd Shock	26/09/1997	09:40:25	6.0	Normal	56.3783	1	0
205	Umbria-Marche 2nd Shock	26/09/1997	09:40:25	5.2	Normal	64.9771	1	0
206	Umbria-Marche 2nd Shock	26/09/1997	09:40:25	5.2	Normal	80.3719	1	0
207	Umbro-Marchigiano	03/10/1997	08:55:22	5.2	Normal	21.2888	1	0
208	Umbro-Marchigiano	03/10/1997	08:55:22	5.2	Normal	5.6392	0	0
209	Umbro-Marchigiano	03/10/1997	08:55:22	5.2	Normal	7.8624	1	0
210	Umbro-Marchigiano	03/10/1997	08:55:22	5.2	Normal	19.4520	0	0
211	Umbro-Marchigiano	03/10/1997	08:55:22	5.2	Normal	39.3226	1	0
212	Umbro-Marchigiano	03/10/1997	08:55:22	5.2	Normal	35.6668	0	0
213	Umbro-Marchigiano	03/10/1997	08:55:22	5.2	Normal	29.4324	1	0
214	Umbro-Marchigiano	03/10/1997	08:55:22	5.2	Normal	6.8554	1	0
N° GM	EQ ID	Date	Hour	5.9	Fault type	R_{epi}	Ss	SA

215	Umbro-Marchigiano	03/10/1997	08:55:22	5.2	Normal	12.0349	1	0
216	Umbro-Marchigiano	03/10/1997	08:55:22	5.4	Normal	8.3117	1	0
217	Umbro-Marchigiano	03/10/1997	08:55:22	5.4	Normal	8.3117	1	0
218	Umbro-Marchigiano	06/10/1997	23:24:53	5.4	Normal	21.9336	1	0
219	Umbro-Marchigiano	06/10/1997	23:24:53	5.4	Normal	3.6392	0	0
220	Umbro-Marchigiano	06/10/1997	23:24:53	5.4	Normal	6.0896	0	0
221	Umbro-Marchigiano	06/10/1997	23:24:53	5.4	Normal	20.9903	0	0
222	Umbro-Marchigiano	06/10/1997	23:24:53	5.4	Normal	36.8883	1	0
223	Umbro-Marchigiano	06/10/1997	23:24:53	5.4	Normal	41.9247	1	0
224	Umbro-Marchigiano	06/10/1997	23:24:53	5.4	Normal	41.6612	0	0
225	Umbro-Marchigiano	06/10/1997	23:24:53	5.4	Normal	38.0659	1	0
226	Umbro-Marchigiano	06/10/1997	23:24:53	5.4	Normal	52.5950	0	0
227	Umbro-Marchigiano	06/10/1997	23:24:53	5.4	Normal	27.8199	1	0
228	Umbro-Marchigiano	06/10/1997	23:24:53	5.4	Normal	9.0178	1	0
229	Umbro-Marchigiano	06/10/1997	23:24:53	5.4	Normal	14.1045	0	1
230	Umbro-Marchigiano	06/10/1997	23:24:53	5.4	Normal	10.6200	1	0
231	Umbro-Marchigiano	06/10/1997	23:24:53	5.4	Normal	10.6200	0	0
232	Umbro-Marchigiano	06/10/1997	23:24:53	5.2	Normal	33.2226	0	0
233	Umbro-Marchigiano	06/10/1997	23:24:53	5.2	Normal	66.3770	1	0
234	Umbro-Marchigiano	12/10/1997	11:08:36	5.2	Normal	18.0780	1	0
235	Umbro-Marchigiano	12/10/1997	11:08:36	5.2	Normal	11.0259	0	0
236	Umbro-Marchigiano	12/10/1997	11:08:36	5.2	Normal	13.8885	0	0
237	Umbro-Marchigiano	12/10/1997	11:08:36	5.2	Normal	14.4084	1	0
238	Umbro-Marchigiano	12/10/1997	11:08:36	5.2	Normal	22.1558	0	0
239	Umbro-Marchigiano	12/10/1997	11:08:36	5.2	Normal	6.6149	1	0
240	Umbro-Marchigiano	12/10/1997	11:08:36	5.2	Normal	23.7669	1	0
241	Umbro-Marchigiano	12/10/1997	11:08:36	5.2	Normal	28.7961	0	1
242	Umbro-Marchigiano	12/10/1997	11:08:36	5.2	Normal	25.3551	1	0
243	Umbro-Marchigiano	12/10/1997	11:08:36	5.2	Normal	25.3551	1	0
244	Umbro-Marchigiano	12/10/1997	11:08:36	5.6	Normal	19.2315	0	1
245	Umbro-Marchigiano	12/10/1997	11:08:36	5.6	Normal	53.4901	0	1
246	Umbria-Marche 3rdShock	14/10/1997	15:23:09	5.6	Normal	17.5786	0	0
247	Umbria-Marche 3rdShock	14/10/1997	15:23:09	5.6	Normal	73.9945	0	0
248	Umbria-Marche 3rdShock	14/10/1997	15:23:09	5.6	Normal	73.9905	0	1
249	Umbria-Marche 3rdShock	14/10/1997	15:23:09	5.6	Normal	68.5319	1	0
250	Umbria-Marche 3rdShock	14/10/1997	15:23:09	5.6	Normal	68.9338	1	0
251	Umbria-Marche 3rdShock	14/10/1997	15:23:09	5.6	Normal	68.4289	0	0
N° GM	EQ ID	Date	Hour	5.9	Fault type	R_{epi}	Ss	SA

252	Umbria-Marche 3rdShock	14/10/1997	15:23:09	5.6	Normal	113.1439	0	0
253	Umbria-Marche 3rdShock	14/10/1997	15:23:09	5.6	Normal	23.7921	1	0
254	Umbria-Marche 3rdShock	14/10/1997	15:23:09	5.6	Normal	18.2678	1	0
255	Umbria-Marche 3rdShock	14/10/1997	15:23:09	5.6	Normal	11.8334	1	0
256	Umbria-Marche 3rdShock	14/10/1997	15:23:09	5.6	Normal	14.5865	0	0
257	Umbria-Marche 3rdShock	14/10/1997	15:23:09	5.6	Normal	15.4006	0	0
258	Umbria-Marche 3rdShock	14/10/1997	15:23:09	5.6	Normal	27.9458	1	0
259	Umbria-Marche 3rdShock	14/10/1997	15:23:09	5.6	Normal	22.0159	1	0
260	Umbria-Marche 3rdShock	14/10/1997	15:23:09	5.6	Normal	29.6812	0	0
261	Umbria-Marche 3rdShock	14/10/1997	15:23:09	5.6	Normal	52.5851	1	0
262	Umbria-Marche 3rdShock	14/10/1997	15:23:09	5.6	Normal	37.6703	0	0
263	Umbria-Marche 3rdShock	14/10/1997	15:23:09	5.6	Normal	29.6406	1	0
264	Umbria-Marche 3rdShock	14/10/1997	15:23:09	5.6	Normal	23.9697	1	0
265	Umbria-Marche 3rdShock	14/10/1997	15:23:09	5.6	Normal	29.0821	0	0
266	Umbria-Marche 3rdShock	14/10/1997	15:23:09	5.6	Normal	25.4635	0	1
267	Umbria-Marche 3rdShock	14/10/1997	15:23:09	5.6	Normal	25.4635	1	0
268	Umbria-Marche 3rdShock	14/10/1997	15:23:09	5.6	Normal	26.1309	0	0
269	Umbria-Marche 3rdShock	14/10/1997	15:23:09	5.6	Normal	20.0486	0	0
270	Umbria-Marche 3rdShock	14/10/1997	15:23:09	5.6	Normal	52.3675	1	0
271	Umbria-Marche 3rdShock	14/10/1997	15:23:09	5.6	Normal	19.7229	0	0
272	Umbria-Marche 3rdShock	14/10/1997	15:23:09	5.0	Normal	23.0047	0	0
273	Umbria-Marche 3rdShock	14/10/1997	15:23:09	5.0	Normal	68.3885	1	0
274	Umbro-Marchigiano	21/03/1998	16:45:09	5.0	Normal	12.5656	1	0
275	Umbro-Marchigiano	21/03/1998	16:45:09	5.0	Normal	13.6758	1	0
276	Umbro-Marchigiano	21/03/1998	16:45:09	5.0	Normal	6.3033	0	0
N° GM	EQ ID	Date	Hour	5.9	Fault type	R_{epi}	Ss	SA

277	Umbro-Marchigiano	21/03/1998	16:45:09	5.0	Normal	6.2465	0	1
278	Umbro-Marchigiano	21/03/1998	16:45:09	5.0	Normal	19.3058	0	1
279	Umbro-Marchigiano	21/03/1998	16:45:09	5.0	Normal	20.9730	0	1
280	Umbro-Marchigiano	21/03/1998	16:45:09	5.0	Normal	21.5020	0	0
281	Umbro-Marchigiano	21/03/1998	16:45:09	5.0	Normal	22.9349	1	0
282	Umbro-Marchigiano	21/03/1998	16:45:09	5.0	Normal	6.6799	0	0
283	Umbro-Marchigiano	21/03/1998	16:45:09	5.3	Normal	6.9470	0	0
284	Umbro-Marchigiano	21/03/1998	16:45:09	5.3	Normal	13.9917	1	0
285	Umbro-Marchigiano	26/03/1998	16:26:17	5.3	Normal	28.6755	1	0
286	Umbro-Marchigiano	26/03/1998	16:26:17	5.3	Normal	10.2775	1	0
287	Umbro-Marchigiano	26/03/1998	16:26:17	5.3	Normal	17.4603	1	0
288	Umbro-Marchigiano	26/03/1998	16:26:17	5.3	Normal	17.4594	0	0
289	Umbro-Marchigiano	26/03/1998	16:26:17	5.3	Normal	15.2166	1	0
290	Umbro-Marchigiano	26/03/1998	16:26:17	5.3	Normal	19.8862	0	0
291	Umbro-Marchigiano	26/03/1998	16:26:17	5.3	Normal	4.7892	0	1
292	Umbro-Marchigiano	26/03/1998	16:26:17	5.3	Normal	1.0286	0	1
293	Umbro-Marchigiano	26/03/1998	16:26:17	5.3	Normal	4.2861	1	0
294	Umbro-Marchigiano	26/03/1998	16:26:17	5.3	Normal	3.1826	0	0
295	Umbro-Marchigiano	26/03/1998	16:26:17	5.1	Normal	30.1095	0	0
296	Umbro-Marchigiano	26/03/1998	16:26:17	5.1	Normal	30.2693	1	0
297	Umbro-Marchigiano	03/04/1998	07:26:36	5.1	Normal	30.5024	1	0
298	Umbro-Marchigiano	03/04/1998	07:26:36	5.1	Normal	15.6766	0	0
299	Umbro-Marchigiano	03/04/1998	07:26:36	5.1	Normal	23.3459	1	0
300	Umbro-Marchigiano	03/04/1998	07:26:36	5.1	Normal	23.3286	1	0
301	Umbro-Marchigiano	03/04/1998	07:26:36	5.1	Normal	23.8980	0	0
302	Umbro-Marchigiano	03/04/1998	07:26:36	5.1	Normal	22.8430	1	0
303	Umbro-Marchigiano	03/04/1998	07:26:36	5.1	Normal	19.7063	0	0
304	Umbro-Marchigiano	03/04/1998	07:26:36	5.1	Normal	9.9801	0	1
305	Umbro-Marchigiano	03/04/1998	07:26:36	5.1	Normal	5.1881	0	1
306	Umbro-Marchigiano	03/04/1998	07:26:36	5.1	Normal	8.4975	1	0
307	Umbro-Marchigiano	03/04/1998	07:26:36	5.1	Normal	7.7991	0	1
308	Umbro-Marchigiano	03/04/1998	07:26:36	5.6	Normal	35.7286	0	0
309	Umbro-Marchigiano	03/04/1998	07:26:36	5.6	Normal	35.8448	1	0
310	Lucano	09/09/1998	11:28:00	5.6	Normal	28.3153	1	0
311	Lucano	09/09/1998	11:28:00	5.6	Normal	6.6332	0	0
312	Lucano	09/09/1998	11:28:00	5.6	Normal	9.8488	0	1
313	Lucano	09/09/1998	11:28:00	5.9	Normal	34.1218	1	0
314	Lucano	09/09/1998	11:28:00	5.9	Normal	13.4839	0	1
315	Tyrrenian	06/09/2002	01:21:29	5.9	Thrust	131.3406	0	0
316	Tyrrenian	06/09/2002	01:21:29	5.9	Thrust	150.5906	0	0
317	Tyrrenian	06/09/2002	01:21:29	5.7	Thrust	118.8001	0	0
318	Tyrrenian	06/09/2002	01:21:29	5.7	Thrust	108.2822	1	0
319	Molise First Shock	31/10/2002	10:32:59	5.7	Strike-slip	40.5172	0	0
N° GM	EQ ID	Date	Hour	5.9	Fault type	R_{epi}	Ss	SA

320	Molise First Shock	31/10/2002	10:32:59	5.7	Strike-slip	25.6405	0	0
321	Molise First Shock	31/10/2002	10:32:59	5.7	Strike-slip	138.4404	0	1
322	Molise First Shock	31/10/2002	10:32:59	5.7	Strike-slip	41.6442	0	1
323	Molise First Shock	31/10/2002	10:32:59	5.7	Strike-slip	45.5861	0	0
324	Molise First Shock	31/10/2002	10:32:59	5.7	Strike-slip	57.9020	0	0
325	Molise First Shock	31/10/2002	10:32:59	5.7	Strike-slip	41.2386	0	0
326	Molise First Shock	31/10/2002	10:32:59	5.7	Strike-slip	46.3770	0	0
327	Molise Second Shock	01/11/2002	15:09:02	5.7	Strike-slip	35.5951	0	1
328	Molise Second Shock	01/11/2002	15:09:02	5.7	Strike-slip	26.7274	0	1
329	Molise Second Shock	01/11/2002	15:09:02	5.7	Strike-slip	133.4609	0	0
330	Molise Second Shock	01/11/2002	15:09:02	5.7	Strike-slip	48.4281	0	0
331	Molise Second Shock	01/11/2002	15:09:02	5.5	Strike-slip	45.7065	0	0
332	Molise Second Shock	01/11/2002	15:09:02	5.5	Strike-slip	42.5201	0	1
333	Jabuka Island	29/03/2003	17:42:16	5.5	Thrust	158.2081	0	0
334	Jabuka Island	29/03/2003	17:42:16	5.5	Thrust	168.2868	0	0
335	Jabuka Island	29/03/2003	17:42:16	5.3	Thrust	149.6150	1	0
336	Jabuka Island	29/03/2003	17:42:16	5.3	Thrust	140.8154	0	0
337	Monghidoro	14/09/2003	21:42:53	5.3	Thrust	33.6886	0	0
338	Monghidoro	14/09/2003	21:42:53	5.3	Thrust	22.9942	0	0
339	Monghidoro	14/09/2003	21:42:53	5.3	Thrust	40.9236	1	0
340	Monghidoro	14/09/2003	21:42:53	5.3	Thrust	11.2473	0	0
341	Monghidoro	14/09/2003	21:42:53	5.4	Thrust	71.0442	0	0
342	Monghidoro	14/09/2003	21:42:53	5.4	Thrust	52.9976	0	0
343	Eolie Islands	05/05/2004	13:39:41	5.4	Thrust	119.7905	0	1
344	Eolie Islands	05/05/2004	13:39:41	5.4	Thrust	145.3876	1	0
345	Eolie Islands	05/05/2004	13:39:41	5.2	Thrust	76.9000	0	1
346	Eolie Islands	05/05/2004	13:39:41	5.2	Thrust	86.9327	0	1
347	Carnic Alps	12/07/2004	13:04:06	5.2	Thrust	27.9074	1	0
348	Carnic Alps	12/07/2004	13:04:06	5.2	Thrust	90.2814	0	0
349	Carnic Alps	12/07/2004	13:04:06	5.3	Thrust	36.7896	0	0
350	Carnic Alps	12/07/2004	13:04:06	5.0	Thrust	55.9599	0	0
351	Southern Garda	24/11/2004	22:59:39	5.0	Thrust	14.4696	0	1
352	Central Adriatic	25/11/2004	06:21:17	5.0	Thrust	185.0606	0	0
353	Central Adriatic	25/11/2004	06:21:17	5.0	Thrust	196.3477	0	0
354	Central Adriatic	25/11/2004	06:21:17	5.0	Thrust	162.7939	0	0
355	Central Adriatic	25/11/2004	06:21:17	5.0	Thrust	168.2735	0	0
356	Central Adriatic	25/11/2004	06:21:17	5.0	Thrust	148.5476	0	0
357	Central Adriatic	25/11/2004	06:21:17	5.8	Thrust	172.2770	0	0
358	Central Adriatic	25/11/2004	06:21:17	5.8	Thrust	159.9102	0	0
359	Western Calabria	26/10/2006	14:28:37	5.8	Normal	119.8968	1	0
360	Western Calabria	26/10/2006	14:28:37	5.8	Normal	73.4626	1	0
361	Western Calabria	26/10/2006	14:28:37	5.8	Normal	63.2866	0	0
362	Western Calabria	26/10/2006	14:28:37	5.8	Normal	112.7980	0	0
N° GM	EQ ID	Date	Hour	5.9	Fault type	R_{epi}	Ss	SA

363	Western Calabria	26/10/2006	14:28:37	5.8	Normal	89.3954	1	0
364	Western Calabria	26/10/2006	14:28:37	5.8	Normal	149.2579	0	0
365	Western Calabria	26/10/2006	14:28:37	5.8	Normal	181.9527	1	0
366	Western Calabria	26/10/2006	14:28:37	5.8	Normal	92.1992	0	0
367	Western Calabria	26/10/2006	14:28:37	5.8	Normal	96.3135	0	0
368	Western Calabria	26/10/2006	14:28:37	5.8	Normal	61.4709	0	0
369	Western Calabria	26/10/2006	14:28:37	5.8	Normal	99.7607	1	0
370	Western Calabria	26/10/2006	14:28:37	5.8	Normal	142.1331	0	1
371	Western Calabria	26/10/2006	14:28:37	5.8	Normal	165.1166	0	0
372	Western Calabria	26/10/2006	14:28:37	5.8	Normal	71.9197	0	0
373	Western Calabria	26/10/2006	14:28:37	5.8	Normal	158.0630	0	0
374	Western Calabria	26/10/2006	14:28:37	5.8	Normal	52.2342	0	1
375	Western Calabria	26/10/2006	14:28:37	5.8	Normal	148.9558	0	1
376	Western Calabria	26/10/2006	14:28:37	5.8	Normal	142.5604	1	0
377	Western Calabria	26/10/2006	14:28:37	5.8	Normal	121.6111	0	1
378	Western Calabria	26/10/2006	14:28:37	5.8	Normal	51.8625	0	1
379	Western Calabria	26/10/2006	14:28:37	5.8	Normal	40.3118	1	0
380	Western Calabria	26/10/2006	14:28:37	5.8	Normal	197.6500	0	1
381	Western Calabria	26/10/2006	14:28:37	5.8	Normal	77.9801	0	1
382	Western Calabria	26/10/2006	14:28:37	5.8	Normal	81.1470	0	1
383	Western Calabria	26/10/2006	14:28:37	5.8	Normal	183.8025	0	0
384	Western Calabria	26/10/2006	14:28:37	5.8	Normal	45.8821	0	0
385	Western Calabria	26/10/2006	14:28:37	5.8	Normal	141.0803	0	1
386	Western Calabria	26/10/2006	14:28:37	5.8	Normal	89.7565	0	1
387	Western Calabria	26/10/2006	14:28:37	5.8	Normal	48.5879	0	1
388	Western Calabria	26/10/2006	14:28:37	5.8	Normal	125.9406	0	1
389	Western Calabria	26/10/2006	14:28:37	5.8	Normal	123.4478	0	1
390	Western Calabria	26/10/2006	14:28:37	5.8	Normal	169.1710	1	0
391	Western Calabria	26/10/2006	14:28:37	5.8	Normal	112.1030	0	1
392	Western Calabria	26/10/2006	14:28:37	5.8	Normal	60.0915	0	0
393	Western Calabria	26/10/2006	14:28:37	5.8	Normal	27.9186	0	0
394	Western Calabria	26/10/2006	14:28:37	5.8	Normal	91.2748	0	1
395	Western Calabria	26/10/2006	14:28:37	5.8	Normal	90.4220	0	0
396	Western Calabria	26/10/2006	14:28:37	5.8	Normal	34.3514	0	0
397	Western Calabria	26/10/2006	14:28:37	5.8	Normal	45.3574	0	0
398	Western Calabria	26/10/2006	14:28:37	5.8	Normal	55.0660	0	1
399	Western Calabria	26/10/2006	14:28:37	5.2	Normal	53.2672	1	0
400	Western Calabria	26/10/2006	14:28:37	5.2	Normal	50.6595	0	0
401	Lipari	04/07/2007	23:55:33	5.2	Normal	78.3214	0	0
402	Lipari	04/07/2007	23:55:33	5.2	Normal	87.5464	0	0
403	Lipari	04/07/2007	23:55:33	5.2	Normal	90.0223	0	0
404	Lipari	04/07/2007	23:55:33	5.2	Normal	134.9575	0	0
405	Lipari	04/07/2007	23:55:33	5.2	Normal	86.5929	0	1
N° GM	EQ ID	Date	Hour	5.9	Fault type	R_{epi}	Ss	SA

406	Lipari	04/07/2007	23:55:33	5.2	Normal	4.0489	1	0
407	Lipari	04/07/2007	23:55:33	5.4	Normal	57.0019	0	0
408	Lipari	04/07/2007	23:55:33	5.4	Normal	75.0991	0	0
409	Parmense	23/12/2008	15:24:21	5.4	Thrust	47.4450	0	0
410	Parmense	23/12/2008	15:24:21	5.4	Thrust	60.1809	0	1
411	Parmense	23/12/2008	15:24:21	5.4	Thrust	91.3460	0	1
412	Parmense	23/12/2008	15:24:21	5.4	Thrust	45.4487	0	0
413	Parmense	23/12/2008	15:24:21	5.4	Thrust	91.4325	0	0
414	Parmense	23/12/2008	15:24:21	5.4	Thrust	37.0555	1	0
415	Parmense	23/12/2008	15:24:21	5.4	Thrust	115.7974	1	0
416	Parmense	23/12/2008	15:24:21	5.4	Thrust	65.6204	0	0
417	Parmense	23/12/2008	15:24:21	5.4	Thrust	42.7683	0	1
418	Parmense	23/12/2008	15:24:21	5.4	Thrust	117.0267	0	0
419	Parmense	23/12/2008	15:24:21	5.4	Thrust	138.7771	0	0
420	Parmense	23/12/2008	15:24:21	5.4	Thrust	59.7263	0	1
421	Parmense	23/12/2008	15:24:21	5.4	Thrust	76.8123	0	1
422	Parmense	23/12/2008	15:24:21	5.4	Thrust	40.8931	0	0
423	Parmense	23/12/2008	15:24:21	5.4	Thrust	37.4667	0	0
424	Parmense	23/12/2008	15:24:21	5.4	Thrust	82.9082	0	0
425	Parmense	23/12/2008	15:24:21	5.4	Thrust	60.7274	0	0
426	Parmense	23/12/2008	15:24:21	5.4	Thrust	32.0546	0	0
427	Parmense	23/12/2008	15:24:21	5.4	Thrust	145.0498	0	0
428	Parmense	23/12/2008	15:24:21	5.4	Thrust	129.1676	0	1
429	Parmense	23/12/2008	15:24:21	5.4	Thrust	121.4985	0	1
430	Parmense	23/12/2008	15:24:21	5.4	Thrust	106.3483	0	0
431	Parmense	23/12/2008	15:24:21	5.4	Thrust	148.9569	0	0
432	Parmense	23/12/2008	15:24:21	5.4	Thrust	140.1155	0	0
433	Parmense	23/12/2008	15:24:21	5.4	Thrust	157.6906	1	0
434	Parmense	23/12/2008	15:24:21	5.4	Thrust	125.2716	0	0
435	Parmense	23/12/2008	15:24:21	5.4	Thrust	90.9597	0	1
436	Parmense	23/12/2008	15:24:21	5.4	Thrust	127.3514	0	1
437	Parmense	23/12/2008	15:24:21	6.3	Thrust	135.6083	0	0
438	Parmense	23/12/2008	15:24:21	6.3	Thrust	126.5805	0	0
439	L'Aquila Mainshock	06/04/2009	01:32:39	6.3	Normal	23.0167	0	1
440	L'Aquila Mainshock	06/04/2009	01:32:39	6.3	Normal	4.6338	0	0
441	L'Aquila Mainshock	06/04/2009	01:32:39	6.3	Normal	4.3919	0	0
442	L'Aquila Mainshock	06/04/2009	01:32:39	6.3	Normal	5.6501	0	0
443	L'Aquila Mainshock	06/04/2009	01:32:39	6.3	Normal	4.8698	0	0
444	L'Aquila Mainshock	06/04/2009	01:32:39	6.3	Normal	198.0726	0	0
445	L'Aquila Mainshock	06/04/2009	01:32:39	6.3	Normal	199.6304	0	0
446	L'Aquila Mainshock	06/04/2009	01:32:39	6.3	Normal	180.3456	1	0
447	L'Aquila Mainshock	06/04/2009	01:32:39	6.3	Normal	88.5157	0	0
448	L'Aquila Mainshock	06/04/2009	01:32:39	6.3	Normal	31.6442	1	0
N° GM	EQ ID	Date	Hour	5.9	Fault type	R_{epi}	Ss	SA

449	L'Aquila Mainshock	06/04/2009	01:32:39	6.3	Normal	138.8717	0	0
450	L'Aquila Mainshock	06/04/2009	01:32:39	6.3	Normal	126.8531	0	1
451	L'Aquila Mainshock	06/04/2009	01:32:39	6.3	Normal	166.8912	0	1
452	L'Aquila Mainshock	06/04/2009	01:32:39	6.3	Normal	32.9025	0	1
453	L'Aquila Mainshock	06/04/2009	01:32:39	6.3	Normal	102.5788	0	0
454	L'Aquila Mainshock	06/04/2009	01:32:39	6.3	Normal	186.5392	0	0
455	L'Aquila Mainshock	06/04/2009	01:32:39	6.3	Normal	19.3193	0	1
456	L'Aquila Mainshock	06/04/2009	01:32:39	6.3	Normal	22.6311	0	1
457	L'Aquila Mainshock	06/04/2009	01:32:39	6.3	Normal	109.7421	0	0
458	L'Aquila Mainshock	06/04/2009	01:32:39	6.3	Normal	39.0218	0	0
459	L'Aquila Mainshock	06/04/2009	01:32:39	6.3	Normal	22.3479	0	0
460	L'Aquila Mainshock	06/04/2009	01:32:39	6.3	Normal	184.4699	0	0
461	L'Aquila Mainshock	06/04/2009	01:32:39	6.3	Normal	139.4246	0	1
462	L'Aquila Mainshock	06/04/2009	01:32:39	6.3	Normal	146.9988	1	0
463	L'Aquila Mainshock	06/04/2009	01:32:39	6.3	Normal	133.6552	0	0
464	L'Aquila Mainshock	06/04/2009	01:32:39	6.3	Normal	50.4190	0	0
465	L'Aquila Mainshock	06/04/2009	01:32:39	6.3	Normal	153.1635	0	0
466	L'Aquila Mainshock	06/04/2009	01:32:39	6.3	Normal	162.4049	0	0
467	L'Aquila Mainshock	06/04/2009	01:32:39	6.3	Normal	191.9978	0	0
468	L'Aquila Mainshock	06/04/2009	01:32:39	6.3	Normal	150.4014	0	0
469	L'Aquila Mainshock	06/04/2009	01:32:39	6.3	Normal	167.9684	0	0
470	L'Aquila Mainshock	06/04/2009	01:32:39	6.3	Normal	56.5273	0	0
471	L'Aquila Mainshock	06/04/2009	01:32:39	6.3	Normal	158.5345	0	0
472	L'Aquila Mainshock	06/04/2009	01:32:39	5.1	Normal	140.9082	0	0
473	L'Aquila Mainshock	06/04/2009	01:32:39	5.1	Normal	129.4068	0	1
474	L'Aquila Aftershock	06/04/2009	02:37:04	5.1	Normal	22.2887	1	0
475	L'Aquila Aftershock	06/04/2009	02:37:04	5.1	Normal	0.8656	1	0
476	L'Aquila Aftershock	06/04/2009	02:37:04	5.1	Normal	5.5384	0	1
477	L'Aquila Aftershock	06/04/2009	02:37:04	5.1	Normal	1.5982	0	0
478	L'Aquila Aftershock	06/04/2009	02:37:04	5.1	Normal	34.5730	1	0
479	L'Aquila Aftershock	06/04/2009	02:37:04	5.1	Normal	21.3478	0	1
480	L'Aquila Aftershock	06/04/2009	02:37:04	5.1	Normal	37.2515	0	1
481	L'Aquila Aftershock	06/04/2009	02:37:04	5.1	Normal	19.2215	0	0
482	Gran Sasso	06/04/2009	23:15:37	5.1	Normal	23.7667	0	1
483	Gran Sasso	06/04/2009	23:15:37	5.1	Normal	12.1648	0	1
484	Gran Sasso	06/04/2009	23:15:37	5.1	Normal	8.3609	0	1
485	Gran Sasso	06/04/2009	23:15:37	5.1	Normal	42.6376	0	0
486	Gran Sasso	06/04/2009	23:15:37	5.1	Normal	34.5910	0	0
487	Gran Sasso	06/04/2009	23:15:37	5.0	Normal	12.7217	0	1
488	Gran Sasso	06/04/2009	23:15:37	5.0	Normal	61.8722	0	1
489	L'Aquila Aftershock	07/04/2009	09:26:28	5.0	Normal	22.9753	0	1
490	L'Aquila Aftershock	07/04/2009	09:26:28	5.0	Normal	3.4971	0	0
491	L'Aquila Aftershock	07/04/2009	09:26:28	5.0	Normal	5.1977	0	0
N° GM	EQ ID	Date	Hour	5.9	Fault type	R_{epi}	Ss	SA

492	L'Aquila Aftershock	07/04/2009	09:26:28	5.0	Normal	4.1747	0	0
493	L'Aquila Aftershock	07/04/2009	09:26:28	5.0	Normal	5.2721	0	1
494	L'Aquila Aftershock	07/04/2009	09:26:28	5.0	Normal	3.9424	0	0
495	L'Aquila Aftershock	07/04/2009	09:26:28	5.0	Normal	32.2668	0	0
496	L'Aquila Aftershock	07/04/2009	09:26:28	5.0	Normal	33.8060	0	0
497	L'Aquila Aftershock	07/04/2009	09:26:28	5.0	Normal	19.9727	0	0
498	L'Aquila Aftershock	07/04/2009	09:26:28	5.0	Normal	38.7166	0	0
499	L'Aquila Aftershock	07/04/2009	09:26:28	5.0	Normal	21.6249	0	0
500	L'Aquila Aftershock	07/04/2009	09:26:28	5.0	Normal	64.5248	0	1
501	L'Aquila Aftershock	07/04/2009	09:26:28	5.0	Normal	56.6707	1	0
502	L'Aquila Aftershock	07/04/2009	09:26:28	5.6	Normal	14.2645	0	1
503	L'Aquila Aftershock	07/04/2009	09:26:28	5.6	Normal	11.3147	0	0
504	L'Aquila Aftershock	07/04/2009	17:47:37	5.6	Normal	35.5135	1	0
505	L'Aquila Aftershock	07/04/2009	17:47:37	5.6	Normal	14.7830	0	1
506	L'Aquila Aftershock	07/04/2009	17:47:37	5.6	Normal	15.1391	0	1
507	L'Aquila Aftershock	07/04/2009	17:47:37	5.6	Normal	9.3502	0	0
508	L'Aquila Aftershock	07/04/2009	17:47:37	5.6	Normal	14.8990	0	1
509	L'Aquila Aftershock	07/04/2009	17:47:37	5.6	Normal	14.4077	0	1
510	L'Aquila Aftershock	07/04/2009	17:47:37	5.6	Normal	15.0648	0	1
511	L'Aquila Aftershock	07/04/2009	17:47:37	5.6	Normal	6.9007	0	0
512	L'Aquila Aftershock	07/04/2009	17:47:37	5.6	Normal	76.2541	0	1
513	L'Aquila Aftershock	07/04/2009	17:47:37	5.6	Normal	21.5943	0	1
514	L'Aquila Aftershock	07/04/2009	17:47:37	5.6	Normal	114.3622	0	1
515	L'Aquila Aftershock	07/04/2009	17:47:37	5.6	Normal	36.5802	0	0
516	L'Aquila Aftershock	07/04/2009	17:47:37	5.6	Normal	92.5870	0	0
517	L'Aquila Aftershock	07/04/2009	17:47:37	5.6	Normal	195.8164	0	0
518	L'Aquila Aftershock	07/04/2009	17:47:37	5.6	Normal	28.6190	0	0
519	L'Aquila Aftershock	07/04/2009	17:47:37	5.6	Normal	21.7366	0	0
520	L'Aquila Aftershock	07/04/2009	17:47:37	5.6	Normal	97.6841	0	0
521	L'Aquila Aftershock	07/04/2009	17:47:37	5.6	Normal	51.4837	0	0
522	L'Aquila Aftershock	07/04/2009	17:47:37	5.6	Normal	33.0281	1	0
523	L'Aquila Aftershock	07/04/2009	17:47:37	5.6	Normal	159.4535	0	0
524	L'Aquila Aftershock	07/04/2009	17:47:37	5.6	Normal	58.0448	0	0
525	L'Aquila Aftershock	07/04/2009	17:47:37	5.6	Normal	121.0915	0	1
526	L'Aquila Aftershock	07/04/2009	17:47:37	5.6	Normal	49.9487	0	1
527	L'Aquila Aftershock	07/04/2009	17:47:37	5.6	Normal	52.0389	0	0
528	L'Aquila Aftershock	07/04/2009	17:47:37	5.6	Normal	150.0863	0	1
529	L'Aquila Aftershock	07/04/2009	17:47:37	5.6	Normal	179.5465	0	1
530	L'Aquila Aftershock	07/04/2009	17:47:37	5.6	Normal	43.9830	0	1
531	L'Aquila Aftershock	07/04/2009	17:47:37	5.6	Normal	128.8902	0	0
532	L'Aquila Aftershock	07/04/2009	17:47:37	5.6	Normal	9.9654	0	0
533	L'Aquila Aftershock	07/04/2009	17:47:37	5.6	Normal	8.8700	0	0
534	L'Aquila Aftershock	07/04/2009	17:47:37	5.4	Normal	5.9015	1	0
N° GM	EQ ID	Date	Hour	5.9	Fault type	R_{epi}	Ss	SA

535	L'Aquila Aftershock	07/04/2009	17:47:37	5.4	Normal	5.3021	1	0
536	Gran Sasso	09/04/2009	00:52:59	5.4	Normal	22.9490	1	0
537	Gran Sasso	09/04/2009	00:52:59	5.4	Normal	12.0529	0	1
538	Gran Sasso	09/04/2009	00:52:59	5.4	Normal	12.2872	0	1
539	Gran Sasso	09/04/2009	00:52:59	5.4	Normal	16.1638	0	0
540	Gran Sasso	09/04/2009	00:52:59	5.4	Normal	11.7146	0	0
541	Gran Sasso	09/04/2009	00:52:59	5.4	Normal	11.3404	0	1
542	Gran Sasso	09/04/2009	00:52:59	5.4	Normal	11.8613	0	0
543	Gran Sasso	09/04/2009	00:52:59	5.4	Normal	27.0320	0	0
544	Gran Sasso	09/04/2009	00:52:59	5.4	Normal	19.3219	0	0
545	Gran Sasso	09/04/2009	00:52:59	5.4	Normal	100.1593	0	1
546	Gran Sasso	09/04/2009	00:52:59	5.4	Normal	46.6580	0	0
547	Gran Sasso	09/04/2009	00:52:59	5.4	Normal	47.4627	0	0
548	Gran Sasso	09/04/2009	00:52:59	5.4	Normal	117.7956	0	1
549	Gran Sasso	09/04/2009	00:52:59	5.4	Normal	30.3534	0	0
550	Gran Sasso	09/04/2009	00:52:59	5.4	Normal	31.8278	0	0
551	Gran Sasso	09/04/2009	00:52:59	5.4	Normal	9.2150	0	1
552	Gran Sasso	09/04/2009	00:52:59	5.4	Normal	83.2534	1	0
553	Gran Sasso	09/04/2009	00:52:59	5.4	Normal	142.4897	0	0
554	Gran Sasso	09/04/2009	00:52:59	5.4	Normal	76.5182	0	0
555	Gran Sasso	09/04/2009	00:52:59	5.4	Normal	168.2970	0	0
556	Gran Sasso	09/04/2009	00:52:59	5.4	Normal	65.5828	0	0
557	Gran Sasso	09/04/2009	00:52:59	5.4	Normal	145.4778	0	0
558	Gran Sasso	09/04/2009	00:52:59	5.4	Normal	19.6003	1	0
559	Gran Sasso	09/04/2009	00:52:59	5.4	Normal	17.9923	0	0
560	Gran Sasso	09/04/2009	00:52:59	5.3	Normal	20.5393	0	1
561	Gran Sasso	09/04/2009	00:52:59	5.3	Normal	26.3089	0	0
562	L'Aquila Aftershock	09/04/2009	19:38:16	5.3	Normal	24.6046	0	0
563	L'Aquila Aftershock	09/04/2009	19:38:16	5.3	Normal	14.0050	0	1
564	L'Aquila Aftershock	09/04/2009	19:38:16	5.3	Normal	14.2516	0	1
565	L'Aquila Aftershock	09/04/2009	19:38:16	5.3	Normal	17.7228	0	0
566	L'Aquila Aftershock	09/04/2009	19:38:16	5.3	Normal	13.0726	0	0
567	L'Aquila Aftershock	09/04/2009	19:38:16	5.3	Normal	13.7855	0	0
568	L'Aquila Aftershock	09/04/2009	19:38:16	5.3	Normal	27.5488	0	0
569	L'Aquila Aftershock	09/04/2009	19:38:16	5.3	Normal	20.4343	0	0
570	L'Aquila Aftershock	09/04/2009	19:38:16	5.3	Normal	48.1404	0	0
571	L'Aquila Aftershock	09/04/2009	19:38:16	5.3	Normal	49.6295	1	0
572	L'Aquila Aftershock	09/04/2009	19:38:16	5.3	Normal	32.5017	0	0
573	L'Aquila Aftershock	09/04/2009	19:38:16	5.3	Normal	16.5890	0	0
574	L'Aquila Aftershock	09/04/2009	19:38:16	5.3	Normal	32.4341	0	0
575	L'Aquila Aftershock	09/04/2009	19:38:16	5.3	Normal	9.4901	0	1
576	L'Aquila Aftershock	09/04/2009	19:38:16	5.1	Normal	77.4762	0	0
577	L'Aquila Aftershock	09/04/2009	19:38:16	5.1	Normal	66.0787	1	0
N° GM	EQ ID	Date	Hour	5.9	Fault type	R_{epi}	Ss	SA

578	L'Aquila Aftershock	13/04/2009	21:14:24	5.1	Normal	15.6019	0	1
579	L'Aquila Aftershock	13/04/2009	21:14:24	5.1	Normal	25.2629	0	1
580	L'Aquila Aftershock	13/04/2009	21:14:24	5.1	Normal	14.6557	0	1
581	L'Aquila Aftershock	13/04/2009	21:14:24	5.1	Normal	17.9396	0	0
582	L'Aquila Aftershock	13/04/2009	21:14:24	5.1	Normal	13.9707	0	1
583	L'Aquila Aftershock	13/04/2009	21:14:24	5.1	Normal	14.1702	0	0
584	L'Aquila Aftershock	13/04/2009	21:14:24	5.1	Normal	27.3907	0	0
585	L'Aquila Aftershock	13/04/2009	21:14:24	5.1	Normal	20.4809	0	0
586	L'Aquila Aftershock	13/04/2009	21:14:24	5.1	Normal	33.1165	0	0
587	L'Aquila Aftershock	13/04/2009	21:14:24	5.1	Normal	16.1338	0	0
588	L'Aquila Aftershock	13/04/2009	21:14:24	Mw	Normal	32.9349	0	1
589	L'Aquila Aftershock	13/04/2009	21:14:24	6.4	Normal	65.8954	0	0

A.2 Regression coefficients for MIDR

Table X.XX Coefficients of equation for MIDR α=0.1

T(s)	b_1	b_2	b_3	b_4	b_5	b_6	σ	R^2
0.10	-2.03000	0.57750	-2.11310	-14.43310	0.27470	0.21400	0.40804	0.72307
0.20	-2.13010	0.61750	-2.01410	-16.02440	0.30510	0.24180	0.40552	0.69820
0.30	-2.75770	0.65760	-1.78130	-13.81550	0.31540	0.27120	0.37805	0.70296
0.40	-3.17680	0.69760	-1.65860	-13.32910	0.30610	0.27360	0.37350	0.68839
0.50	-3.52190	0.73510	-1.58420	-13.11160	0.32390	0.26090	0.37093	0.68115
0.75	-4.24600	0.81190	-1.45200	-11.37600	0.38290	0.26880	0.36763	0.68384
1.00	-4.65600	0.85530	-1.39930	-10.75060	0.41740	0.29140	0.36505	0.69085
1.50	-5.15430	0.89680	-1.30560	-10.38440	0.41330	0.30200	0.37156	0.67425
2.00	-5.45300	0.91710	-1.25710	-9.33800	0.38960	0.29480	0.36860	0.67466
2.50	-5.52070	0.90930	-1.23280	-9.28780	0.36610	0.29400	0.36381	0.67248
3.00	-5.61450	0.91770	-1.23840	-9.71740	0.36680	0.27780	0.36404	0.67131
3.50	-5.69010	0.92670	-1.25430	-10.08220	0.36610	0.27360	0.36182	0.67621
4.00	-5.74450	0.92920	-1.25960	-10.01840	0.35880	0.26970	0.35837	0.68106
4.50	-5.80790	0.93580	-1.27160	-10.06850	0.36040	0.26010	0.35857	0.68327
5.00	-5.89390	0.94570	-1.28080	-9.98800	0.36860	0.26510	0.35994	0.68642

Table X.XX Coefficients of equation for MIDR α=8

T(s)	b_1	b_2	b_3	b_4	b_5	b_6	σ	R^2
0.10	-2.11690	0.58570	-2.06300	-14.09290	0.28260	0.21780	0.40307	0.72415
0.20	-2.20840	0.62180	-1.97030	-15.43450	0.30590	0.24160	0.40033	0.70137
0.30	-2.75190	0.65300	-1.75480	-13.34740	0.31810	0.26550	0.37046	0.71055
0.40	-3.10720	0.69360	-1.66930	-13.08610	0.32550	0.26980	0.36403	0.70477
0.50	-3.39660	0.72370	-1.59760	-12.88310	0.33190	0.25830	0.36695	0.69337
0.75	-4.13850	0.80290	-1.46510	-11.23700	0.38090	0.27220	0.36387	0.69082
1.00	-4.49410	0.83450	-1.40200	-10.58620	0.40580	0.29980	0.36440	0.69132
1.50	-5.03400	0.88690	-1.31450	-10.41100	0.40720	0.30030	0.36696	0.67810
2.00	-5.34430	0.91650	-1.28340	-9.65250	0.39240	0.29110	0.36866	0.67727

2.50	-5.51590	0.92170	-1.24920	-9.35700	0.38960	0.29720	0.36860	0.67598
3.00	-5.59050	0.92360	-1.24580	-9.96450	0.39140	0.29060	0.37260	0.67189
3.50	-5.72210	0.93660	-1.24490	-10.09370	0.39190	0.28870	0.37448	0.66996
4.00	-5.84470	0.94770	-1.24060	-9.78980	0.38190	0.28640	0.37139	0.67042
4.50	-5.96200	0.96040	-1.24230	-9.80030	0.37540	0.28350	0.37218	0.67243
5.00	-6.01370	0.96380	-1.24870	-10.04460	0.37060	0.28180	0.37288	0.67406

Table X.XX Coefficients of equation for MIDR α=30

T(s)	b_1	b_2	b_3	b_4	b_5	b_6	σ	R^2
0.10	-2.29910	1.61710	-0.16350	-5.17240	0.52480	-16.07820	0.40025	0.72507
0.20	-3.60030	1.89560	-0.16920	-4.51270	0.42190	-17.48360	0.39830	0.70221
0.30	-5.07260	2.05580	-0.16470	-3.68870	0.32010	-14.78060	0.37175	0.70793
0.40	-5.19470	1.98180	-0.15220	-3.50340	0.30220	-14.61870	0.36691	0.70103
0.50	-6.13360	2.21020	-0.16710	-3.35820	0.28870	-14.48060	0.36924	0.68715
0.75	-7.04410	2.29550	-0.16390	-3.05500	0.26250	-12.56280	0.36635	0.68781
1.00	-6.82040	1.97900	-0.12100	-2.45480	0.17200	-11.35460	0.36229	0.69231
1.50	-7.34210	2.16500	-0.14600	-2.87490	0.26180	-11.68950	0.36771	0.67798
2.00	-7.33280	2.11150	-0.14200	-2.97010	0.28460	-11.01630	0.37047	0.67544
2.50	-7.69320	2.09040	-0.13110	-2.58910	0.22510	-10.31570	0.36971	0.67278
3.00	-8.19870	2.19670	-0.13660	-2.44200	0.19990	-10.84580	0.37239	0.66596
3.50	-8.32120	2.16100	-0.12880	-2.30590	0.17550	-10.98630	0.37356	0.66598
4.00	-7.86710	1.94340	-0.10650	-2.19140	0.15720	-10.54050	0.37275	0.66842
4.50	-7.29290	1.78460	-0.09750	-2.41830	0.19670	-10.72530	0.37564	0.66665
5.00	-7.55890	1.87610	-0.10630	-2.47490	0.20510	-11.04230	0.37189	0.67103

A.3 Regression coefficients for IDR(x)

Table X.XX Coefficients of equation for IDR(x=0.25) α=0.1

T(s)	b_1	b_2	b_3	b_4	b_5	b_6	σ	R^2
0.10	-2.34450	0.58060	-2.09310	-14.30880	0.27780	0.21550	0.40496	0.72373
0.20	-2.45690	0.62120	-1.99560	-15.85610	0.30690	0.24260	0.40315	0.69874
0.30	-3.09700	0.66500	-1.76970	-13.79630	0.31540	0.27350	0.37829	0.70098
0.40	-3.53230	0.70550	-1.64120	-13.23720	0.30060	0.27460	0.37539	0.68342
0.50	-3.89430	0.74540	-1.56680	-13.12270	0.31940	0.26360	0.37516	0.67316
0.75	-4.64840	0.82600	-1.43270	-11.41140	0.37880	0.26680	0.37259	0.67512
1.00	-5.05720	0.86910	-1.38490	-10.95220	0.42730	0.29320	0.36943	0.68495
1.50	-5.58850	0.91330	-1.28630	-10.52960	0.42360	0.29810	0.37425	0.67044
2.00	-5.94000	0.93930	-1.22990	-9.30780	0.38400	0.29030	0.37121	0.66977
2.50	-5.98680	0.92540	-1.20300	-9.41150	0.36070	0.29240	0.36671	0.66517
3.00	-6.06820	0.92840	-1.20290	-9.73520	0.35850	0.28190	0.36561	0.66443
3.50	-6.12870	0.93780	-1.23110	-10.43340	0.35410	0.27330	0.36463	0.66783
4.00	-6.18480	0.93970	-1.23380	-10.16970	0.34850	0.26790	0.36162	0.67260
4.50	-6.24350	0.94680	-1.25260	-10.30800	0.35010	0.26430	0.36179	0.67614
5.00	-6.29310	0.95260	-1.26920	-10.34020	0.34920	0.26230	0.35894	0.68307

Table X.XX Coefficients of equation for IDR(x=0.25) α=8

T(s)	b_1	b_2	b_3	b_4	b_5	b_6	σ	R^2
0.10	-2.13640	0.58310	-2.07640	-14.18170	0.28020	0.21640	0.40253	0.72432
0.20	-2.23740	0.62200	-1.98340	-15.66320	0.30550	0.24090	0.39961	0.70149
0.30	-2.82000	0.65860	-1.76330	-13.54940	0.30910	0.26590	0.37155	0.70787
0.40	-3.17010	0.69470	-1.66630	-13.17920	0.31990	0.26700	0.36572	0.70055
0.50	-3.50500	0.73250	-1.59570	-12.83780	0.33420	0.25580	0.36974	0.68725
0.75	-4.21080	0.80640	-1.46310	-11.66340	0.37090	0.26960	0.36943	0.68027
1.00	-4.64630	0.84810	-1.39430	-10.71860	0.40320	0.29910	0.36964	0.68281
1.50	-5.18960	0.89530	-1.29150	-10.42000	0.40520	0.30350	0.37135	0.67076
2.00	-5.55160	0.93350	-1.25880	-10.18720	0.38640	0.29140	0.36980	0.67147
2.50	-5.73130	0.94310	-1.23610	-9.58800	0.37920	0.28530	0.36902	0.67190
3.00	-5.82450	0.94360	-1.22670	-9.83440	0.39740	0.29150	0.37202	0.66802
3.50	-5.88850	0.94600	-1.23280	-10.19290	0.39400	0.29110	0.37399	0.66506
4.00	-5.96920	0.94930	-1.22710	-10.17920	0.38530	0.28320	0.37361	0.66370
4.50	-6.15470	0.96500	-1.20210	-9.53280	0.37720	0.28000	0.37306	0.66500
5.00	-6.27690	0.98090	-1.21190	-9.51030	0.37220	0.27710	0.37408	0.66784

Table X.XX Coefficients of equation for IDR(x=0.25) α=30

T(s)	b_1	b_2	b_3	b_4	b_5	b_6	σ	R^2
0.10	-2.08310	0.58110	-2.09350	-14.30380	0.27770	0.21540	0.40491	0.72390
0.20	-2.17880	0.61920	-1.99660	-15.79510	0.30540	0.24150	0.40245	0.69995
0.30	-2.77340	0.65400	-1.76510	-13.56750	0.31290	0.26820	0.37466	0.70488
0.40	-3.15420	0.69550	-1.66780	-13.30330	0.31770	0.27080	0.36987	0.69529
0.50	-3.49220	0.73120	-1.59010	-12.88880	0.33080	0.25930	0.37122	0.68379
0.75	-4.21990	0.80920	-1.45920	-11.50040	0.37790	0.26830	0.36874	0.68232
1.00	-4.63910	0.84860	-1.38980	-10.63540	0.40700	0.29550	0.36713	0.68562
1.50	-5.18120	0.89860	-1.29930	-10.51870	0.41470	0.30500	0.37049	0.67435
2.00	-5.51030	0.92830	-1.26100	-9.71650	0.38930	0.29690	0.37478	0.66808
2.50	-5.68580	0.93390	-1.22680	-9.33230	0.37560	0.29390	0.37180	0.66685
3.00	-5.79800	0.94250	-1.22770	-9.95960	0.38090	0.28580	0.37633	0.66004
3.50	-5.91440	0.95320	-1.23030	-10.09880	0.38430	0.28630	0.37638	0.66214
4.00	-5.99230	0.95540	-1.22360	-9.88850	0.37130	0.28090	0.37543	0.66177
4.50	-6.11790	0.96910	-1.22780	-9.79580	0.36840	0.28080	0.37883	0.66117
5.00	-6.20930	0.98050	-1.23840	-9.96830	0.36410	0.27750	0.37549	0.66754

Table X.XX Coefficients of equation for IDR(x=0.50) α=0.1

T(s)	b_1	b_2	b_3	b_4	b_5	b_6	σ	R^2
0.10	-2.11800	0.57870	-2.10520	-14.38630	0.27590	0.21460	0.40681	0.72333
0.20	-2.22400	0.61910	-2.00670	-15.96700	0.30590	0.24220	0.40462	0.69831
0.30	-2.86490	0.66170	-1.77560	-13.82550	0.31590	0.27290	0.37845	0.70164
0.40	-3.30970	0.70470	-1.64950	-13.43220	0.30410	0.27670	0.37658	0.68271
0.50	-3.69560	0.74770	-1.57240	-13.32590	0.32300	0.26640	0.37714	0.67133
0.75	-4.55640	0.84180	-1.42520	-11.66320	0.36880	0.27120	0.38699	0.65644

1.00	-5.05560	0.89490	-1.36150	-11.41990	0.40270	0.29540	0.38989	0.65540
1.50	-5.73620	0.95580	-1.24620	-11.08730	0.42340	0.30080	0.39522	0.64410
2.00	-6.15110	0.98740	-1.18130	-9.88950	0.39740	0.28540	0.38910	0.64809
2.50	-6.30510	0.98510	-1.14910	-9.38210	0.38650	0.28880	0.38483	0.64868
3.00	-6.51980	1.00700	-1.14650	-9.25700	0.38230	0.27280	0.38502	0.65155
3.50	-6.49970	0.99430	-1.16010	-9.61190	0.37010	0.26770	0.38453	0.64842
4.00	-6.50560	0.98420	-1.16270	-9.44790	0.35440	0.26150	0.37849	0.65248
4.50	-6.54060	0.98360	-1.17770	-9.61810	0.34140	0.26190	0.37530	0.65661
5.00	-6.58920	0.98490	-1.18710	-9.47090	0.33480	0.25930	0.37141	0.66293

Table X.XX Coefficients of equation for IDR(x=0.50) α=8

T(s)	b_1	b_2	b_3	b_4	b_5	b_6	σ	R^2
0.10	-2.09570	0.57540	-2.12720	-14.51930	0.27280	0.21330	0.41017	0.72269
0.20	-2.17590	0.61250	-2.02570	-16.03380	0.30290	0.24010	0.40681	0.69866
0.30	-2.77800	0.64920	-1.79290	-13.83390	0.31760	0.26920	0.37774	0.70520
0.40	-3.19410	0.69110	-1.67630	-13.39070	0.31530	0.27170	0.37205	0.69347
0.50	-3.54740	0.73060	-1.60120	-13.13560	0.32170	0.25850	0.37268	0.68171
0.75	-4.31210	0.80970	-1.45480	-11.47150	0.37370	0.27170	0.37084	0.67898
1.00	-4.77310	0.85770	-1.38810	-10.56700	0.39940	0.29210	0.37357	0.67828
1.50	-5.38520	0.91810	-1.29460	-10.73470	0.41090	0.29920	0.37723	0.66674
2.00	-5.71840	0.94490	-1.25000	-9.80690	0.39560	0.29160	0.37677	0.66653
2.50	-5.88040	0.94430	-1.20420	-9.24070	0.38100	0.28960	0.37523	0.66134
3.00	-6.05940	0.95920	-1.19440	-9.68950	0.38990	0.29060	0.37649	0.65995
3.50	-6.15350	0.96950	-1.20890	-10.31530	0.37860	0.28280	0.37522	0.66127
4.00	-6.23570	0.97400	-1.20810	-10.13900	0.36210	0.26770	0.37532	0.65986
4.50	-6.37010	0.98860	-1.21400	-9.88370	0.35880	0.26680	0.37558	0.66413
5.00	-6.44330	0.99510	-1.22330	-10.08360	0.35400	0.27100	0.37711	0.66403

Table X.XX Coefficients of equation for IDR(x=0.50) α=30

T(s)	b_1	b_2	b_3	b_4	b_5	b_6	σ	R^2
0.10	-2.12680	0.57150	-2.14780	-14.57510	0.26950	0.21090	0.41393	0.72198
0.20	-2.17690	0.60580	-2.04630	-16.04320	0.29910	0.23880	0.40893	0.69983
0.30	-2.72210	0.63760	-1.82050	-13.90920	0.31730	0.26200	0.37760	0.70942
0.40	-3.10720	0.67670	-1.70930	-13.35420	0.31590	0.26920	0.37059	0.70116
0.50	-3.38930	0.70660	-1.63910	-13.26160	0.31850	0.25890	0.36784	0.69217
0.75	-4.16120	0.79000	-1.49630	-11.29300	0.36980	0.26410	0.36545	0.69172
1.00	-4.57250	0.82860	-1.42070	-10.53150	0.39170	0.29510	0.36568	0.68976
1.50	-5.17430	0.89230	-1.33540	-10.58590	0.40500	0.29880	0.37233	0.67579
2.00	-5.51420	0.92000	-1.28300	-9.87570	0.39300	0.29650	0.37585	0.66888
2.50	-5.81480	0.94500	-1.23670	-9.77010	0.38020	0.29430	0.37651	0.66330
3.00	-5.95960	0.95650	-1.22880	-10.31700	0.38350	0.29130	0.38143	0.65581
3.50	-6.08510	0.96760	-1.22970	-10.41820	0.37760	0.28680	0.38321	0.65456
4.00	-6.23120	0.97910	-1.21670	-10.21670	0.37850	0.28190	0.38458	0.65369
4.50	-6.39420	0.99780	-1.21480	-10.40090	0.37080	0.28120	0.38575	0.65408
5.00	-6.46860	1.00200	-1.21460	-10.98410	0.37530	0.28050	0.38731	0.65104

Table X.XX Coefficients of equation for IDR(x=0.75) α=0.1

T(s)	b_1	b_2	b_3	b_4	b_5	b_6	σ	R^2
0.10	-2.04190	0.57770	-2.11170	-14.42520	0.27490	0.21410	0.40783	0.72312
0.20	-2.14300	0.61770	-2.01280	-16.01670	0.30530	0.24180	0.40537	0.69820
0.30	-2.77370	0.65840	-1.78020	-13.81830	0.31550	0.27150	0.37814	0.70269
0.40	-3.19850	0.69900	-1.65670	-13.35230	0.30610	0.27440	0.37408	0.68729
0.50	-3.55100	0.73750	-1.58180	-13.15980	0.32400	0.26210	0.37205	0.67929
0.75	-4.30290	0.81760	-1.44590	-11.42140	0.38100	0.26900	0.37084	0.67906
1.00	-4.73710	0.86330	-1.38940	-10.80700	0.41660	0.29220	0.36878	0.68533
1.50	-5.29500	0.91210	-1.29020	-10.48670	0.41500	0.30330	0.37770	0.66646
2.00	-5.64960	0.93980	-1.23830	-9.44450	0.38920	0.29680	0.37673	0.66514
2.50	-5.76870	0.93550	-1.20230	-9.31790	0.36390	0.29990	0.37415	0.65932
3.00	-5.91020	0.94850	-1.20110	-9.78770	0.36770	0.28370	0.37472	0.65775
3.50	-6.02110	0.96180	-1.21560	-10.33320	0.36520	0.27650	0.37478	0.65941
4.00	-6.09930	0.96800	-1.22170	-10.43870	0.35630	0.26890	0.37353	0.66119
4.50	-6.17640	0.97660	-1.23700	-10.57760	0.35540	0.26080	0.37505	0.66227
5.00	-6.28930	0.98800	-1.23950	-10.51130	0.36010	0.26320	0.37714	0.66336

Table X.XX Coefficients of equation for IDR(x=0.75) α=8

T(s)	b_1	b_2	b_3	b_4	b_5	b_6	σ	R^2
0.10	-2.15560	0.56160	-2.22750	-14.92420	0.25920	0.20910	0.42598	0.72107
0.20	-2.07780	0.58160	-2.12280	-16.19330	0.28340	0.22610	0.41709	0.70275
0.30	-2.49150	0.60080	-1.90720	-14.13160	0.30340	0.24880	0.38186	0.71740
0.40	-2.77410	0.63710	-1.82490	-13.90050	0.31000	0.24930	0.37159	0.71573
0.50	-2.99220	0.66710	-1.77500	-13.76400	0.31810	0.24140	0.37421	0.70548
0.75	-3.60440	0.72550	-1.62160	-12.57220	0.35080	0.26820	0.36147	0.70554
1.00	-4.08660	0.77030	-1.51530	-11.02330	0.35090	0.28370	0.36457	0.69585
1.50	-4.65290	0.82940	-1.40850	-11.52960	0.36500	0.29240	0.36986	0.67360
2.00	-5.10040	0.87890	-1.35190	-10.71780	0.38100	0.28540	0.37384	0.67083
2.50	-5.37520	0.90630	-1.32190	-10.61580	0.39620	0.28780	0.37483	0.67071
3.00	-5.60090	0.92670	-1.29540	-10.87490	0.42310	0.29890	0.38318	0.66202
3.50	-5.76190	0.94130	-1.27980	-11.07880	0.41720	0.30010	0.38463	0.65860
4.00	-5.94910	0.95760	-1.25450	-10.81100	0.41320	0.29510	0.38250	0.66028
4.50	-6.13760	0.97110	-1.22550	-9.97280	0.41100	0.29470	0.38522	0.65840
5.00	-6.30280	0.99080	-1.21910	-9.91890	0.38800	0.29030	0.38642	0.65717

Table X.XX Coefficients of equation for IDR(x=0.75) α=30

T(s)	b_1	b_2	b_3	b_4	b_5	b_6	σ	R^2
0.10	-2.21690	0.55120	-2.32690	-15.17790	0.24620	0.20300	0.44449	0.71814
0.20	-2.02810	0.56280	-2.22390	-16.65830	0.26600	0.22060	0.42854	0.70468
0.30	-2.36500	0.57510	-2.00750	-14.58740	0.30040	0.24000	0.39331	0.71991
0.40	-2.63840	0.61460	-1.92830	-14.44720	0.31310	0.24920	0.38923	0.71212
0.50	-2.81570	0.63620	-1.86530	-14.74950	0.31370	0.24070	0.38218	0.70550
0.75	-3.50770	0.69860	-1.67650	-12.58200	0.33650	0.26360	0.36472	0.70944

1.00	-3.89230	0.73080	-1.56850	-11.73500	0.32920	0.28230	0.36364	0.69754
1.50	-4.51540	0.80650	-1.47630	-11.70460	0.37220	0.28900	0.36357	0.69087
2.00	-4.98640	0.85600	-1.39910	-10.55030	0.37740	0.27700	0.37346	0.67710
2.50	-5.28470	0.88390	-1.35660	-10.68570	0.39600	0.29450	0.37474	0.67379
3.00	-5.50920	0.90640	-1.33070	-10.88680	0.40570	0.30200	0.38251	0.66388
3.50	-5.74890	0.92840	-1.29360	-10.57100	0.40880	0.30740	0.38440	0.66109
4.00	-5.91450	0.93740	-1.25630	-9.89710	0.40090	0.30930	0.38583	0.65713
4.50	-6.09450	0.95890	-1.24760	-9.87080	0.39020	0.30090	0.38270	0.66145
5.00	-6.20660	0.96830	-1.23500	-10.28310	0.37750	0.29920	0.38188	0.65869

Table X.XX Coefficients of equation for IDR(x=1.00) α=0.1

T(s)	b_1	b_2	b_3	b_4	b_5	b_6	σ	R^2
0.10	-2.03000	0.57750	-2.11310	-14.43310	0.27470	0.21400	0.40804	0.72307
0.20	-2.13010	0.61750	-2.01410	-16.02440	0.30510	0.24180	0.40552	0.69820
0.30	-2.75770	0.65760	-1.78130	-13.81550	0.31540	0.27120	0.37805	0.70296
0.40	-3.17680	0.69760	-1.65860	-13.32910	0.30610	0.27360	0.37350	0.68839
0.50	-3.52190	0.73510	-1.58420	-13.11160	0.32390	0.26090	0.37093	0.68115
0.75	-4.24600	0.81190	-1.45200	-11.37600	0.38290	0.26880	0.36763	0.68384
1.00	-4.65600	0.85530	-1.39930	-10.75060	0.41740	0.29140	0.36505	0.69085
1.50	-5.15430	0.89680	-1.30560	-10.38440	0.41330	0.30200	0.37156	0.67425
2.00	-5.45300	0.91710	-1.25710	-9.33800	0.38960	0.29480	0.36860	0.67466
2.50	-5.52070	0.90930	-1.23280	-9.28780	0.36610	0.29400	0.36381	0.67248
3.00	-5.61450	0.91770	-1.23840	-9.71740	0.36680	0.27780	0.36404	0.67131
3.50	-5.69010	0.92670	-1.25430	-10.08220	0.36610	0.27360	0.36182	0.67621
4.00	-5.74450	0.92920	-1.25960	-10.01840	0.35880	0.26970	0.35837	0.68106
4.50	-5.80790	0.93580	-1.27160	-10.06850	0.36040	0.26010	0.35857	0.68327
5.00	-5.89390	0.94570	-1.28080	-9.98800	0.36860	0.26510	0.35994	0.68642

Table X.XX Coefficients of equation for IDR(x=1.00) α=8

T(s)	b_1	b_2	b_3	b_4	b_5	b_6	σ	R^2
0.10	-1.52750	0.50630	-2.69870	-18.23920	0.20320	0.19420	0.49997	0.70321
0.20	-1.84150	0.54400	-2.35450	-17.34920	0.24700	0.20970	0.44803	0.70205
0.30	-2.19560	0.55980	-2.11600	-15.42730	0.28230	0.23110	0.40775	0.71702
0.40	-2.44200	0.59120	-2.01460	-14.91320	0.29220	0.23320	0.39435	0.71694
0.50	-2.55260	0.61170	-1.97430	-15.30940	0.30760	0.23380	0.39829	0.70356
0.75	-3.10250	0.65910	-1.79290	-14.02630	0.33030	0.25680	0.36786	0.71545
1.00	-3.56450	0.69760	-1.65610	-11.97810	0.33160	0.26750	0.36356	0.71077
1.50	-4.04440	0.74920	-1.54870	-12.19100	0.35670	0.27840	0.35813	0.70056
2.00	-4.48260	0.79910	-1.48120	-11.21910	0.37630	0.27920	0.36175	0.69601
2.50	-4.75890	0.82050	-1.41750	-10.32910	0.38170	0.28220	0.36167	0.69233
3.00	-4.96280	0.83990	-1.38720	-10.42740	0.40780	0.29430	0.36356	0.68944
3.50	-5.19930	0.86900	-1.36530	-10.45020	0.40630	0.30170	0.36956	0.68227
4.00	-5.31260	0.87610	-1.33960	-10.35380	0.39540	0.30480	0.36944	0.67826
4.50	-5.47980	0.89190	-1.31670	-9.86570	0.39440	0.29750	0.37146	0.67605
5.00	-5.64430	0.91160	-1.30580	-9.72340	0.38700	0.29540	0.37380	0.67416

Table X.XX Coefficients of equation for IDR(x=1.00) α=30

T(s)	b_1	b_2	b_3	b_4	b_5	b_6	σ	R^2
0.10	-2.87470	0.58900	-2.04560	-13.93670	0.28650	0.21960	0.39729	0.72642
0.20	-2.91020	0.61760	-1.96160	-15.07360	0.30190	0.23890	0.39377	0.70764
0.30	-3.31120	0.63610	-1.77720	-12.97050	0.31670	0.25660	0.36630	0.72004
0.40	-3.55270	0.66830	-1.71600	-12.59350	0.32190	0.25610	0.36203	0.71714
0.50	-3.70380	0.68520	-1.66820	-12.83620	0.33130	0.24570	0.36190	0.70707
0.75	-4.21260	0.73840	-1.56180	-11.14640	0.37950	0.25950	0.35218	0.71732
1.00	-4.36030	0.74830	-1.51730	-10.74540	0.37640	0.27690	0.34673	0.71896
1.50	-4.66270	0.78270	-1.47140	-10.96760	0.38220	0.28920	0.35134	0.70748
2.00	-4.91150	0.81090	-1.44240	-10.07070	0.36490	0.28340	0.35592	0.70294
2.50	-5.06260	0.81560	-1.39570	-9.88860	0.36910	0.29140	0.35621	0.69603
3.00	-5.13070	0.82030	-1.38890	-10.62440	0.36900	0.29420	0.36354	0.68217
3.50	-5.33530	0.84810	-1.38390	-10.72670	0.37400	0.29960	0.36709	0.68082
4.00	-5.47470	0.86330	-1.36860	-10.42660	0.36200	0.29200	0.37132	0.67495
4.50	-5.66540	0.88430	-1.34490	-10.12810	0.36510	0.28940	0.37288	0.67345
5.00	-5.76170	0.89340	-1.33490	-10.24670	0.36570	0.28830	0.37309	0.67200

A.4 Regression coefficients for PFA(x)

Table X.XX Coefficients of equation for PFA(x=0.25) α=0.1

T(s)	b_1	b_2	b_3	b_4	b_5	b_6	σ	R^2
0.10	-1.28300	0.61710	-1.86180	-12.31270	0.31800	0.23350	0.37312	0.73262
0.20	-1.33880	0.61910	-1.83950	-12.27710	0.30790	0.23390	0.36816	0.73327
0.30	-1.34490	0.61590	-1.83140	-11.61440	0.30550	0.22950	0.36758	0.73701
0.40	-1.24580	0.60970	-1.85610	-11.83130	0.29940	0.21590	0.36985	0.73667
0.50	-1.18420	0.60960	-1.88400	-12.35320	0.30270	0.22340	0.37249	0.73562
0.75	-1.11500	0.60670	-1.90040	-12.46940	0.32230	0.23940	0.38134	0.73048
1.00	-1.10630	0.61610	-1.92200	-12.76550	0.30800	0.23840	0.38678	0.72574
1.50	-1.07930	0.60120	-1.88420	-13.25200	0.28960	0.23610	0.37195	0.72883
2.00	-1.19880	0.61430	-1.86320	-12.49780	0.31020	0.24160	0.37131	0.73311
2.50	-1.21830	0.62310	-1.87220	-12.86970	0.31500	0.23480	0.37103	0.73250
3.00	-1.22970	0.62650	-1.87170	-13.28270	0.31570	0.22920	0.37941	0.72031
3.50	-1.36810	0.64070	-1.84210	-13.23310	0.31710	0.24210	0.37423	0.72153
4.00	-1.38330	0.63300	-1.81930	-13.08450	0.32490	0.24660	0.36623	0.72749
4.50	-1.47070	0.63960	-1.80040	-12.76380	0.32690	0.24890	0.36036	0.73305
5.00	-1.56670	0.64780	-1.78350	-12.51280	0.32870	0.25340	0.35907	0.73367

Table X.XX Coefficients of equation for PFA (x=0.25) α=8

T(s)	b_1	b_2	b_3	b_4	b_5	b_6	σ	R^2
0.10	-1.03380	0.60640	-1.93020	-12.69290	0.30860	0.22930	0.38009	0.73430
0.20	-0.95360	0.60150	-1.92710	-13.23430	0.28520	0.22270	0.37854	0.72933
0.30	-1.06410	0.61100	-1.89690	-12.74070	0.30960	0.23810	0.37308	0.73547
0.40	-1.07740	0.61860	-1.90220	-13.01750	0.32020	0.23560	0.37532	0.73277

0.50	-1.15070	0.62990	-1.89000	-13.30800	0.31770	0.23330	0.38400	0.71913
0.75	-1.32870	0.62660	-1.80080	-12.50610	0.31610	0.24770	0.36008	0.73414
1.00	-1.50100	0.64260	-1.76180	-12.08220	0.30970	0.24330	0.36395	0.72535
1.50	-1.61670	0.65910	-1.77210	-12.99610	0.33180	0.25310	0.36098	0.72650
2.00	-1.85520	0.67510	-1.71450	-12.02280	0.35180	0.25480	0.36176	0.72391
2.50	-1.94800	0.67500	-1.68480	-12.16870	0.34760	0.26130	0.35592	0.72355
3.00	-2.09310	0.68290	-1.65080	-11.76080	0.35030	0.25820	0.35495	0.72137
3.50	-2.28290	0.70440	-1.62990	-11.56760	0.35070	0.26690	0.35176	0.72385
4.00	-2.31800	0.69870	-1.61040	-11.30230	0.34270	0.26620	0.35154	0.72108
4.50	-2.34370	0.70030	-1.61710	-11.59510	0.34110	0.26380	0.34943	0.72262
5.00	-2.46610	0.71030	-1.59600	-11.27310	0.34440	0.26050	0.34932	0.72150

Table X.XX Coefficients of equation for PFA (x=0.25) α=30

T(s)	b_1	b_2	b_3	b_4	b_5	b_6	σ	R^2
0.10	-0.86510	0.59890	-1.97470	-13.13450	0.30170	0.22510	0.38564	0.73273
0.20	-0.85210	0.60050	-1.94530	-13.96020	0.28630	0.22820	0.38260	0.72315
0.30	-1.03390	0.60320	-1.86670	-12.67030	0.31120	0.24270	0.37168	0.73201
0.40	-1.12700	0.62310	-1.86920	-13.15610	0.31720	0.24460	0.37683	0.72417
0.50	-1.24090	0.63430	-1.83890	-13.46870	0.31610	0.23220	0.37174	0.72117
0.75	-1.58520	0.64980	-1.73540	-11.75580	0.34110	0.25160	0.36148	0.72829
1.00	-1.73080	0.66030	-1.70340	-12.28070	0.33370	0.25830	0.35694	0.72335
1.50	-2.08840	0.70110	-1.67460	-12.44960	0.34760	0.26440	0.35370	0.72356
2.00	-2.35500	0.71300	-1.60950	-11.74400	0.35140	0.26560	0.35281	0.71792
2.50	-2.56660	0.72270	-1.56590	-11.20730	0.35510	0.27920	0.35045	0.71745
3.00	-2.69710	0.72810	-1.53490	-10.98800	0.35750	0.27290	0.34878	0.71497
3.50	-2.85610	0.74380	-1.52160	-10.89610	0.36130	0.27290	0.34798	0.71539
4.00	-2.91280	0.74800	-1.52630	-10.78750	0.35740	0.27030	0.34664	0.71844
4.50	-2.99210	0.75380	-1.52010	-10.56880	0.36130	0.26610	0.34378	0.72258
5.00	-3.05090	0.75720	-1.51610	-10.36030	0.36400	0.26360	0.34402	0.72328

Table X.XX Coefficients of equation for PFA(x=0.50) α=0.1

T(s)	b_1	b_2	b_3	b_4	b_5	b_6	σ	R^2
0.10	-0.86420	0.60060	-1.97690	-13.47520	0.29900	0.22600	0.38691	0.72908
0.20	-1.09430	0.62250	-1.89720	-13.78070	0.30810	0.24010	0.38216	0.71823
0.30	-1.35280	0.62570	-1.79300	-11.77490	0.29630	0.23420	0.36426	0.73167
0.40	-1.33940	0.62510	-1.79030	-11.38110	0.27460	0.21150	0.36419	0.73189
0.50	-1.25050	0.61920	-1.81790	-11.93230	0.28590	0.20950	0.36405	0.73374
0.75	-1.17150	0.62430	-1.86900	-12.24520	0.33830	0.23910	0.38101	0.72802
1.00	-1.18190	0.63540	-1.88830	-12.97900	0.34140	0.25540	0.39354	0.71409
1.50	-1.36590	0.64150	-1.81410	-13.48350	0.32100	0.26390	0.37758	0.71191
2.00	-1.58720	0.64770	-1.74060	-12.14710	0.30020	0.25250	0.36561	0.71874
2.50	-1.66260	0.65150	-1.71990	-12.23610	0.29460	0.24560	0.35797	0.72183
3.00	-1.68650	0.65020	-1.71250	-12.51320	0.29960	0.23320	0.35257	0.72413
3.50	-1.79280	0.66370	-1.70870	-12.28560	0.32730	0.24110	0.35251	0.72816
4.00	-1.85290	0.67290	-1.71500	-12.10990	0.35330	0.24580	0.34878	0.73742

4.50	-1.94600	0.68500	-1.71110	-11.68170	0.35900	0.24710	0.35044	0.73886
5.00	-1.96250	0.68730	-1.71560	-11.49430	0.34920	0.24240	0.35484	0.73530

Table X.XX Coefficients of equation for PFA (x=0.50) α=8

T(s)	b_1	b_2	b_3	b_4	b_5	b_6	σ	R^2
0.10	-0.52550	0.58510	-2.06260	-13.72920	0.28400	0.21790	0.40027	0.72794
0.20	-0.56880	0.59600	-2.00880	-14.53200	0.28230	0.22540	0.39611	0.71614
0.30	-0.83190	0.60250	-1.89440	-13.13980	0.29230	0.23760	0.37253	0.73126
0.40	-0.96710	0.62290	-1.87580	-13.34910	0.31100	0.23780	0.36973	0.73080
0.50	-1.05740	0.63460	-1.85880	-13.50430	0.32420	0.22900	0.38108	0.71517
0.75	-1.40860	0.65760	-1.76550	-12.98540	0.33060	0.24780	0.35912	0.72698
1.00	-1.68530	0.66520	-1.67070	-11.44660	0.33190	0.26080	0.35328	0.72724
1.50	-1.86500	0.68570	-1.66810	-11.84650	0.34170	0.26110	0.35586	0.72269
2.00	-2.08270	0.70710	-1.64550	-11.59590	0.34150	0.25770	0.35167	0.72571
2.50	-2.18520	0.70270	-1.61050	-11.07320	0.35250	0.26500	0.34820	0.72753
3.00	-2.30210	0.70860	-1.58940	-10.73420	0.36170	0.26710	0.34593	0.72955
3.50	-2.35840	0.71480	-1.59400	-10.67630	0.36440	0.27250	0.35291	0.72377
4.00	-2.35220	0.71130	-1.59700	-11.11990	0.35800	0.26840	0.35036	0.72321
4.50	-2.39880	0.71480	-1.59810	-11.19820	0.35580	0.26380	0.35092	0.72204
5.00	-2.47480	0.72150	-1.59360	-11.21210	0.35690	0.26310	0.34877	0.72399

Table X.XX Coefficients of equation for PFA (x=0.50) α=30

T(s)	b_1	b_2	b_3	b_4	b_5	b_6	σ	R^2
0.10	-0.42780	0.58220	-2.09090	-14.10320	0.28030	0.21580	0.40404	0.72605
0.20	-0.54810	0.59950	-2.01460	-15.17310	0.28880	0.23030	0.39884	0.71001
0.30	-0.94330	0.60790	-1.84980	-13.22800	0.30550	0.24550	0.36999	0.72615
0.40	-1.19460	0.63780	-1.80710	-12.90680	0.31300	0.24340	0.36732	0.72441
0.50	-1.32690	0.64730	-1.76920	-13.03960	0.31940	0.23380	0.36740	0.71631
0.75	-1.74950	0.67890	-1.68120	-11.78190	0.35680	0.24880	0.35382	0.72834
1.00	-1.93650	0.68750	-1.63490	-11.29230	0.34370	0.26140	0.35069	0.72622
1.50	-2.19010	0.70910	-1.61040	-11.80440	0.36060	0.27460	0.35006	0.72189
2.00	-2.44460	0.73090	-1.58200	-10.97340	0.35780	0.26480	0.35338	0.71887
2.50	-2.55050	0.72850	-1.55310	-10.88260	0.34960	0.27060	0.34983	0.71728
3.00	-2.64710	0.73260	-1.54210	-11.26330	0.35800	0.27180	0.34794	0.71583
3.50	-2.80780	0.74580	-1.52590	-10.99580	0.36770	0.27600	0.34558	0.71929
4.00	-2.87000	0.74980	-1.52770	-10.96320	0.36250	0.27560	0.34833	0.71648
4.50	-2.93610	0.75240	-1.51780	-10.77830	0.36090	0.27130	0.34572	0.71863
5.00	-2.97990	0.75500	-1.51840	-10.78210	0.35870	0.26430	0.34380	0.72060

Table X.XX Coefficients of equation for PFA(x=0.75) α=0.1

T(s)	b_1	b_2	b_3	b_4	b_5	b_6	σ	R^2
0.10	-0.35770	0.57850	-2.10650	-14.40270	0.27580	0.21470	0.40694	0.72329
0.20	-0.66800	0.61860	-2.00540	-15.86580	0.30610	0.24170	0.40420	0.69928
0.30	-1.38120	0.65610	-1.78050	-13.65780	0.31290	0.26820	0.37682	0.70494
0.40	-1.82190	0.68790	-1.66290	-12.73960	0.29540	0.26250	0.36863	0.69708

0.50	-2.12700	0.71370	-1.60420	-12.34070	0.31380	0.24670	0.36304	0.69658
0.75	-2.54050	0.74490	-1.54090	-10.27720	0.37850	0.24830	0.34682	0.72508
1.00	-2.51710	0.73900	-1.57530	-9.60230	0.37780	0.25440	0.34814	0.73462
1.50	-2.24940	0.70070	-1.62710	-9.72910	0.33340	0.24130	0.36581	0.71798
2.00	-1.85880	0.66090	-1.72520	-10.23930	0.32200	0.24240	0.37780	0.71863
2.50	-1.62560	0.64660	-1.80060	-11.09260	0.30550	0.23560	0.38376	0.71886
3.00	-1.42030	0.63110	-1.85700	-12.24560	0.31880	0.23750	0.39296	0.71191
3.50	-1.30440	0.62630	-1.89870	-13.40440	0.31150	0.23620	0.39050	0.71279
4.00	-1.21250	0.61150	-1.90720	-13.80280	0.31030	0.24190	0.38244	0.71969
4.50	-1.29350	0.62340	-1.90470	-13.79440	0.31210	0.24480	0.37907	0.72330
5.00	-1.34650	0.62240	-1.87940	-13.47410	0.31820	0.25010	0.37643	0.72440

Table X.XX Coefficients of equation for PFA (x=0.75) α=8

T(s)	b_1	b_2	b_3	b_4	b_5	b_6	σ	R^2
0.10	-0.24400	0.57410	-2.13580	-14.57370	0.27120	0.21280	0.41150	0.72239
0.20	-0.53100	0.61280	-2.03390	-16.05540	0.30190	0.23910	0.40679	0.69995
0.30	-1.19300	0.64240	-1.80550	-13.62910	0.30750	0.25900	0.37449	0.71127
0.40	-1.54000	0.66510	-1.70510	-12.82670	0.30500	0.25430	0.36294	0.71065
0.50	-1.78700	0.68640	-1.65700	-12.42760	0.31850	0.23580	0.35761	0.71117
0.75	-2.14370	0.71680	-1.60640	-10.95920	0.35950	0.23970	0.34858	0.72730
1.00	-2.19560	0.71520	-1.60760	-10.50760	0.37080	0.25750	0.34915	0.73168
1.50	-2.23350	0.71580	-1.63000	-10.94740	0.36430	0.27600	0.35816	0.72323
2.00	-2.22280	0.70780	-1.63650	-11.16250	0.34450	0.26310	0.36453	0.71308
2.50	-2.22460	0.70020	-1.63760	-11.62080	0.33650	0.26300	0.35947	0.71460
3.00	-2.30600	0.69840	-1.61900	-11.78220	0.35300	0.26800	0.35463	0.71683
3.50	-2.41230	0.70950	-1.61900	-11.71120	0.34450	0.27010	0.36027	0.71093
4.00	-2.49070	0.71400	-1.60620	-11.80510	0.33050	0.26850	0.35455	0.71328
4.50	-2.58530	0.71530	-1.57820	-11.74410	0.33260	0.26660	0.35310	0.70994
5.00	-2.71700	0.73290	-1.57960	-11.99860	0.33550	0.27230	0.35125	0.71245

Table X.XX Coefficients of equation for PFA (x=0.75) α=30

T(s)	b_1	b_2	b_3	b_4	b_5	b_6	σ	R^2
0.10	-0.22690	0.57340	-2.14000	-14.55300	0.27080	0.21230	0.41242	0.72238
0.20	-0.50110	0.60910	-2.03380	-15.87190	0.30190	0.23940	0.40774	0.70034
0.30	-1.13220	0.63800	-1.81610	-13.69910	0.30990	0.25730	0.37579	0.71136
0.40	-1.50350	0.66330	-1.71070	-12.74670	0.29740	0.25530	0.36435	0.71018
0.50	-1.73530	0.67970	-1.65600	-12.53310	0.30940	0.24220	0.35781	0.70918
0.75	-2.17490	0.72090	-1.59840	-11.25390	0.37220	0.25090	0.34889	0.72523
1.00	-2.38180	0.73770	-1.58160	-10.95100	0.39200	0.27360	0.35151	0.72501
1.50	-2.70770	0.75990	-1.53570	-11.09600	0.37330	0.28550	0.35607	0.71054
2.00	-2.95750	0.76640	-1.48400	-10.51480	0.35270	0.29360	0.35526	0.70431
2.50	-3.13670	0.77520	-1.45570	-10.67480	0.33560	0.28860	0.35260	0.69967
3.00	-3.27410	0.78870	-1.45800	-11.23040	0.33820	0.27510	0.35545	0.69383
3.50	-3.44300	0.80630	-1.45490	-11.48790	0.35120	0.27450	0.35491	0.69534
4.00	-3.55690	0.81350	-1.44610	-11.13750	0.35460	0.26950	0.35248	0.69950

4.50	-3.70420	0.82800	-1.43990	-11.04800	0.36980	0.26220	0.35437	0.69931
5.00	-3.80390	0.83260	-1.42580	-10.77170	0.37390	0.26130	0.34817	0.70655

Table X.XX Coefficients of equation for PFA(x=1.00) α=0.1

T(s)	b_1	b_2	b_3	b_4	b_5	b_6	σ	R^2
0.10	0.00990	0.56570	-2.20270	-14.92310	0.26160	0.20880	0.42210	0.00990
0.20	-0.21630	0.59660	-2.09030	-16.27090	0.29690	0.23490	0.41362	-0.21630
0.30	-0.78690	0.61470	-1.86160	-13.64010	0.30250	0.24830	0.37783	-0.78690
0.40	-1.05980	0.63290	-1.77510	-12.33650	0.28770	0.23620	0.36540	-1.05980
0.50	-1.16690	0.64130	-1.75060	-12.46070	0.29690	0.22630	0.35755	-1.16690
0.75	-1.34360	0.66280	-1.74270	-11.59330	0.35700	0.23870	0.35831	-1.34360
1.00	-1.34370	0.66480	-1.75960	-11.70320	0.35310	0.25860	0.37042	-1.34370
1.50	-1.37990	0.65840	-1.73440	-12.01140	0.32410	0.25760	0.36347	-1.37990
2.00	-1.40460	0.65040	-1.71830	-11.32500	0.32380	0.25400	0.36148	-1.40460
2.50	-1.40050	0.65420	-1.73630	-11.66020	0.31170	0.24400	0.35957	-1.40050
3.00	-1.32810	0.64790	-1.76030	-12.27900	0.31760	0.23870	0.36439	-1.32810
3.50	-1.34140	0.64760	-1.76030	-12.52500	0.32530	0.24100	0.36354	-1.34140
4.00	-1.35370	0.64710	-1.76280	-12.64550	0.33380	0.24450	0.35780	-1.35370
4.50	-1.47850	0.66260	-1.75270	-12.23430	0.33250	0.24420	0.35577	-1.47850
5.00	-1.54240	0.66360	-1.73190	-11.75730	0.33630	0.24730	0.35456	-1.54240

Table X.XX Coefficients of equation for PFA (x=1.00) α=8

T(s)	b_1	b_2	b_3	b_4	b_5	b_6	σ	R^2
0.10	-0.12070	0.56890	-2.16860	-14.47440	0.26850	0.21210	0.41675	-0.12070
0.20	-0.20500	0.58520	-2.08340	-15.43060	0.28200	0.22390	0.41106	-0.20500
0.30	-0.58570	0.59600	-1.91790	-13.89400	0.29560	0.24330	0.37954	-0.58570
0.40	-0.86630	0.62390	-1.84990	-13.41470	0.30250	0.23850	0.37022	-0.86630
0.50	-1.03290	0.64380	-1.82430	-13.40240	0.31470	0.23400	0.37308	-1.03290
0.75	-1.44940	0.67200	-1.72180	-12.21500	0.34010	0.24620	0.35429	-1.44940
1.00	-1.69230	0.68500	-1.66000	-11.04460	0.33450	0.25540	0.35351	-1.69230
1.50	-1.80810	0.69130	-1.65140	-11.58670	0.34910	0.26520	0.34770	-1.80810
2.00	-1.93560	0.70550	-1.65360	-11.42450	0.35230	0.25460	0.35401	-1.93560
2.50	-2.01050	0.70020	-1.62240	-11.01340	0.35190	0.25880	0.35184	-2.01050
3.00	-2.02400	0.69550	-1.62430	-11.23650	0.35510	0.26380	0.34878	-2.02400
3.50	-2.13550	0.70720	-1.61940	-11.09140	0.35670	0.27020	0.35143	-2.13550
4.00	-2.13020	0.70360	-1.62350	-11.41430	0.35180	0.27520	0.35146	-2.13020
4.50	-2.17550	0.70540	-1.61910	-11.29210	0.34170	0.26590	0.34928	-2.17550
5.00	-2.23890	0.70740	-1.60380	-11.10470	0.34030	0.25550	0.34726	-2.23890

Table X.XX Coefficients of equation for PFA (x=1.00) α=30

T(s)	b_1	b_2	b_3	b_4	b_5	b_6	σ	R^2
0.10	-0.19570	0.57060	-2.14610	-14.35830	0.26970	0.21000	0.41408	-0.19570
0.20	-0.32540	0.59350	-2.06580	-15.50130	0.28720	0.22980	0.40763	-0.32540
0.30	-0.73460	0.60330	-1.88960	-13.70000	0.31030	0.24700	0.37710	-0.73460
0.40	-1.02430	0.63140	-1.82160	-13.31690	0.31070	0.24810	0.37111	-1.02430

0.50	-1.20620	0.64590	-1.77550	-13.31420	0.31660	0.23860	0.36497	-1.20620
0.75	-1.69080	0.68010	-1.66460	-11.44070	0.34410	0.25080	0.35193	-1.69080
1.00	-1.91390	0.69770	-1.63150	-11.18190	0.35160	0.26310	0.35086	-1.91390
1.50	-2.15980	0.71860	-1.60590	-11.51640	0.35330	0.26900	0.34834	-2.15980
2.00	-2.35800	0.73060	-1.58010	-10.87500	0.36150	0.26680	0.35323	-2.35800
2.50	-2.41430	0.72510	-1.56440	-10.83470	0.35170	0.26390	0.34607	-2.41430
3.00	-2.45210	0.72340	-1.56550	-11.02690	0.36080	0.26950	0.34778	-2.45210
3.50	-2.51220	0.72400	-1.55720	-10.89770	0.36340	0.26680	0.34269	-2.51220
4.00	-2.57300	0.73280	-1.57250	-10.76150	0.35700	0.26860	0.34371	-2.57300
4.50	-2.59200	0.73120	-1.57410	-10.57710	0.35580	0.26660	0.34450	-2.59200
5.00	-2.55020	0.72340	-1.58520	-10.64730	0.35430	0.26380	0.34518	-2.55020

A.5 Structural analysis for IDR(x) & MIDR

```
clear all
clc

damping_ratio=5;

T1_range=[0.1
0.20
0.30
0.40
0.50
0.75
1.00
1.50
2.00
2.50
3.00
3.50
4.00
4.50
5.00];

alpha_range= [0.1;8;30];

dx=0.01;

x=0:dx:1;
x=x';

for index_alpha=1:1:length(alpha_range);
```

```
for index_T=1:1:length(T1_range);

alpha=alpha_range(index_alpha);

T1=T1_range(index_T);

H=(T1/0.0488)^(1/0.75);

[GAMMA T_modal phi
derivative_phi]=miranda_model_x_MIDR_spectrum(alpha,
T1);
[record_names]=textread('list.txt', '%s');

for index_ground_motion_x=1:1:length(record_names)

    index_ground_motion_x


name_file_x=['ITACA_database\',record_names{index_ground
_motion_x}, 'xa_record.mat'];

    load(name_file_x);
    record(1)=[];
    DT=record(1,1);
    record(1)=[];
    acceleration=record;


    for i=1:length(T_modal)

displacement_time_history(:,i)=SDoF(acceleration,T_modal
(i),DT);

u_i(:,:,i)=GAMMA(i,1).*derivative_phi(:,i)*displacement_
time_history(:,i)';
    end

    IDR=(1./H).*sum(u_i,3);

max_time_IDR_x(index_ground_motion_x,:,index_T,index_alp
ha)=max(abs(IDR),[],2);


GIDS_x(index_ground_motion_x,index_T,index_alpha)=max(ma
```

```
x_time_IDR_x(index_ground_motion_x,:,index_T,index_alpha
),[],2);

    clear displacement_time_history
    clear u_i



end


for index_ground_motion_y=1:1:length(record_names)

  index_ground_motion_y;


name_file_y=['ITACA_database\',record_names{index_ground
_motion_y}, 'ya_record.mat'];

   load(name_file_y);
    record(1)=[];
   DT=record(1,1);
    record(1)=[];
    acceleration=record;
    clear record

    for i=1:length(T_modal)

displacement_time_history(:,i)=SDoF(acceleration,T_modal
(i),DT);

u_i(:,:,i)=GAMMA(i,1).*derivative_phi(:,i)*displacement_
time_history(:,i)';
    end

    IDR=(1./H).*sum(u_i,3);

max_time_IDR_y(index_ground_motion_y,:,index_T,index_alp
ha)=max(abs(IDR),[],2);


GIDS_y(index_ground_motion_y,index_T,index_alpha)=max(ma
x_time_IDR_y(index_ground_motion_y,:,index_T,index_alpha
),[],2);
```

```
    clear displacement_time_history
   clear u_i
    clear IDR

end


 save max_time_IDR_x
 save GIDS_x

 save max_time_IDR_y
 save GIDS_y

end

end
```

A.6 Structural analysis for PFA(x)

```
clear all
clc

damping_ratio=5;
T1_range= [0.10
0.20
0.30
0.40
0.50
0.75
1.00
1.50
2.00
2.50
3.00
3.50
4.00
4.50
5.00];

alpha_range= [0.1 ;8;30];
dx= 0.01;

x=0:dx:1;
x=x';
```

```
for index_alpha=1:1:length(alpha_range);

for index_T=1:1:length(T1_range);

alpha=alpha_range(index_alpha);

T1=T1_range(index_T);

H=(T1/0.0488)^(1/0.75);

[GAMMA, T_modal, phi,
derivative_phi]=miranda_model_x_MIDR_spectrum(alpha,
T1);

[record_names]=textread('list.txt', '%s');

for index_ground_motion_x=1:1:length(record_names)

    index_ground_motion_x


name_file_x=['ITACA_database\',record_names{index_ground
_motion_x}, 'xa_record.mat'];

    load(name_file_x);
    record(1)=[];
    DT=record(1,1);
    record(1)=[];
    acceleration=record;
    clear record

    for i=1:length(T_modal)

acceleration_time_history(:,i)=SDoF_acc(acceleration,T_m
odal(i),DT);

floor_acc_i(:,:,i)=GAMMA(i,1).*phi(:,i)*acceleration_tim
e_history(:,i)';
    end

    RELATIVE_FLOOR_ACC=sum(floor_acc_i,3);

    for p=1:length(x)

FLOOR_ACC(p,:)=acceleration'+RELATIVE_FLOOR_ACC(p,:);
```

```
    end


PEAK_FLOOR_ACC_x(index_ground_motion_x,:,index_T,index_a
lpha)=max(abs(FLOOR_ACC),[],2);

    clear acceleration_time_history
    clear floor_acc_i
    clear FLOOR_ACC

end

for index_ground_motion_y=1:1:length(record_names)

    index_ground_motion_y


name_file_y=['ITACA_database\',record_names{index_ground
_motion_y}, 'ya_record.mat'];



    load(name_file_y);
    record(1)=[];
    DT=record(1,1);
    record(1)=[];
    acceleration=record;
    clear record

    for i=1:length(T_modal)

acceleration_time_history(:,i)=SDoF_acc(acceleration,T_m
odal(i),DT);

floor_acc_i(:,:,i)=GAMMA(i,1).*phi(:,i)*acceleration_tim
e_history(:,i)';
    end

  RELATIVE_FLOOR_ACC=sum(floor_acc_i,3);

    for p=1:length(x)

FLOOR_ACC(p,:)=acceleration'+RELATIVE_FLOOR_ACC(p,:);
    end
```

```
PEAK_FLOOR_ACC_y(index_ground_motion_y,:,index_T,index_a
lpha)=max(abs(FLOOR_ACC),[],2);

    clear acceleration_time_history
   clear floor_acc_i
    clear FLOOR_ACC

end

 save PEAK_FLOOR_ACC_x
 save PEAK_FLOOR_ACC_y


end

end

PFA=sqrt(PEAK_FLOOR_ACC_x.*PEAK_FLOOR_ACC_y);
```

A.7 Modal analysis for linear-MDOF

```
function eigenvalues=compute_eigenvalues(alpha);
alpha=0.1
gamma=0.05:0.0001:20;
gamma=gamma';

beta_1=sqrt((alpha^2)+(gamma.^2));

first_numerator=alpha^4;
first_denominator=(gamma.^2).*(beta_1.^2);
first_ratio=first_numerator./first_denominator;
first_bracket=[2+first_ratio];

second_numerator=alpha^2;
second_denominator=gamma.*beta_1;
second_ratio=second_numerator./second_denominator;
second_bracket=second_ratio;

F=2+first_bracket.*cos(gamma).*cosh(beta_1)+second_brack
et.*sin(gamma).*sinh(beta_1);

k=1;

for i=2:1:length(F);
```

```
    if F(i,1)>0 & F(i-1,1)<0;
        save_indexes1(k,1)=i;
        k=k+1;
    end
end
k=1;
for i=2:1:length(F);
    if F(i,1)<0 & F(i-1,1)>0;
        save_indexes2(k,1)=i;
        k=k+1;
    end
end
indices=sort([save_indexes1; save_indexes2]);
eigenvalues=gamma(indices);
function
[GAMMA,T,phi,derivative_phi]=miranda_model_x_MIDR_spectr
um(alpha, T1)
dx=0.01;
x=0:dx:1;
x=x';
eigenvalues=compute_eigenvalues(alpha);
gamma1=eigenvalues(1,1);
number_of_modes=6;
phi=zeros(length(x), number_of_modes);
derivative_phi=zeros(length(x), number_of_modes);
```

```
GAMMA=zeros(number_of_modes,1);
T=zeros(number_of_modes,1);
T(1,1)=T1;

for j=2:1:number_of_modes;

gamma=eigenvalues(j,1);
beta=sqrt(alpha^2+gamma^2);
T(j,1)=((gamma1/(gamma*beta))*sqrt(gamma1^2+alpha^2))*T(
1,1);

clear gamma
clear beta

end

for i=1:1:number_of_modes;

gamma=eigenvalues(i,1);
beta=sqrt(alpha^2+gamma^2);
eta=((gamma^2)*sin(gamma)+gamma*beta*sinh(beta))/((gamma
^2)*cos(gamma)+(beta^2)*cosh(beta));
phi(:,i)=sin(gamma.*x)-(gamma/beta).*sinh(x.*beta)-
eta.*cos(gamma.*x)+eta.*cosh(beta.*x);
phi(:,i)=(phi(:,i))./(sin(gamma)-
(gamma/beta).*sinh(beta)-
eta.*cos(gamma)+eta.*cosh(beta));
derivative_phi(:,i)=gamma.*cos(gamma.*x)-
gamma.*cosh(x.*beta)+eta.*gamma.*sin(gamma.*x)+eta.*beta
.*sinh(beta.*x);
derivative_phi(:,i)=(derivative_phi(:,i))./(sin(gamma)-
(gamma/beta).*sinh(beta)-
eta.*cos(gamma)+eta.*cosh(beta));
GAMMA(i,1)=(dx.*trapz(phi(:,i))).*(dx.*trapz((phi(:,i)).
^2));

clear gamma
clear beta
clear eta

end
```

A.8 Numerical time integration scheme for displacement

```
function
displacement_time_history=SDoF(acceleration,T,DT)

Kel=1;
sm=5/100;
acc=acceleration;

    for p=1:length(T)
        w(p)=2*3.14/T(p);
        Mu(p)=Kel/w(p)^2;
        C(p)=2*sm*(Mu(p)*Kel)^0.5;
        gamma=1/2;
        beta=1/4;

k(p)=Kel(p)+gamma*C(p)/(beta*DT)+Mu/(beta*(DT^2));
        ap(p)=Mu/(beta*DT)+gamma*C(p)/beta;
        bp(p)=Mu/(2*beta)+C(p)*DT*(gamma/(2*beta)-1);

        for i=1:length(acc)
            ACCs(i)=acc(i);
            Ps(i)=(-1)*Mu*ACCs(i);
        end

        PGA=max(abs(ACCs));

        Xs(1)=0;
        Vs(1)=0;
        As(1)=(-C(p)*Vs(1)-Kel(p)*Xs(1)+Ps(1))/Mu;
        DPs(1)=Ps(2)-Ps(1);
        Dps(1)=DPs(1)+ap(p)*Vs(1)+bp(p)*As(1);
        DXs(1)=Dps(1)/k(p);
        DVs(1)=gamma*DXs(1)/(beta*DT)-
gamma*Vs(1)/beta+DT*As(1)*(1-(gamma/(2*beta)));
        Atots(1)=As(1)+ACCs(1);

        for i=2:length(acc)
            DPs(i)=Ps(i)-Ps(i-1);
            DPs(length(acc))=0-Ps(length(acc));
            Xs(i)=Xs(i-1)+DXs(i-1);
            Vs(i)=Vs(i-1)+DVs(i-1);
            As(i)=(-C(p)*Vs(i)-Kel(p)*Xs(i)+Ps(i))/Mu;
            Dps(i)=DPs(i)+ap(p)*Vs(i)+bp(p)*As(i);
            DXs(i)=Dps(i)/k(p);
```

```
            DVs(i)=gamma*DXs(i)/(beta*DT)-
gamma*Vs(i)/beta+DT*As(i)*(1-(gamma/(2*beta)));
            Atots(i)=As(i)+ACCs(i);
        end

        displacement_time_history=Xs';

    end
```

A.9 Numerical time integration scheme for acceleration

```
function
acceleration_time_history=SDoF_acc(acceleration,T,DT)

Kel=1;
sm=5/100;
acc=acceleration;


    for p=1:length(T)
        w(p)=2*3.14/T(p);
        Mu(p)=Kel/w(p)^2;
        C(p)=2*sm*(Mu*Kel(p))^0.5;
        gamma=1/2;
        beta=1/4;

k(p)=Kel(p)+gamma*C(p)/(beta*DT)+Mu/(beta*(DT^2));
        ap(p)=Mu/(beta*DT)+gamma*C(p)/beta;
        bp(p)=Mu/(2*beta)+C(p)*DT*(gamma/(2*beta)-1);

        for i=1:length(acc)
            ACCs(i)=acc(i);
            Ps(i)=(-1)*Mu*ACCs(i);
        end

        PGA=max(abs(ACCs));

        Xs(1)=0;
        Vs(1)=0;
        As(1)=(-C(p)*Vs(1)-Kel(p)*Xs(1)+Ps(1))/Mu;
        DPs(1)=Ps(2)-Ps(1);
        Dps(1)=DPs(1)+ap(p)*Vs(1)+bp(p)*As(1);
```

```
        DXs(1)=Dps(1)/k(p);
        DVs(1)=gamma*DXs(1)/(beta*DT)-
gamma*Vs(1)/beta+DT*As(1)*(1-(gamma/(2*beta)));
        Atots(1)=As(1)+ACCs(1);

        for i=2:length(acc)
            DPs(i)=Ps(i)-Ps(i-1);
            DPs(length(acc))=0-Ps(length(acc));
            Xs(i)=Xs(i-1)+DXs(i-1);
            Vs(i)=Vs(i-1)+DVs(i-1);
            As(i)=(-C(p)*Vs(i)-Kel(p)*Xs(i)+Ps(i))/Mu;
            Dps(i)=DPs(i)+ap(p)*Vs(i)+bp(p)*As(i);
            DXs(i)=Dps(i)/k(p);
            DVs(i)=gamma*DXs(i)/(beta*DT)-
gamma*Vs(i)/beta+DT*As(i)*(1-(gamma/(2*beta)));
            Atots(i)=As(i)+ACCs(i);
        end

        acceleration_time_history=As';

    end
```

A.10 Regression analysis for MIDR

```
clc
clear all
close all

load X.mat
load ('Y.mat','Y')

[m n p]=size(Y);

%X=[M   R^2  Ss  Sa]independent variable
%    1   2   3   4
for j=1:p

for i=1:n

y=Y(:,i,j);
modelfun=@(b,x)b(1)+b(2).*x(:,1)+0.5.*b(3).*log10(x(:,2)
+b(4).^2)+b(5).*x(:,3)+b(6).*x(:,4);
beta0=[0.5 0.5 0.5 0.5 0.5 0.5];
mdl=NonLinearModel.fit(XA,y,modelfun,beta0);
coefficients_Bindi(i,j,:)=mdl.Coefficients.Estimate;
```

```
residual(i,j,:)=mdl.Residuals.Raw;
R2(i,j,:)=mdl.Rsquared.Ordinary;
SE_Bindi(i,j,:)=mdl.RMSE;
p_val_MIDR = mdl.Coefficients.pValue;
end
end
```

A.11 Regression analysis for IDR(x)

```
clc
clear all
close all

load X.mat
load ('log10_IDR_geom.mat','log10_IDR_geom')

[m n p q]=size(log10_IDR_geom);

%X=[M   R^2  Ss  Sa]independent variable
%    1   2   3   4
for k=1:q

for j=1:p
for i=1:n

y=log10_IDR_geom(:,i,j,k);
modelfun=@(b,x)b(1)+b(2).*x(:,1)+0.5.*b(3).*log10(x(:,2)
+b(4).^2)+b(5).*x(:,3)+b(6).*x(:,4);
beta0=[0.5 0.5 0.5 0.5 0.5 0.5];
mdl=NonLinearModel.fit(XA,y,modelfun,beta0);
coefficients_IDR_A(i,j,k,:)=mdl.Coefficients.Estimate;
residual(i,j,k,:)=mdl.Residuals.Raw;
R2(i,j,k,:)=mdl.Rsquared.Ordinary;
SE_IDR_A(i,j,k,:)=mdl.RMSE;
p_val_IDR = mdl.Coefficients.pValue;
end
end
end
```

A.12 Regression analysis for PFA(x)

```
clc
clear all
```

```
close all

load XA.mat
load ('Y_PFA.mat','Y_PFA')

[m n p q]=size(Y_PFA);

%X=[M   R^2  Ss  Sa]independent variable
%    1   2   3   4
for k=1:q

for j=1:p
for i=1:n

y=Y_PFA(:,i,j,k);
modelfun=@(b,x)b(1)+b(2).*x(:,1)+0.5.*b(3).*log10(x(:,2)
+b(4).^2)+b(5).*x(:,3)+b(6).*x(:,4);
beta0=[0.5 0.5 0.5 0.5 0.5 0.5];
mdl=NonLinearModel.fit(XA,y,modelfun,beta0);
coefficients_PFA_A(i,j,k,:)=mdl.Coefficients.Estimate;
residual_PFA(i,j,k,:)=mdl.Residuals.Raw;
R2_PFA(i,j,k,:)=mdl.Rsquared.Ordinary;
SE_PFA_A(i,j,k,:)=mdl.RMSE;
p_val_PFA = mdl.Coefficients.pValue;
end
end
end
```

A.13 Real-time hazard curves for PGA

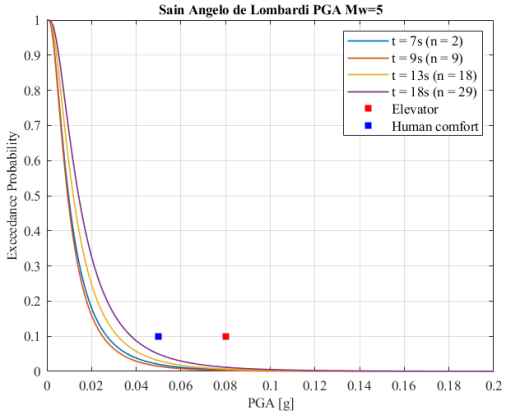

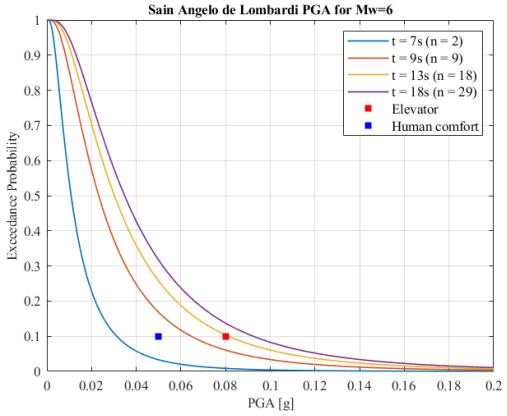

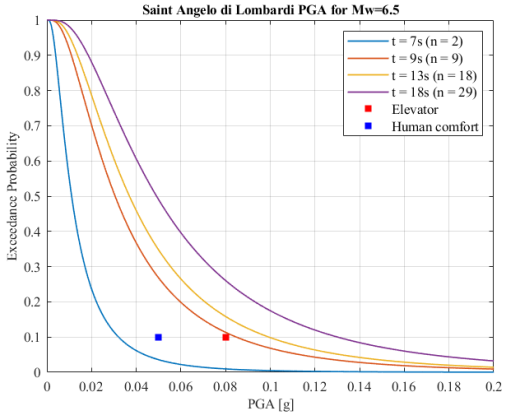

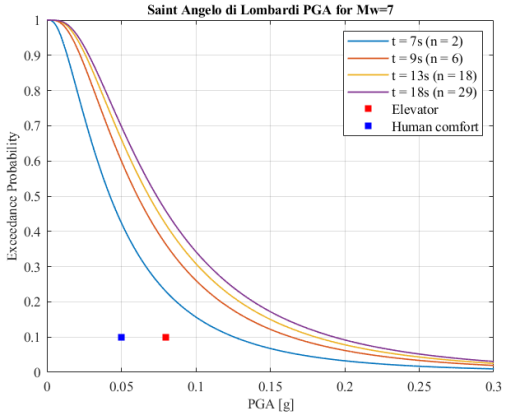

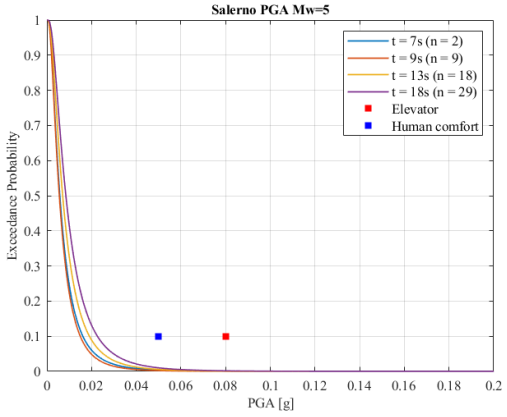

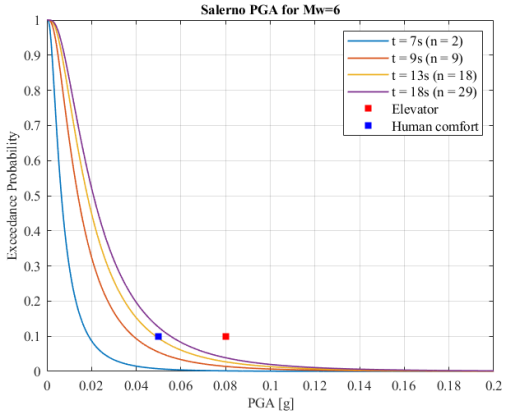

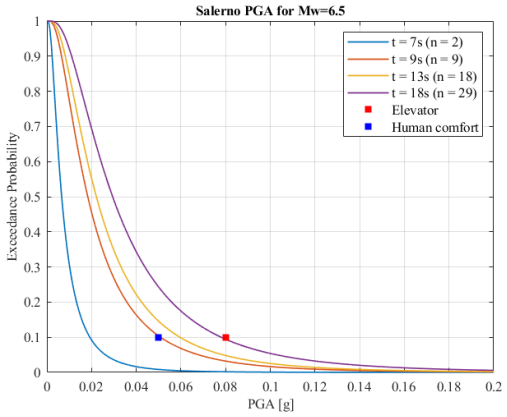
Salerno PGA for Mw=6.5
t = 7s (n = 2)
t = 9s (n = 9)
t = 13s (n = 18)
t = 18s (n = 29)
Elevator
Human comfort
Exceedance Probability
PGA [g]

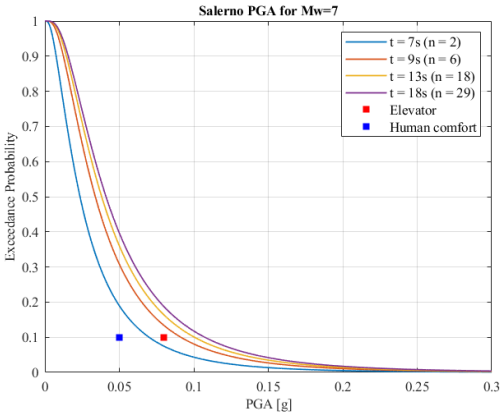
Salerno PGA for Mw=7
t = 7s (n = 2)
t = 9s (n = 6)
t = 13s (n = 18)
t = 18s (n = 29)
Elevator
Human comfort
Exceedance Probability
PGA [g]

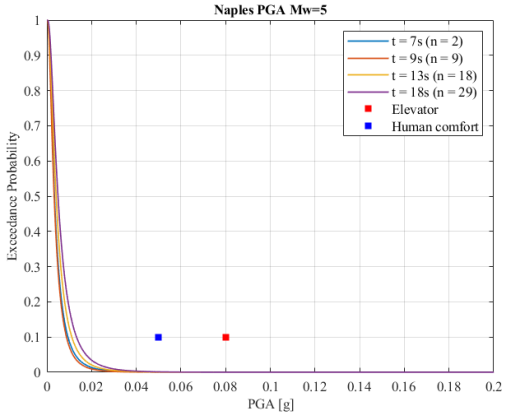
Naples PGA Mw=5
t = 7s (n = 2)
t = 9s (n = 9)
t = 13s (n = 18)
t = 18s (n = 29)
Elevator
Human comfort
Exceedance Probability
PGA [g]

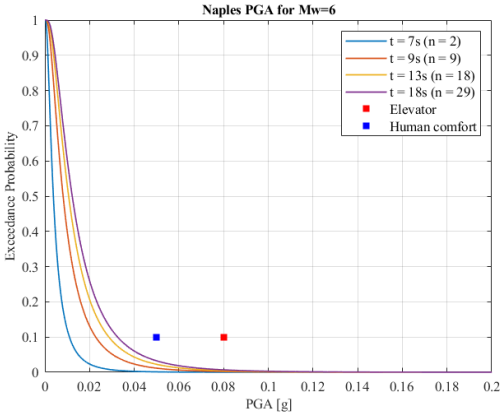
Naples PGA for Mw=6
t = 7s (n = 2)
t = 9s (n = 9)
t = 13s (n = 18)
t = 18s (n = 29)
Elevator
Human comfort
Exceedance Probability
PGA [g]

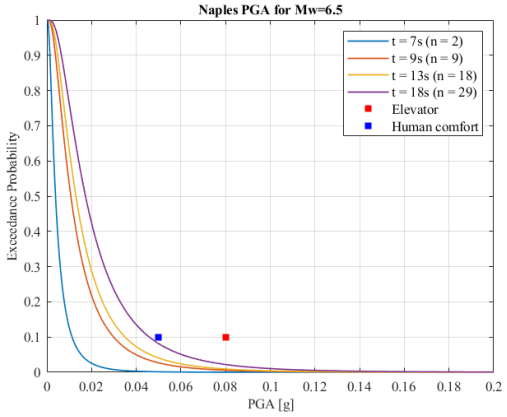
Naples PGA for Mw=6.5
t = 7s (n = 2)
t = 9s (n = 9)
t = 13s (n = 18)
t = 18s (n = 29)
Elevator
Human comfort
Exceedance Probability
PGA [g]

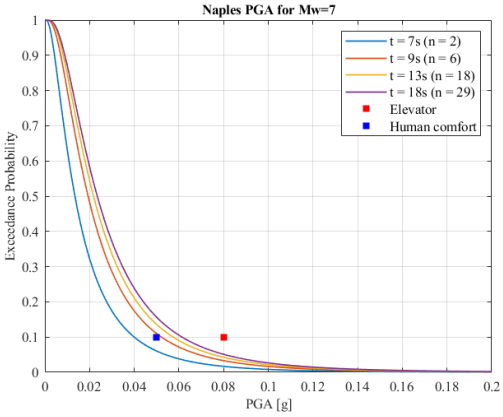
Naples PGA for Mw=7
t = 7s (n = 2)
t = 9s (n = 6)
t = 13s (n = 18)
t = 18s (n = 29)
Elevator
Human comfort
Exceedance Probability
PGA [g]

A.14 Real-time hazard curves for Mw=6

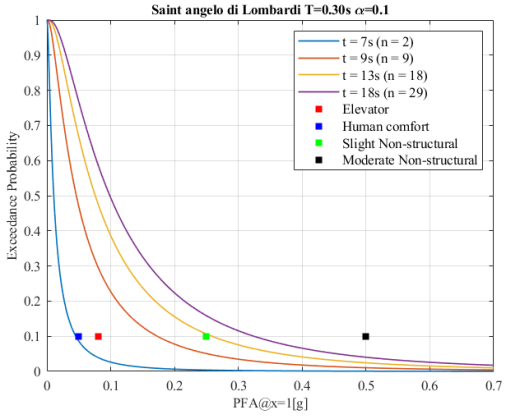

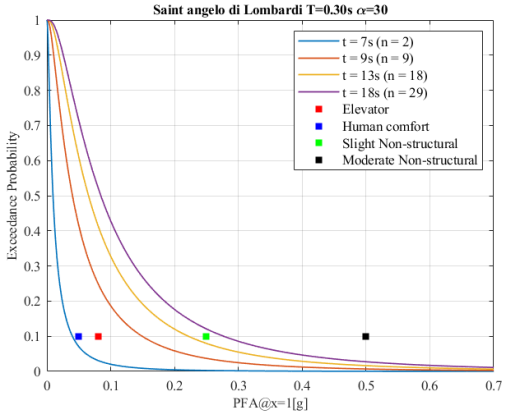

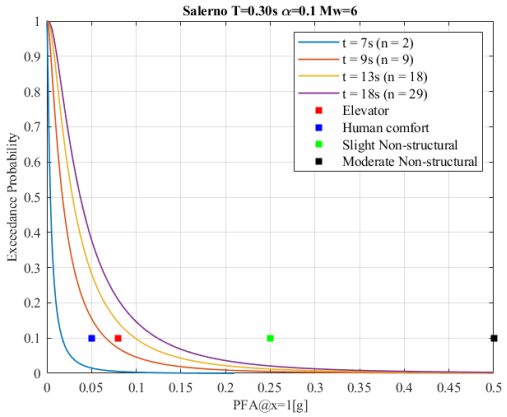

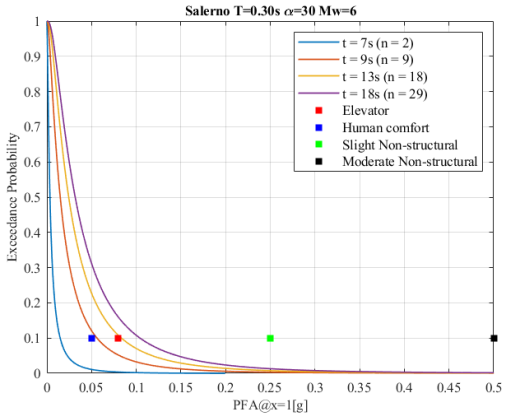

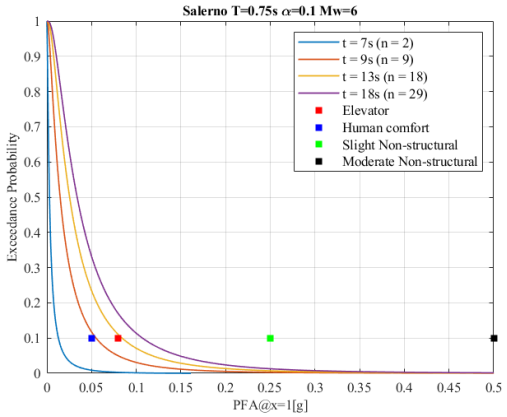

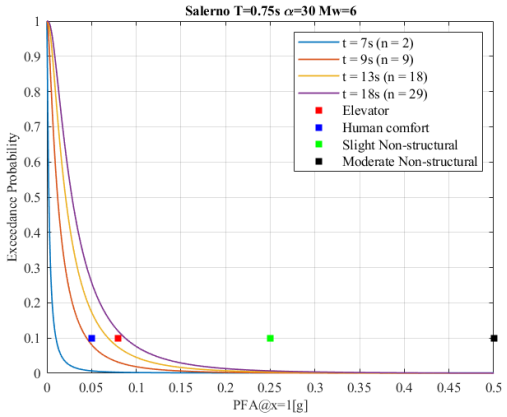

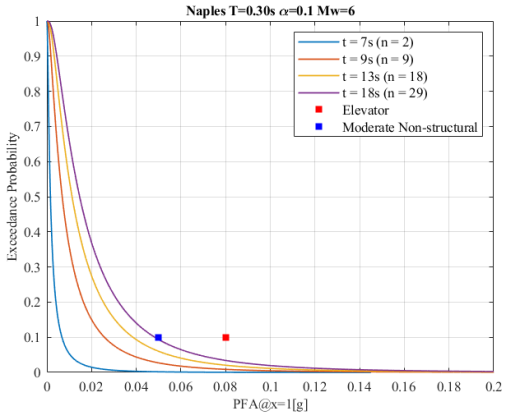
Naples T=0.30s α=0.1 Mw=6
t = 7s (n = 2)
t = 9s (n = 9)
t = 13s (n = 18)
t = 18s (n = 29)
Elevator
Moderate Non-structural
Exceedance Probability
PFA@x=1[g]

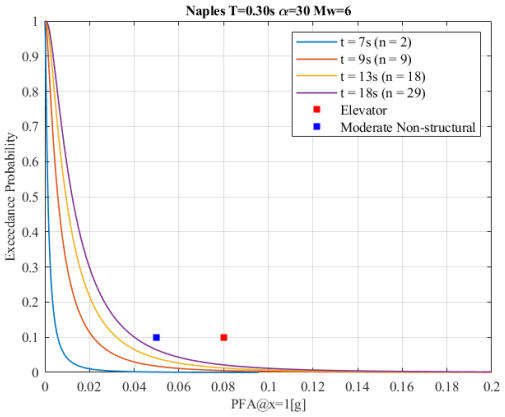
Naples T=0.30s α=30 Mw=6
t = 7s (n = 2)
t = 9s (n = 9)
t = 13s (n = 18)
t = 18s (n = 29)
Elevator
Moderate Non-structural
Exceedance Probability
PFA@x=1[g]

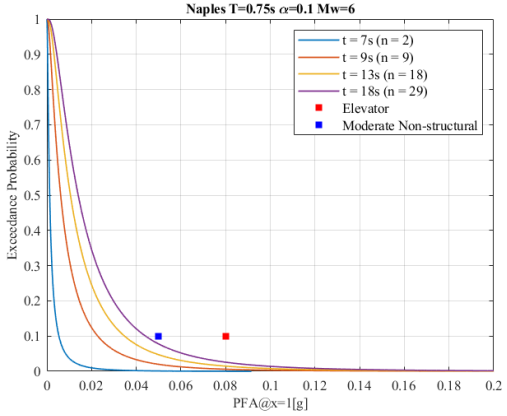
Naples T=0.75s α=0.1 Mw=6
t = 7s (n = 2)
t = 9s (n = 9)
t = 13s (n = 18)
t = 18s (n = 29)
Elevator
Moderate Non-structural
Exceedance Probability
PFA@x=1[g]

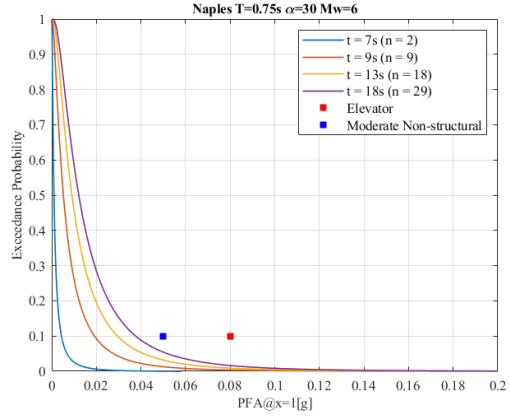
Naples T=0.75s α=30 Mw=6
t = 7s (n = 2)
t = 9s (n = 9)
t = 13s (n = 18)
t = 18s (n = 29)
Elevator
Moderate Non-structural
Exceedance Probability
PFA@x=1[g]

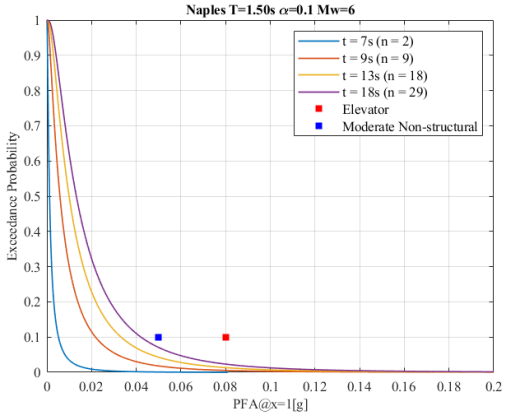
Naples T=1.50s α=0.1 Mw=6
t = 7s (n = 2)
t = 9s (n = 9)
t = 13s (n = 18)
t = 18s (n = 29)
Elevator
Moderate Non-structural
Exceedance Probability
PFA@x=1[g]

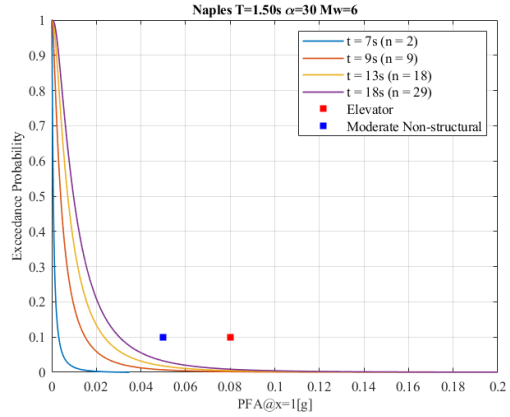
Naples T=1.50s α=30 Mw=6
t = 7s (n = 2)
t = 9s (n = 9)
t = 13s (n = 18)
t = 18s (n = 29)
Elevator
Moderate Non-structural
Exceedance Probability
PFA@x=1[g]

A.15 Real-time hazard curves for Mw=6.5

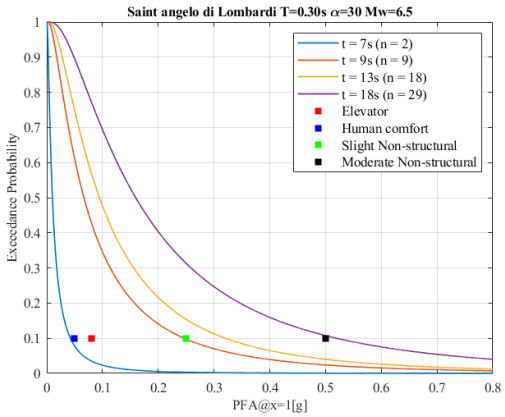

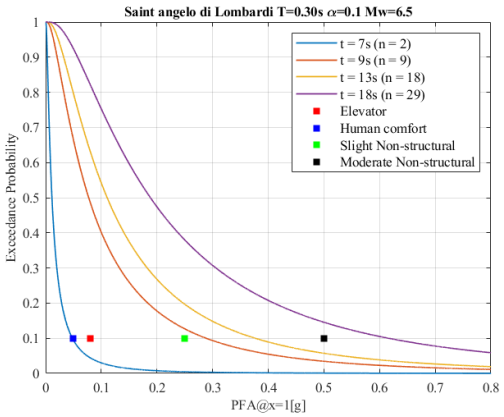

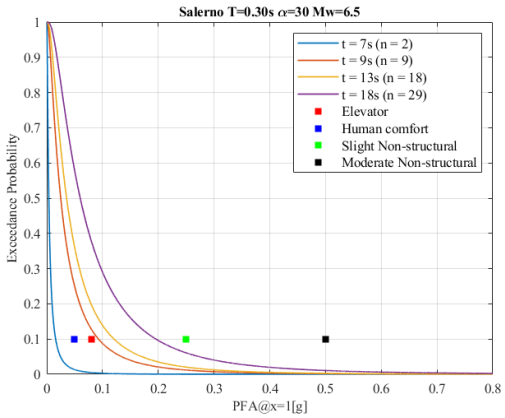

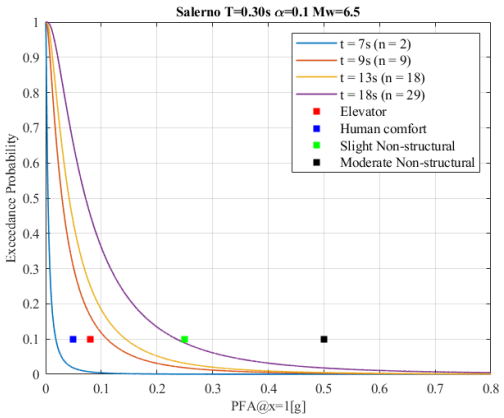

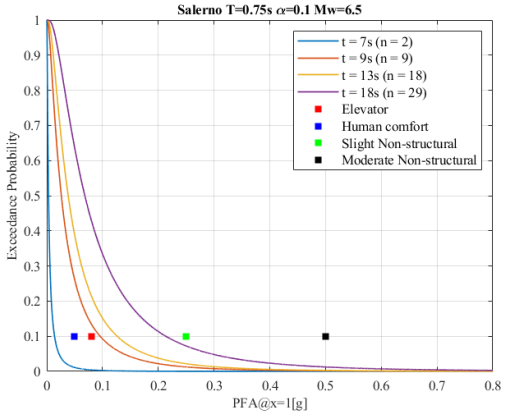

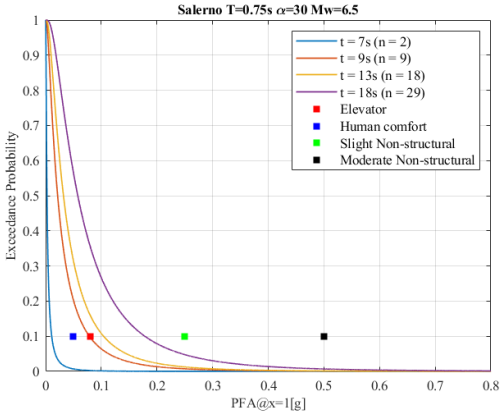

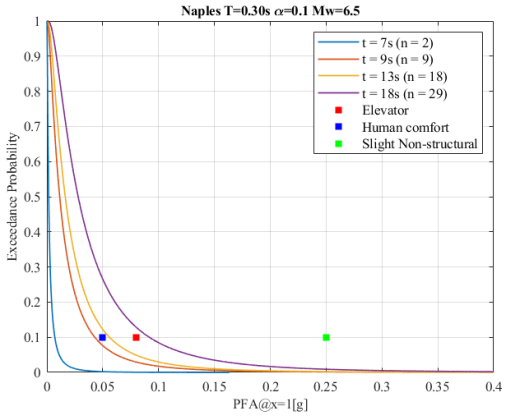
Naples T=0.30s α=0.1 Mw=6.5
t = 7s (n = 2)
t = 9s (n = 9)
t = 13s (n = 18)
t = 18s (n = 29)
Elevator
Human comfort
Slight Non-structural
Exceedance Probability
PFA@x=1[g]

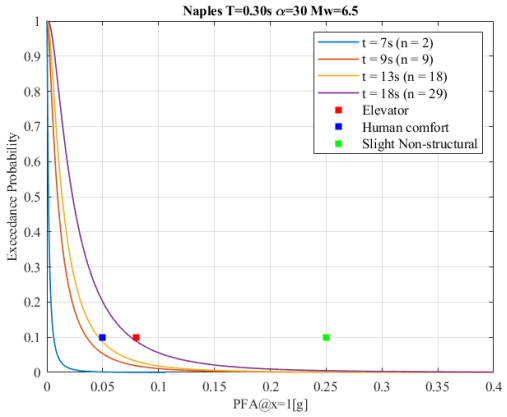
Naples T=0.30s α=30 Mw=6.5
t = 7s (n = 2)
t = 9s (n = 9)
t = 13s (n = 18)
t = 18s (n = 29)
Elevator
Human comfort
Slight Non-structural
Exceedance Probability
PFA@x=1[g]

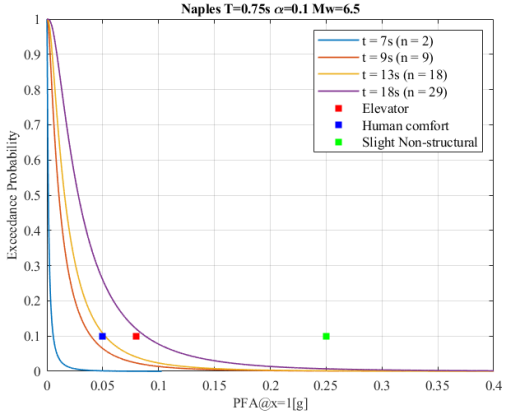
Naples T=0.75s α=0.1 Mw=6.5
t = 7s (n = 2)
t = 9s (n = 9)
t = 13s (n = 18)
t = 18s (n = 29)
Elevator
Human comfort
Slight Non-structural
Exceedance Probability
PFA@x=1[g]

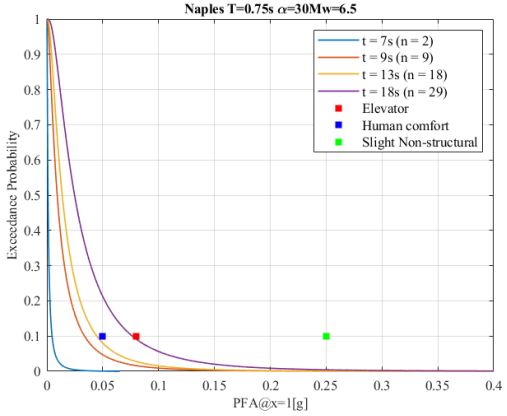
Naples T=0.75s α=30Mw=6.5
t = 7s (n = 2)
t = 9s (n = 9)
t = 13s (n = 18)
t = 18s (n = 29)
Elevator
Human comfort
Slight Non-structural
Exceedance Probability
PFA@x=1[g]

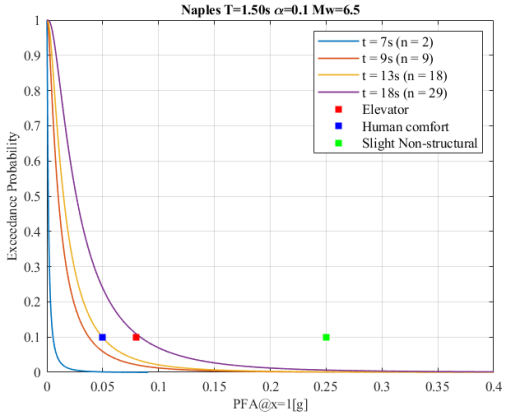
Naples T=1.50s α=0.1 Mw=6.5
t = 7s (n = 2)
t = 9s (n = 9)
t = 13s (n = 18)
t = 18s (n = 29)
Elevator
Human comfort
Slight Non-structural
Exceedance Probability
PFA@x=1[g]

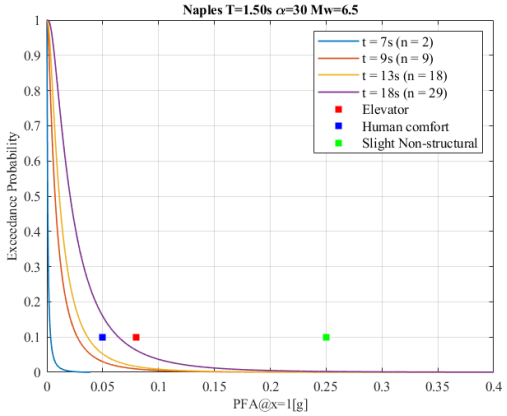
Naples T=1.50s α=30 Mw=6.5
t = 7s (n = 2)
t = 9s (n = 9)
t = 13s (n = 18)
t = 18s (n = 29)
Elevator
Human comfort
Slight Non-structural
Exceedance Probability
PFA@x=1[g]

A.16 Real-time hazard curves for Mw=7.0

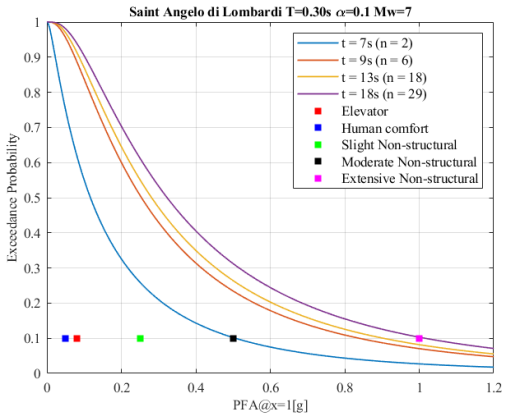

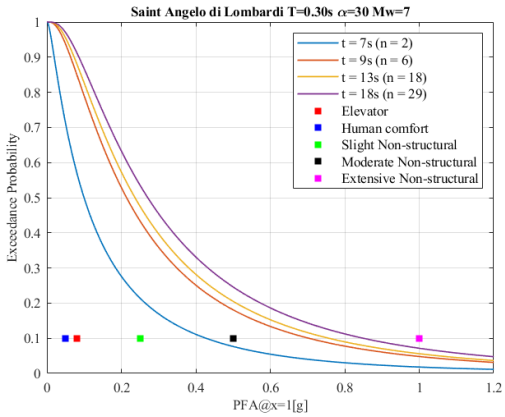

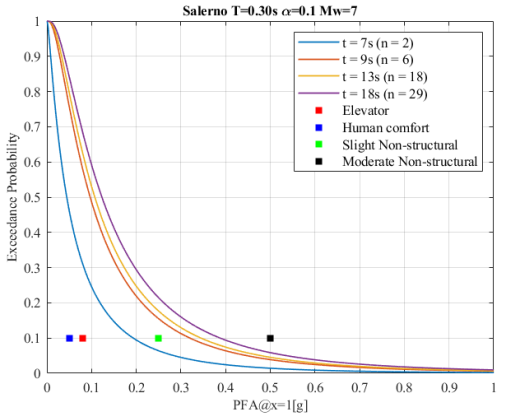

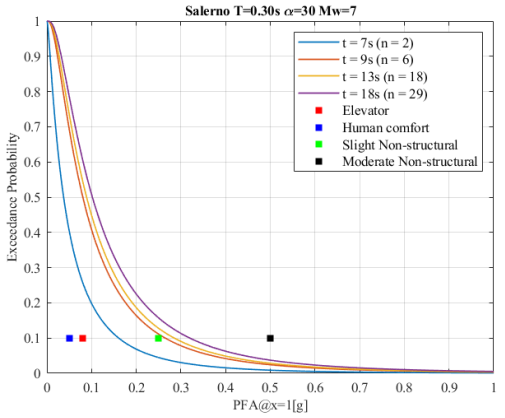

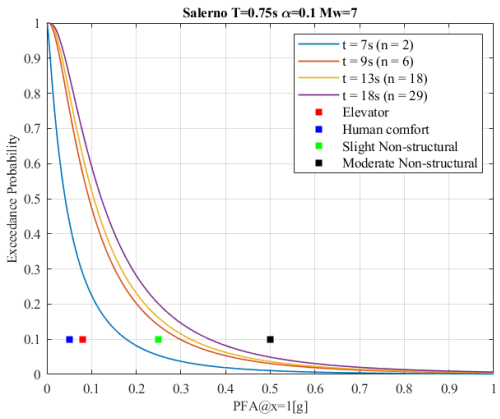
Salerno T=0.75s α=0.1 Mw=7
t = 7s (n = 2)
t = 9s (n = 6)
t = 13s (n = 18)
t = 18s (n = 29)
Elevator
Human comfort
Slight Non-structural
Moderate Non-structural
Exceedance Probability
PFA@x=1[g]

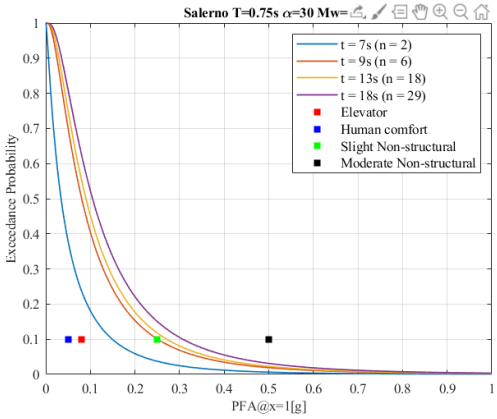
Salerno T=0.75s α=30 Mw=
t = 7s (n = 2)
t = 9s (n = 6)
t = 13s (n = 18)
t = 18s (n = 29)
Elevator
Human comfort
Slight Non-structural
Moderate Non-structural
Exceedance Probability
PFA@x=1[g]

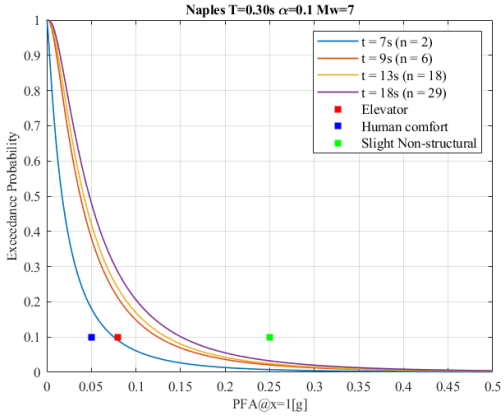
Naples T=0.30s α=0.1 Mw=7
t = 7s (n = 2)
t = 9s (n = 6)
t = 13s (n = 18)
t = 18s (n = 29)
Elevator
Human comfort
Slight Non-structural
Exceedance Probability
PFA@x=1[g]

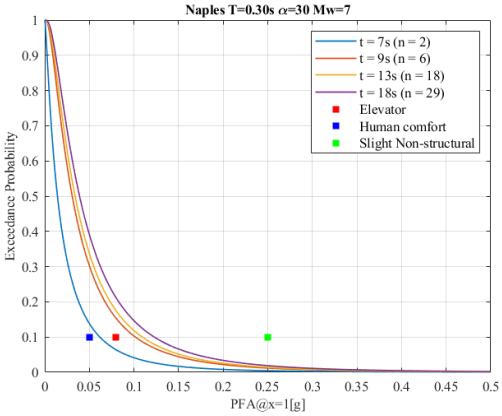
Naples T=0.30s α=30 Mw=7
t = 7s (n = 2)
t = 9s (n = 6)
t = 13s (n = 18)
t = 18s (n = 29)
Elevator
Human comfort
Slight Non-structural
Exceedance Probability
PFA@x=1[g]

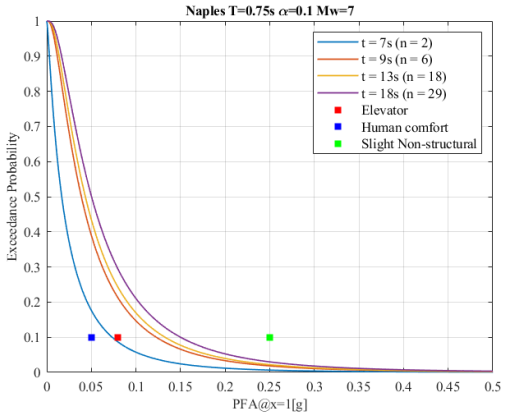
Naples T=0.75s α=0.1 Mw=7
t = 7s (n = 2)
t = 9s (n = 6)
t = 13s (n = 18)
t = 18s (n = 29)
Elevator
Human comfort
Slight Non-structural
Exceedance Probability
PFA@x=1[g]

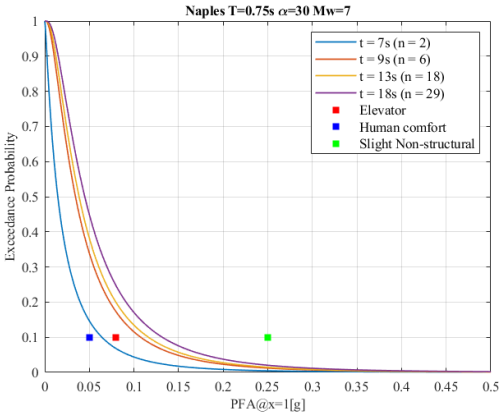
Naples T=0.75s α=30 Mw=7
t = 7s (n = 2)
t = 9s (n = 6)
t = 13s (n = 18)
t = 18s (n = 29)
Elevator
Human comfort
Slight Non-structural
Exceedance Probability
PFA@x=1[g]

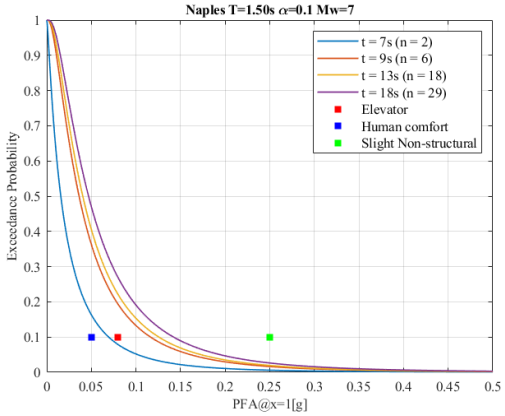
Naples T=1.50s α=0.1 Mw=7
t = 7s (n = 2)
t = 9s (n = 6)
t = 13s (n = 18)
t = 18s (n = 29)
Elevator
Human comfort
Slight Non-structural
Exceedance Probability
PFA@x=1[g]

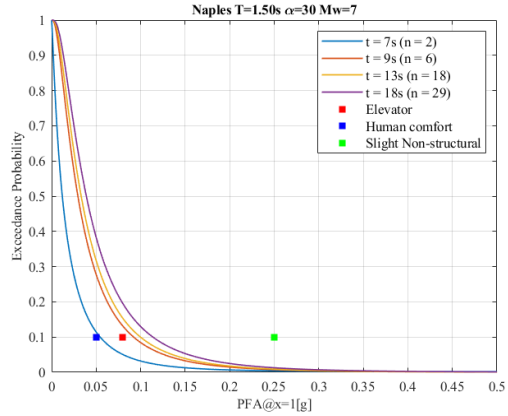
Naples T=1.50s α=30 Mw=7
t = 7s (n = 2)
t = 9s (n = 6)
t = 13s (n = 18)
t = 18s (n = 29)
Elevator
Human comfort
Slight Non-structural
Exceedance Probability
PFA@x=1[g]